EFFECTS OF BINDER TYPES ON IRON SULFIDE OXIDATION OF AGGREGATES IN CONCRETE

BY

NIRAPORN PORNSIRI

A THESIS SUBMITTED IN PARTIAL FULFILLMENT OF THE
REQUIREMENTS FOR THE DEGREE OF MASTER OF SCIENCE
(ENGINEERING AND TECHNOLOGY)
SIRINDHORN INTERNATIONAL INSTITUTE OF TECHNOLOGY
THAMMASAT UNIVERSITY
ACADEMIC YEAR 2022

THAMMASAT UNIVERSITY

SIRINDHORN INTERNATIONAL INSTITUTE OF TECHNOLOGY

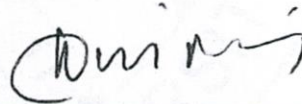THESIS

BY

NIRAPORN PORNSIRI

ENTITLED

EFFECTS OF BINDER TYPES ON IRON SULFIDE OXIDATION

OF AGGREGATES IN CONCRETE

was approved as partial fulfillment of the requirements for

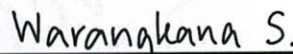the degree of Master of Science (Engineering and Technology)
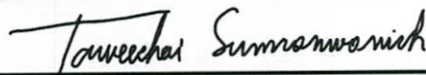
on June 27, 2023

Chairperson

_____
(Professor Somnuk Tangtermsirikul, D.Eng.)

Member and Advisor

Warangkana S.
_____
(Associate Professor Warangkana Saengsoy, Ph.D.)

Member

Taweechai Sumranwanich
_____
(Associate Professor Taweechai Sumranwanich, Ph.D.)

Member

Krittiya K
_____
(Krittiya Kaewmanee, Ph.D.)

Director

_____
(Professor Pruettha Nanakorn, D.Eng.)

Thesis Title	EFFECTS OF BINDER TYPES ON IRON SULFIDE OXIDATION OF AGGREGATES IN CONCRETE
Author	Niraporn Pornsiri
Degree	Master of Science (Engineering and Technology)
Faculty/University	Sirindhorn International Institute of Technology/ Thammasat University
Thesis Advisor	Associate Professor Warangkana Saengsoy, Ph.D.
Academic Years	2022

ABSTRACT

There are many types of deterioration that cause concrete structures to be damaged earlier than their expected life. Deterioration due to iron sulfide oxidation is one of the deterioration types that becomes widespread recently. This oxidation takes place in the aggregates that contain iron sulfide minerals. The oxidation is initiated when moisture and oxygen come into contact with these iron sulfide minerals. It causes the map cracking, pop-out of concrete, and rust staining on the concrete structures.

Even though deterioration due to iron sulfide oxidation is not a new problem, there are still no proper solution to overcome this issue. Here, a three-part solution is proposed. The solutions are 1) screening of aggregates, 2) use of proper mix proportions, and 3) protection and repair of the concrete structures. This study aims to study the second part of the solution which is the study of the effects of types of binders on expansion and rust stain due to iron sulfide oxidation. The study also includes the microstructural tests to obtain better understanding about the mechanisms of expansion and rust stain due to the iron sulfide oxidation.

In this study, five types of cement replacing materials were studied. They were high CaO and low CaO fly ashes, limestone powder, calcined clay, and silica fume.

Along with OPC cement. The aggregates used in the study was Pyrrhotite mineral which was very reactive. After the samples underwent the modified accelerated mortar bar test, two evaluations were used i.e. length change to evaluate expansion, and image analysis to evaluate rust staining.

From the obtained results, it was obvious that expansion and rust staining due to iron sulfide oxidation was governed by different mechanisms. The expansion involved the amount of calcium hydroxide in the mixtures and pore structure, while rust staining is mainly controlled by the alkalinity level of the concrete system but minorly the pore structure. Chance of iron sulfide oxidation occurrence can be reduced by reducing the penetration of moisture and oxygen into the concrete. This can be achieved by a denser pore structure. For expansion, when the amount of calcium hydroxide in the concrete system is reduced, the expansive products can be reduced. However, this lower amount of calcium hydroxide causes lower alkalinity in concrete which is favorable for formation of rust. The alkalinity level of the concrete system should be kept high to reduce rust staining due to iron sulfide oxidation. It was found from this study that the mixture system that best overcome the problems of expansion and rust staining when compared to a controlled OPC-only mixture is the ternary binder system of low CaO fly ash and limestone powder.

ACKNOWLEDGEMENTS

My deepest appreciation goes to Assoc. Prof. Dr. Warangkana Saengsoy, my advisor, who teaches me bundles of useful skills; not only laboratory work, but also how to be an ethic researcher, how to communicate properly, how to use all the technical tools and technology, such as those search engines, photo editing, Microsoft programs especially Microsoft Excel wisely. She does not only take care of my research work, but also my well-being. She is always there that many times it makes me feel that I'm home with family and close friends. She always support and concern about fellows.

Also, I would like to extend my gratitude to Prof. Dr. Somnuk Tangtermsirikul, who gives me enlightenment in concrete field and useful knowledge for my study. Every time that I reach out to him or have discussion with him for the research work, he always make it seems very simple and comprehensive. His vision in concrete research field is beyond anyone's expectation.

Special thanks to SIIT, CONTEC and Thammasat University for giving me this opportunity to pursue a higher level of study. I also would like to thank the thesis committee members which include Assoc. Prof. Dr. Taweechai Sumranwanich and Dr. Krittiya Kaewmanee for responding to my research actively and sharing different perspective to improve my research work. Special thanks are also extended to Mr. Pawee Sinlapasertsakulwong who has been helping and giving advices both in laboratory work and analysis work, as well as sharing useful idea about the research. Even though not presenting at the campus, he always keeps in touch. Furthermore, I appreciated him for providing convenience and accompany me in purchasing laboratory equipment. Thanks to Mr. Jeyakaran Thuraisingam for being a supportive lab buddy, who gives assistance and advices, and for accompanying me to operate lab work outside the campus. Thanks to all the seniors and juniors who have supported me in the laboratory work and gave advices when I was facing problems in research work. Thanks are also conveyed to the staff and security guards for being kind and nice and ensuring that I am safe working in the campus.

And the most important people to be grateful to are my beloved family and friends. Thanks for being superb supporters and are always there by my side. Thanks

for giving encouragement and will power when I struggled. The ones who always provide me with shelter and abundant food. Thank you for BTS and ARMY, TV series, music, and podcast channels that stay with me while working all days and nights.

Niraporn Pornsiri

TABLE OF CONTENTS

LIST OF TABLES

LIST OF FIGURES

LIST OF SYMBOLS/ABBREVIATIONS

Symbols/Abbreviations	Terms
°C	Degree Celsius
°C/ min	Degree Celsius per Minute
%RH	Percentage of Relative Humidity
AMBT	Accelerated Mortar Bar Test
ASTM	American Society for Testing and Materials
ASR	Alkali Silica Reactivity
Al_2O_3	Aluminum Oxide
C_3A	Tri Calcium Aluminate
C_2S	Di Calcium Silicate
C_3S	Tri Calcium Silicate
C_3H_6O	Acetone
$CaCO_3$	Calcium Carbonate
CaO	Calcium Oxide
$Ca(OH)_2$	Calcium Hydroxide
CAH	Calcium Aluminate Hydrate
CC	Calcined Clay
CH	Calcium Hydroxide
CO_2	Carbon di-oxide
CRM	Cement Replacing Material
CSH	Calcium Silicate Hydrate
DTG	Derivative Thermogravimetric
EDS	Energy Dispersive X-ray Spectroscopy
FAM	Mae Moh Fly Ash (High CaO Fly Ash)
FAB	BLCP Fly Ash (Low CaO Fly Ash)
Fe(III)	Iron (III)

Symbols/Abbreviations	Terms
$Fe(OH)_3$	Ferrihydrite
$Fe(OH)_3$	Ferric Hydroxide
$FeO(OH)$	Goethite
$Fe_{1-x}S$	Pyrrhotite
FeS_2	Pyrite
Fe_2O_3	Ferric Oxide
$FeSi$	Ferrosilicon
GU-PC	General Use Portland Cement
H_2O	Water
H_2O_2	Hydrogen Peroxide
H_2SO_4	Sulfuric Acid
hr	Hour
kV	Kilo-Voltage
L_0	Initial Length
$L(t)$	Length after test at exposure period
LC^3	Limestone Calcined Clay
LP	Limestone Powder
mm	Millimeter
mA	Milli-Ampere
MIP	Mercury Intru Porosimetry
NaOCl	Sodium Hypochlorite
NaOH	Sodium Hydroxide
O_2	Oxygen
OPC	Ordinary Portland Cement
PC	Portland Cement
PR	Pyrrhotite
rpm	Revolution per Minute
SCM	Supplementary Cementitious Material
SCG	Siam Cement Group
SEM	Scanning Electron Microscopy

Symbols/Abbreviations	Terms
SF	Silica Fume
SiO_2	Silicon Di-oxide
SO_3	Sulfur Tri-oxide
SRI	Siam Research and Innovation Co., Ltd.
TGA	Thermogravimetric Analysis
TIS	Thailand Industrial Standard
XRD	X-Ray Diffraction Analysis
μm	Micrometer
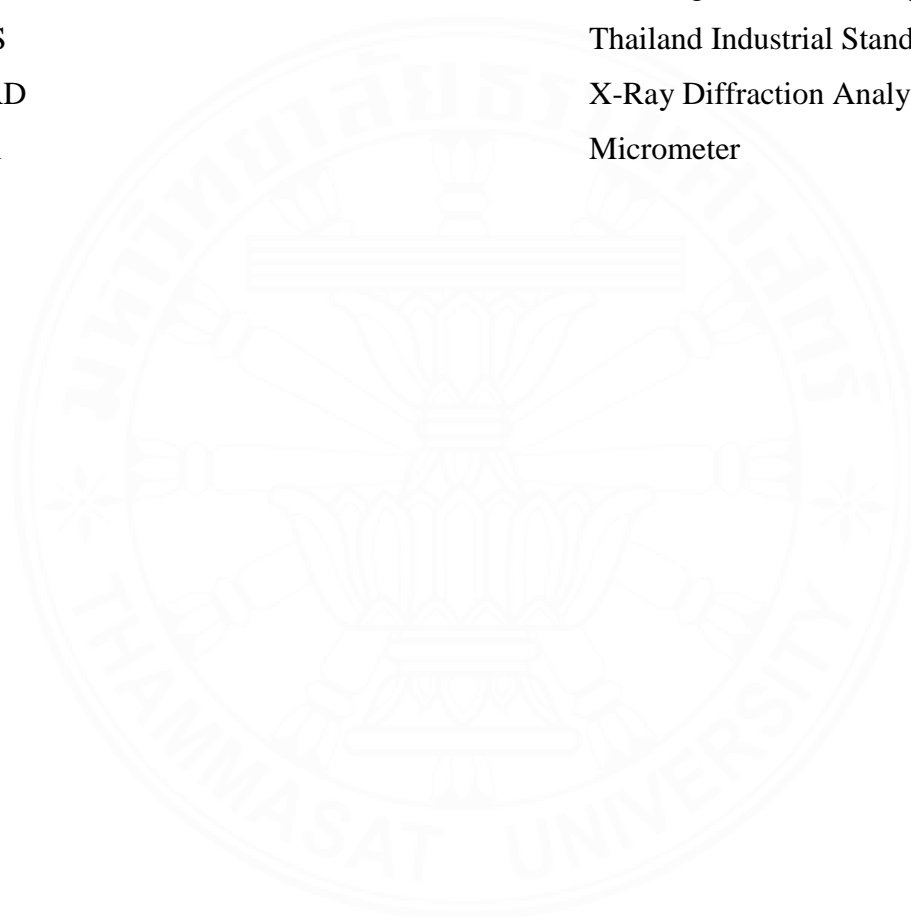
CHAPTER 1
INTRODUCTION

1.1 Background

Concrete is ranked the second most consumed material in the world after water (Daniele Di Stefano, 2021). Cement, along with water, aggregates, and sometimes additional admixtures, are used to produce concrete. Concrete is used to construct many kinds of infrastructures such as roads, bridges, houses, dams, etc. Concrete structures can be seen everywhere nowadays both indoor and outdoor. The outdoor concrete structures are more prone to get deteriorated than the indoor concrete structures. Some common concrete deteriorations that are well heard are the steel corrosion, which is a common problem when reinforced concrete is subjected to chloride or moisture; carbonation, which is the deterioration from exposure to carbon dioxide, etc. The outdoor members that are subjected to rain (water) and air (oxygen) most of the time may result in one deterioration which is the combination of rust stain, cracks, and the pop out of concrete on the concrete surface (Figures 1.1, 1.2, 1.3). This occurrence is due to the oxidation of the iron sulfide. The iron sulfide that is present in the aggregates can react with moisture and oxygen from the surrounding environment or inside the concrete, causing damages. The deterioration causes the structure to lose the aesthetic appearance.

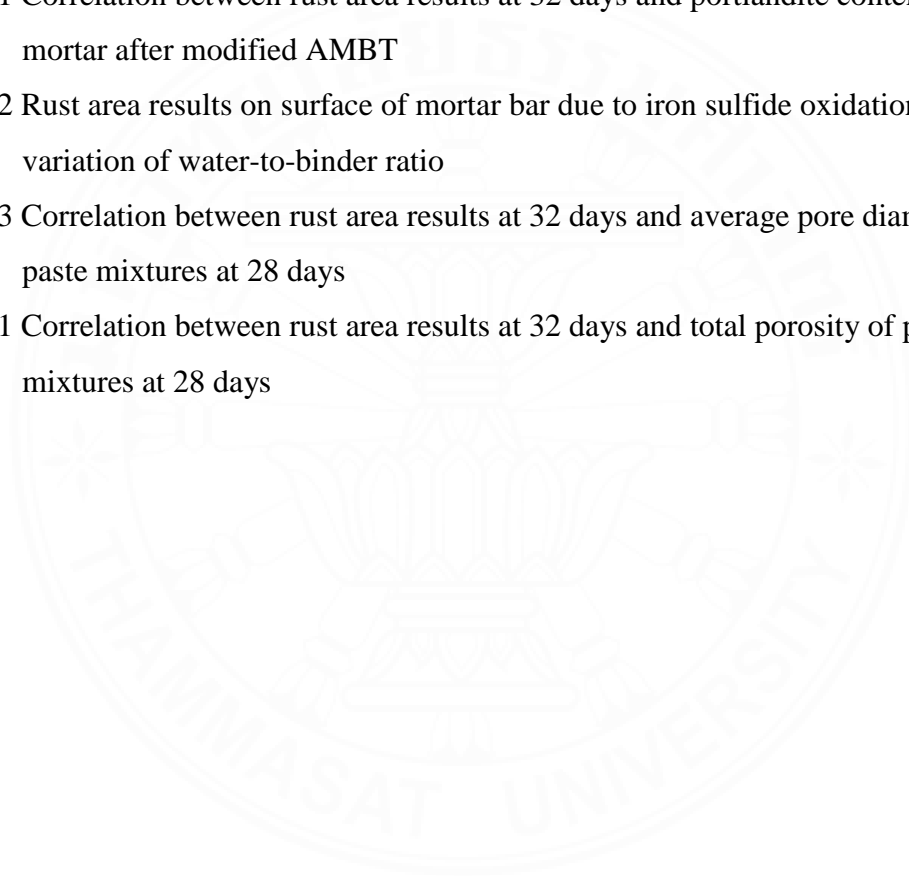**Figure 1.1** A reinforced concrete beam in a water retaining wall with iron sulfide

deterioration showing rust staining on the concrete surface (Jana, 2018)
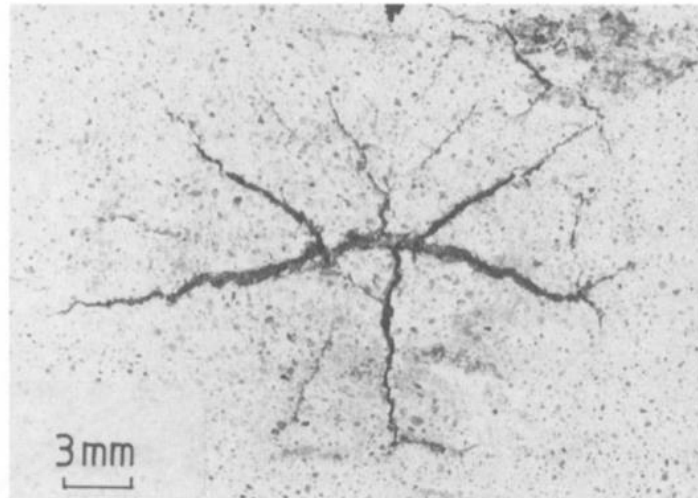
Figure 1.2 A concrete slab showing blistering due to iron sulfide deterioration
(Shayan, 1988)

Figure 1.3 A reinforced concrete beam in a water retaining wall with iron sulfide
deterioration showing pop-out of concrete (Saengsoy et al., 2021)

The concrete structures in Quebec, Canada were found to be deteriorated. Many houses suffered from map cracking and rust staining. The deterioration was later reported to be due to the use of aggregates which contained iron sulfide. The deteriorated structures showed the damage five years after the construction (Rodrigues et al., 2015). The problem of damages due to the iron sulfide oxidation has been reported since 1974. The damage due to iron sulfide was found in many parts of the world including in South Africa and United Kingdom (Guirguis et al., 2018). Graus Dam in

Spain was also reported to have damage due to the iron sulfide in the aggregates, in which the Pyrrhotite bands were found in the aggregates (Oliveira et al., 2014). Zhong and Wille (2018) reported a similar concrete deterioration that became a problem to many house and property owners in Eastern Connecticut (United States of America). The deterioration showed cracks with wide opening and map cracking. The deteriorated concrete structures were cored to investigate the cause(s) of deterioration. Later, it was reported that this deterioration was due to the aggregates that contain iron sulfide. Furthermore, in Thailand, this deterioration due to aggregates containing iron sulfide is known. Mostly, the affected sectors are the house owners, real estate and construction companies, etc. But still, practically, no effective solution to the problems is invented.

1.2 Statement of problem

As mentioned in the background, the iron sulfide oxidation has become a noticeable problem in many parts of the world. It damages concrete structures by causing rust stain, cracks, and pop-out of concrete on the concrete surface. However, there is still no proper solutions to solve this problem. The only solution that is generally done now is to remove the damaged concrete and patch with the new concrete. It is obvious that this is not a sustainable solution. Sooner or later, this new concrete will show damages again since the problematic aggregates are still present in the structure. Plentiful attempts and studies have been done over decades to reproduce the conditions that can best promote the iron sulfide oxidation onsite, but still not all possible parameters that may be the factors affecting the iron sulfide oxidation are included. Especially in Thailand, there is an increasing number of places found to be affected by this iron sulfide-containing aggregates. However, only few studies have been made. This implies the glimpse of understanding about the problem.

Some research showed that a proper mix proportion can be used to reduce the damages due to iron sulfide oxidation when the iron sulfide-containing aggregates are inevitably present in the concrete (El-Mosallamy & Shehata, 2020; Guirguis et al., 2018). However, the cement replacing materials used in those studies are different from the ones available in Thailand. This means that the chemical compositions of the materials are different and it is possible to give different mechanisms. Furthermore, the

studies were done only to evaluate the expansion results of the mortar bars. Damages from rust stain were neglected. Therefore, this research is carried out.

Here, possible solutions to tackle the deterioration due to iron sulfide oxidation are proposed. Figure 1.4 demonstrates a diagram of the solutions which consists of three parts that are independent of each other. These three parts take place at different phases of concrete construction; quarry, concrete plant, and construction site. The first operation is to screen the aggregates that are mined from quarries. Here all the aggregates obtained are going through series of chemical tests to detect whether or not they contain iron and sulfur. The second operation is at the concrete plant where proper mix designs are used to curtail iron sulfide oxidation from any possible iron sulfide containing aggregates that may still present in the concrete. The last operation is the protection (and repair) of the concrete structures at construction sites or at the product level. Even though the design of proper mix proportion can ease degree of the problem, it alone cannot terminate the problem. The coating in the last part of the solution may be necessary. For the best problem solving to be achieved, these three parts have to be integrated. The second part of this solution is where this thesis rests upon. (For more information, the first part of chemical tests to detect iron sulfide in aggregates was studied by Sinlapasertsakulwong (2019) and Saengsoy et al. (2021) and the last part of coating and repair was studied by Jeyakaran et al. (2023))

1.3 Significance of the study

When the iron sulfide-containing aggregates are inevitably present in the concrete, with sufficient amount of water and oxygen, the deterioration due to iron sulfide oxidation can occur. Waiting for the cracks, rust stain, and pop-out to occur then repair the concrete structures is not a wise solution. The use of proper mix proportion can be another solution to alleviate the deterioration damages due to the iron sulfide oxidation. However, there are many types of cement replacing materials available in Thailand that have not been studied to cope with the deterioration due to iron sulfide oxidation. Also, the study includes the evaluation of rust staining on concrete surface due to iron sulfide oxidation, in addition to the expansion, by using different types of cement replacing materials which has never been evaluated in any research. With the use of proper mix proportion, the cost of repair and construction waste can be reduced.

Longer structure's life cycle is achieved. Also, the carbon emission is further reduced from the use of cement replacing materials.

1.4 Objectives

From the above background, there are still research gaps that can be further studied. This leads to the main objective of this study, which is,

➢ To reduce damages involving expansion and rust stain caused by the iron sulfide oxidation using cement replacing materials available in Thailand

In order to obtain this objective, it is necessary to divide it into smaller goals, which are:

1. To study the effects of types of binders on expansion of mortar bars due to iron sulfide oxidation

2. To study the effects of types of binders on rust staining on mortar bars' surface due to iron sulfide oxidation

3. To study the mechanisms of the effects of types of binders on the expansion and rust stain of mortar bars due to iron sulfide oxidation
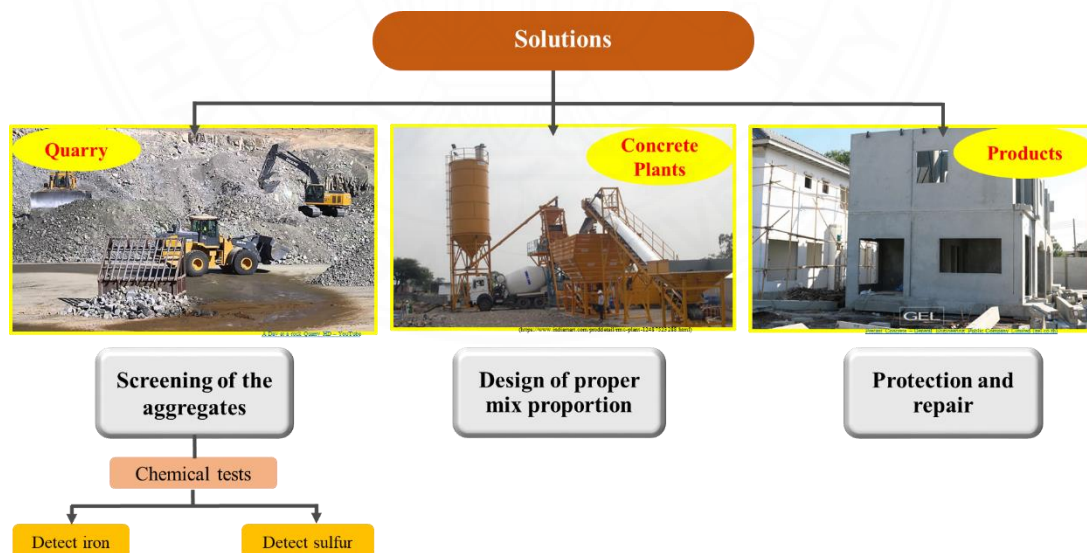
Figure 1.4 Diagram of the three-part solution to solve the deterioration due to iron sulfide oxidation

1.5 Scopes

➤ Materials:

➤ Ordinary Portland cement (OPC) from Siam Cement Group (SCG) Public Company Limited, Thailand, is used as the main binder for the study.

➤ Five types of cement replacing materials are used, consisting of

- High CaO fly ash from Mae Moh power plant, Lampang province, the northern part of Thailand

- Low CaO fly ash from BLCP power plant, Rayong province, the eastern part of Thailand

- Calcined clay from Siam Research and Innovation (SRI) of Siam Cement Group (SCG) Public Company Limited, Thailand

- Limestone powder from Siam Research and Innovation (SRI) of Siam Cement Group (SCG) Public Company Limited, Thailand

- Silica fume from China

- Iron sulfide-containing aggregate, obtained from China. It is the only aggregate used in the study and it is a very reactive aggregate. The size of the aggregate used is in the range of 2.36 to 4.75 mm, which are the aggregates that pass through sieve no. 4 and retain on sieve no. 8.

➤ Mix design:

- Three different replacements are used in the study, which are 10, 30, and 45% by weight of total binders.

- 10% replacement: is used in binary system for limestone powder and silica fume

- 30% replacement: is used in binary and ternary systems for high CaO fly ash, low CaO fly ash, limestone powder, and silica fume

- 45% replacement: is used in binary, ternary and quaternary systems for high CaO fly ash, low CaO fly ash, calcined clay, and limestone powder

- The water-to-binder ratio is kept constant for all mix proportions at 0.45.

- The aggregate-to-binder ratio is kept constant for all mix proportions at 2.25.

➢ Experiments:

• The modified accelerated mortar bar test is carried out to accelerate the expansion of mortar bars

• Two different evaluations are used to evaluate the expansion and rust staining of mortar bars.

  • To evaluate expansion of mortar bars, a length comparator is used.

  • To evaluate rust area of mortar bars, the image analysis is used.

CHAPTER 2
REVIEW OF LITERATURE

2.1 Iron sulfide aggregates

Iron sulfide is one kind of the metal sulfide minerals, which can be found in many forms in nature. The 2 most common forms of the iron sulfide found in the aggregates are Pyrite (FeS_2) (Figure 2.1) and Pyrrhotite ($Fe_{1-x}S$) (Figure 2.2). They are found to be minor minerals that are embedded in the rocks. Also, in the sulfide ore, Pyrite is found as a major mineral and Pyrrhotite as the minor mineral. These 2 minerals are shiny and metallic. As in Figure 2.1, Pyrite possesses yellowish-white color and it has a cubic structure. While Figure 2.2 shows Pyrrhotite with bronze or brownish-red color and it has a hexagonal structure (Jana, 2018). They are sometimes called as Fool's Gold. Naturally, Pyrite is more stable than Pyrrhotite, therefore, Pyrrhotite degrades more severely than the Pyrite (Rodrigues et al., 2015). According to Rodrigues, Duchesne and Fournier (2015), the iron sulfide oxidation usually takes place within Pyrrhotite minerals (Figure 2.3) more often than with Pyrite minerals (Figure 2.4). This is due to the fact that Pyrite has crystalline microstructures, while Pyrrhotite is more likely amorphous microstructures.

Figure 2.1 Microstructure of Pyrite (FeS_2) mineral (mindat.org, n.d.)

Figure 2.2 Microstructure of Pyrrhotite ($Fe_{1-x}S$) mineral (mindat.org, n.d.)
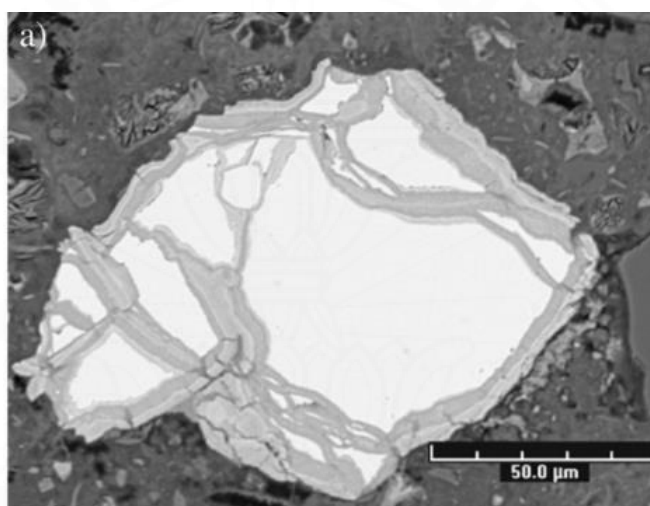
Figure 2.3 Oxidation of Pyrite mineral in aggregate (Schmidt et al., 2011)
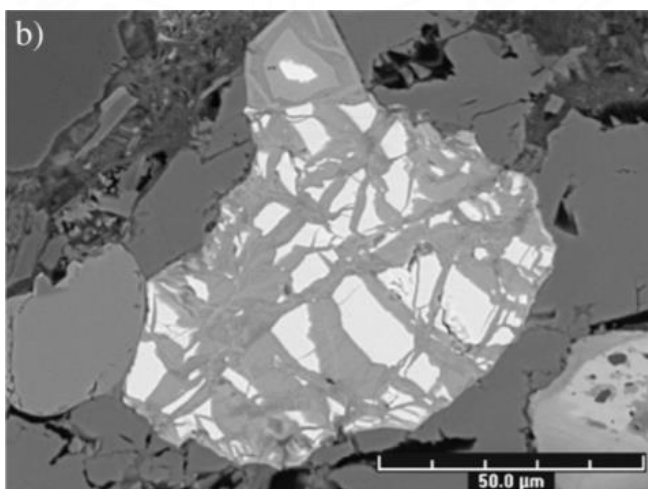
Figure 2.4 Oxidation of Pyrrhotite mineral in aggregate (Schmidt et al., 2011)

2.2 Mechanisms of iron sulfide oxidation

Iron sulfide oxidation is considered as a harmful reaction that causes deterioration in concrete structures. The mechanisms of iron sulfide oxidation start when the iron sulfide (FeS_2) (here, pyrite mineral is used for the explanation) comes into contact with oxygen (O_2) and water (H_2O) (Eq. 1.1). The series of oxidation then occurs following Eqs. 1.1, 1.2 and 1.3. Overall, ferric oxy-hydroxides or rust (Fe_2O_3) and sulfuric acid (H_2SO_4) are formed. At this stage, the mechanism is called as the primary expansion in which the expansion that occurs in the concrete matrix is generated from the products of oxidation (i.e. rust products) (Eq. 1.4) (Jana, 2018). The sulfuric acid (H_2SO_4) from the oxidation then reacts with the calcium hydroxide ($Ca(OH)_2$) or CH, which is already presented from the hydration reaction of cement and forms gypsum (Eq. 1.5). This gypsum then reacts with calcium aluminate hydrate (CAH), the existing substances in Ordinary Portland cement mixtures, and produces secondary ettringite, which is an expansive substance (Eq. 1.6). Eqs. 1.5 and 1.6 are called as the secondary expansion. This stage is simply where the sulfuric acid or the released sulfate reacts with the substances in the concrete system and forms the mentioned expansive products (gypsum and secondary ettringite). It is worth knowing that the primary ettringite is the product during the hydration reaction mainly before getting hardened, which is the reaction from cement and water and it is different from the secondary ettringite that causes deterioration in the concrete that contains iron sulfide containing aggregates.

$$FeS_2 + H_2O + 3.5O_2 \rightarrow Fe^{2+} + 2SO_4^{2-} + 2H^+ \tag{1.1}$$

$$2Fe^{2+} + 3SO_4^{2-} + 2H^+ \rightarrow 2FeSO_4 + H_2SO_4 \tag{1.2}$$

$$4FeSO_4 + 6H_2O + O_2 \rightarrow 2Fe_2O_3 + 2H_2O + 4H_2SO_4 \tag{1.3}$$

$$4FeS_2 + 8H_2O + 15O_2 \rightarrow 2Fe_2O_3 + 8H_2SO_4 \tag{1.4}$$

$$H_2SO_4 + Ca(OH)_2 \rightarrow CaSO_4 \cdot 2H_2O \tag{1.5}$$

$$Ca_3Al_2O_6 + 3CaSO_4 \cdot 2H_2O + 30H_2O \rightarrow 6CaO \cdot Al_2O_3 \cdot 3CaSO_4 \cdot 32H_2O \tag{1.6}$$
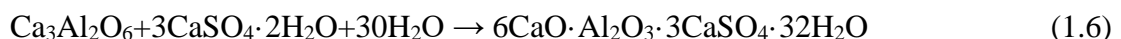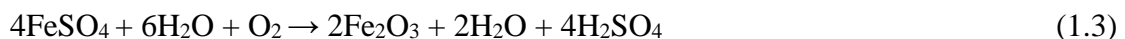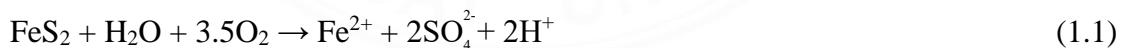
Therefore, from the mechanisms of iron sulfide oxidation, three main products are formed. Start with the ferric oxy-hydroxides or simply the rust products. This

includes ferric oxide (Fe_2O_3), goethite ($FeO(OH)$), ferrihydrite ($Fe(OH)_3$). It is reported that the rust products also shows expansion, but not to the high degree as gypsum and secondary ettringite. They contribute 1.3 times more volume than the original substances (Schmidt et al., 2011). Mainly, the rust products cause rust staining on the concrete's surface. The second product formed is gypsum ($CaSO_4 \cdot 2H_2O$) which causes one to two times of volume change (Eglington, 1998). Lastly, the secondary ettringite from the iron sulfide oxidation yields three to eight times larger volume than that of the original pyritic substance (Tagnit-Hamou et al., 2005). This is the reason why the iron sulfide deteriorates concrete.

These three products together contribute to the expansion inside the concrete in which later result in pop-out and cracking on the surface of the concrete. In addition, rust products also causes rusting on the concrete surface. Overall, the structure loses the aesthetic appearance.

The rate of reaction of iron sulfide oxidation depends on many factors such as surface area of the aggregates, morphology of the aggregates, amount of moisture and oxygen that are in contact with the iron sulfide mineral, etc. The products from iron sulfide oxidation can further react with many other substances in the concrete to form deleterious products. The type of products to be formed in concrete depends on the type of rocks that the iron sulfide minerals embedded in and the environmental condition (Shayan, 1988).

From Zhong and Wille (2018), the area involving with oxidation of iron sulfide is divided into three zones (Figure 2.5). The oxidation begins at the surface of the iron sulfide containing aggregates and continues toward the core of the aggregate. The three zones are 1) oxidized zone, which is the area at the surface of the iron sulfide-containing aggregates, 2) intermediate zone, and 3) unaltered zone, which is at the core of the aggregate. Oxidized zone, closest to the surface of iron sulfide mineral, the area that is first in contact with water and moisture, has high concentration of iron and sulfur, which indicates that iron sulfide oxidation takes place. Almost all of the iron sulfide mineral are oxidized in this zone. Moving toward the aggregate core, the next zone is intermediate zone. In this zone, iron sulfide mineral oxidizes partially. Lastly, the unaltered zone, it is the zone at the aggregate core where no oxidation occurs.
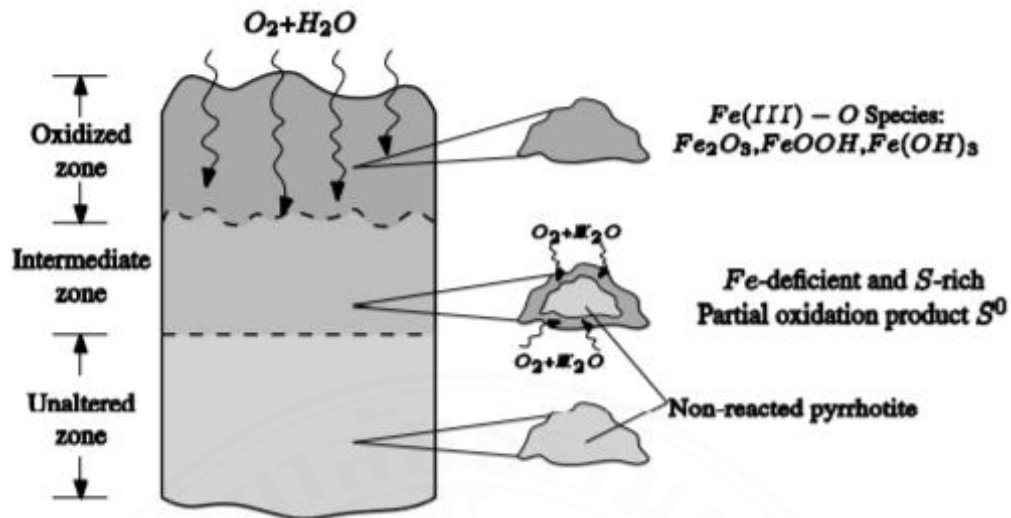
Figure 2.5 Zones of iron sulfide oxidation in aggregates (Zhong & Wille, 2018)

Shayan (1988) stated that the pyritic aggregates that are deep inside the concrete structure remain sound since they are protected by the mortar portion around them. In addition, the water and oxygen cannot easily penetrate inside the concrete structure.

2.3 Screening of aggregates using chemical tests

To use the aggregates in the concrete production and to avoid the unexpected harmful substances that may present in the aggregates, the detection of these harmful substances before using the aggregates must be done. The substances that are considered to be deleterious to concrete are, for instance, organic particles, alkali materials, iron sulfide, etc.

There are some existing standards and specifications published that limit the amount of sulfur (SO_3) that is allowed to be present in the concrete. General German Assembly study of mineral deposits (1960) and French standard [AFNOR NF P 18-540] (1997) limited amount of SO_3 to be less than 1% of total aggregate mass. BS EN 13242 limited amount of total sulfur to be less than 1%. And if Pyrrhotite is present, special precautions have to be carried out according to BS EN 12620: 2008 *Section 6.3.2.* French standard [AFNOR NF P 18-540] (1997) stated that if the aggregate is contaminated with Pyrite, the Pyrite content should not exceed 0.75% of aggregate mass. No standards mention the limitation of iron (Fe) or iron sulfide that can be present in the aggregates or concrete.

For the detection of iron sulfide in the aggregates, chemical tests can be carried out. However, there are still no standards for the detection of iron sulfide minerals published. The only means to detect the reactivity of the aggregates due to iron sulfide is through the detection of iron and sulfur contents separately using different test methods. Those testes are time consuming and some methods require at least 90 days to confirm the safety of aggregates to be used in concrete production (Rodrigues, 2015)

The iron that presents in nature comes in many forms such as Fe (II) or ferrous, Fe (III) or ferric. In order to detect iron in the aggregates, Saengsoy, Yongchaitrakul, Sinlapasertsakulwong and Tangtermsirikul (2021) came up with Cation group III and H_2O_2 tests. With Cation group III, potassium thiocyanate is used to detect Fe (III) ions. If the test solution change color from clear to bloody red color, it indicates the presence of Fe (III) ions. While with H_2O_2 test, hydrogen peroxide is used. If Fe ions are present, the solution changes from clear to turbid light orange color also rusting is observed on aggregate's surface. Midgley (1958) also proposed a test which was named after him, Midgley test. He used saturated lime water to detect the iron ions. The blue-green gelatinous precipitate and rusting on aggregate's surface should be visible to indicate the presence of Fe ions. Later, Ramos, Rodrigues, Fournier and Duchesne (2016) suggested saturated lime water made from 3% sodium hypochlorite (NaOCl) for effective test results.

To detect sulfur, Rodrigues et al. (2016) invented oxygen consumption test. The method detects sulfide from the rate of oxygen consumption. In a latter year, Guirguis and Shehata (2017) proposed a mass loss test. They soaked iron sulfide mineral in solution over a period of time. The mass loss of the aggregates and the color change of the soaking solution indicates the presence of sulfide oxidation.

Recently, Sinlapasertsakulwong (2019) proposed a guideline flow chart of series of chemical tests that detects iron and sulfur in the tested aggregates within short period of time and is practically convenient to be done at the quarry.
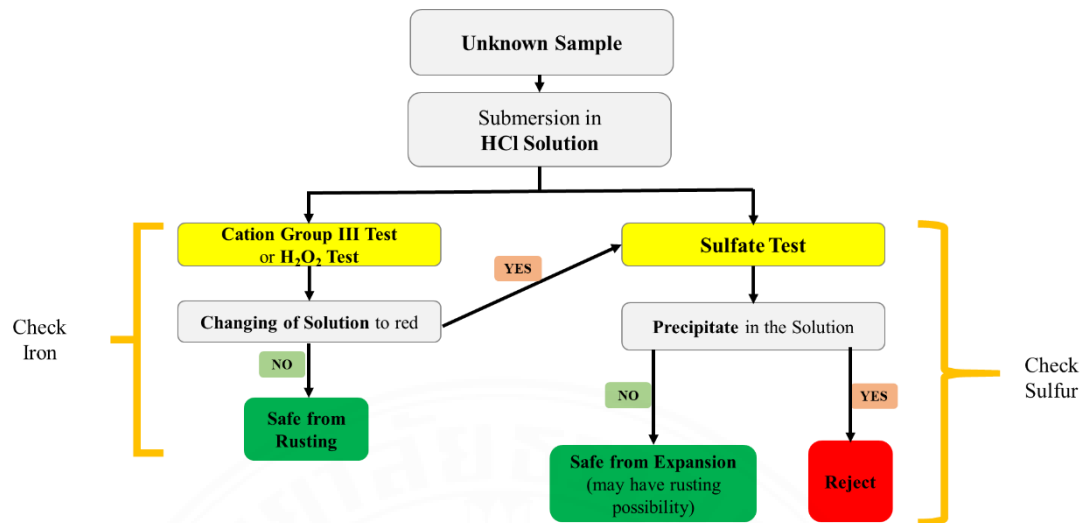
Figure 2.6 Guideline for chemical tests to screen aggregates (Sinlapasertsakulwong, 2019)

2.4 Accelerated mortar bar test (AMBT)

Accelerated mortar bar test is a test method to detect the deterioration potential of the iron sulfide-containing aggregates on mortar bars. The test is modified from the ASTM C1260, which is the standard test method to detect the potential of alkali-silica reactivity (ASR). The test evaluates the mortar bars by their length changes over a period of time. This length changes are measured using a length comparator. The specimens used in the test are mortar bars of sizes $25 \times 25 \times 285$ mm. According to the ASTM C1260 (ASTM, 1994), the original mortar bar test to detect the alkali-silica reactivity, the mortar bars are subjected to soaking period in the sodium hydroxide (NaOH) solution at 80℃ for 14 days. The expansion results after 14 days of the mortar bars were then used to check whether or not the aggregates have ASR potential.

This mortar bar test was then later modified by many researchers to be used as means to evaluate the expansion results caused by the iron sulfide oxidation (El-Mosallamy & Shehata, 2020; Guirguis & Shehata, 2017; Rodrigues et al., 2015). The researchers varied the parameters that were believed to affect the rate of iron sulfide oxidation, including sizes of aggregates, types of iron sulfide, %relative humidity (%RH), ambient temperature, submerging solution during the soaking period, etc. Also, they introduced the wet-dry cycles to the tested mortar bars. Wet cycle refers to the period when the mortar bars are soaked in a solution. On the other hand, dry cycle refers

to the period when the mortar bars are not soaked in any solutions. Some researchers (Rodrigues et al., 2015; Guirguis & Shehata, 2017; El-Mosallamy & Shehata, 2020) conducted experiments in which they divided the test program into 2 phases; the phase promoting iron sulfide oxidation and the phase promoting secondary ettringite or thaumasite formation. Still no any studies have come up with the best test conditions that include all the possible parameters that affect the iron sulfide oxidation and can be promoted for application onsite. Listed below are literature reviews of some of the main measurable parameters that affect the iron sulfide oxidation.

2.4.1 Measurable parameters affecting iron sulfide oxidation

2.4.1.1 Effects of size of aggregates

Saengsoy, Yongchaitrakul, Sinlapasertsakulwong and Tangtermsirikul (2021) conducted an experiment on mortar bars made from two different ranges of aggregate size to study the effect of size of aggregates on the iron sulfide oxidation. The accelerated mortar bar test, which was modified from ASTM C1260, was used to accelerate the oxidation, and the length changes of the mortar bars were used to evaluate the expansion. The aggregate size ranges used in the study were 0.15 to 4.75 mm and 2.36 to 4.75 mm. Two types of reactive aggregates were used; Pyrite and Pyrrhotite minerals. The test was conducted with 4 wet-dry cycles/ 2 weeks in which dry cycle was set at 50 ℃. After 35 days of the experiment, the results showed that the mortar bars with aggregates of sizes between 0.15 to 4.75 mm expanded more than the mortar bars with aggregates of sizes between 2.36 to 4.75 mm (Figure 2.7). This same trend was observed in both specimens with Pyrite and Pyrrhotite minerals. This reasons can be due to the increase in surface area when a smaller aggregate size range was used. Therefore, higher degree of iron sulfide oxidation takes place, which yields more expansion.
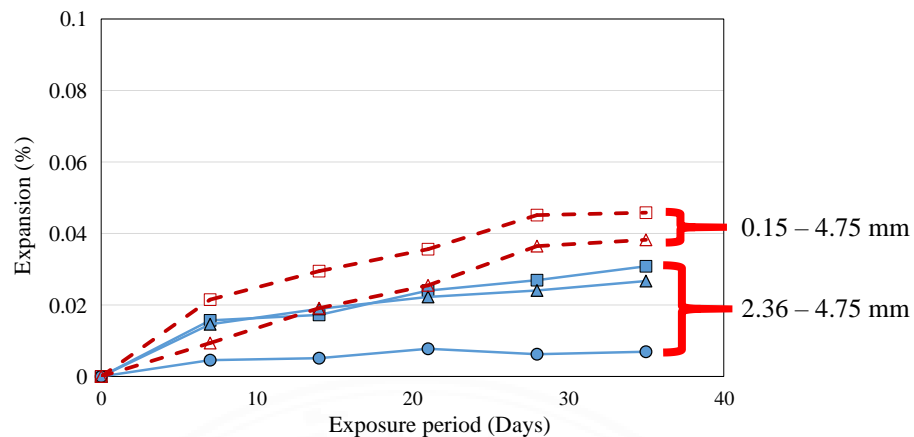
Figure 2.7 Effects of size of aggregates on expansion (Saengsoy et al., 2021)

2.4.1.2 Effects of storing relative humidity (%)

Rodrigues, Duchesne and Fournier (2015) carried out a laboratory test which was aimed to reproduce the deterioration of concrete due to iron sulfide oxidation occurred in Quebec, Canada. The experiment was conducted through the accelerated mortar bar test method which was based on the standard mortar bar test method for alkali-silica reactivity (ASR), ASTM C1260. The test evaluation was done based on the expansion of the mortar bars. The mortar bars used for the study were made up of iron sulfide-containing aggregates that caused the deterioration in Quebec, Canada. They came up with 2 values of %relative humidity (%RH); 60% and 80%. The test was carried out with 2 wet-dry cycles/ 1 week, the specimens were soaked in 6% sodium hypochlorite solution, and kept at 80 ℃ for dry cycle for over 120 days. From the results (Figure 2.8), even though the two test values of % relative humidity gave a very similar results, with 80%RH, the specimens expanded more than 60%RH.

2.4.1.3 Effects of storing temperature

Temperature is another parameter that many studies mentioned that it has effect on the iron sulfide oxidation (Rodrigues et al., 2015). The rate of reaction of iron sulfide oxidation increases with the increase in temperature. Saengsoy, Yongchaitrakul, Sinlapasertsakulwong and Tangtermsirikul (2021) conducted accelerated mortar bar test to find whether or not the higher temperature would yield higher iron sulfide oxidation rate. He did the test on three different storing temperatures (during the dry

cycle); 50, 60, and 80℃. The test, when conducted with mortar bars made with iron sulfide minerals, showed that at 50℃ and 60℃, the expansion rate were very similar where at 50℃, mortar bars showed slightly lower expansion than at 60℃ (Figure 2.9). At 80℃, the mortar bars initially expanded at the same degree as the mortar bars subjected to 50℃ and 60℃, however, the expansion dropped after 5 days and became constant from 20 to 35 days. This drop in expansion at 80℃ may be due to the fact that the ettringite becomes unstable when the temperature is higher than 70℃ (Fridrichová et al., 2016). Therefore, from this results, high temperature accelerated the iron sulfide oxidation. However, the temperature should not exceed 70℃, otherwise the ettringite will become unstable and the condition for iron sulfide oxidation is not well reproduced.
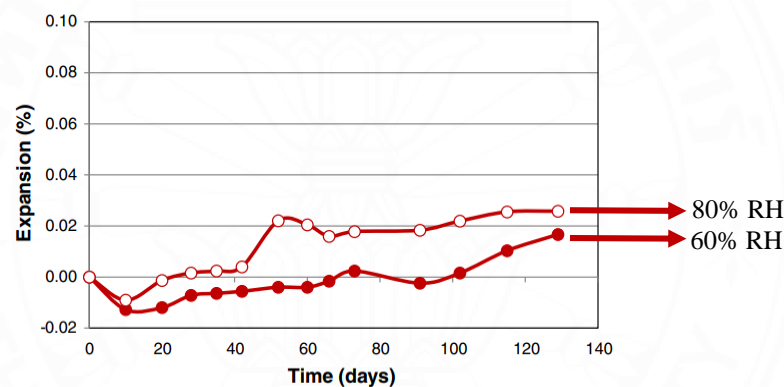
Figure 2.8 Effects of storing % relative humidity on expansion (Rodrigues et al., 2015)
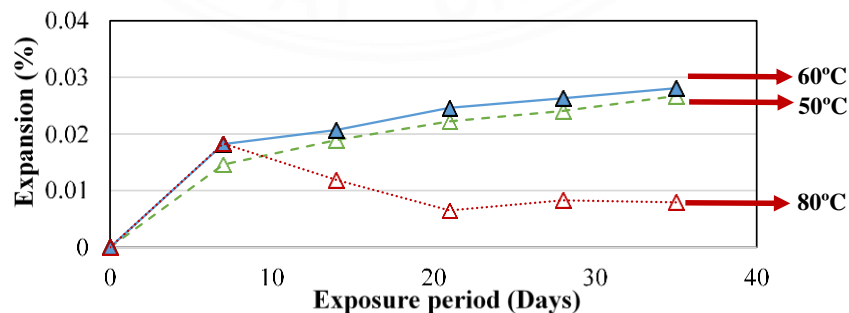
Figure 2.9 Effects of storing temperature on expansion (Saengsoy et al., 2021)

2.4.1.4 Effects of submerging solution

Sinlapasertsakulwong (2019) also studied the effects of submerging solution used in the accelerated mortar bar test to find the most suitable condition that would best promote the deterioration of concrete due to iron sulfide oxidation as occurred onsite. Two oxidizing agents were used to accelerate the mortar bar test. They were hydrogen peroxide (H_2O_2) and sodium hypochlorite or bleach solution (NaOCl). The solutions of 3% hydrogen peroxide and 6% sodium hypochlorite were prepared. Mortar bars were also subjected to another test condition which was without submerging in any solution. From the experimental results (Figure 2.10), sodium hypochlorite gave a more effective result than 3% hydrogen peroxide. This is due to the reason that hydrogen peroxide has a lower pH than that of sodium hypochlorite. This means that hydrogen peroxide is more susceptible to lose its oxidizing power than sodium hypochlorite. Therefore, sodium hypochlorite was selected to be a better condition to promote condition for iron sulfide oxidation.
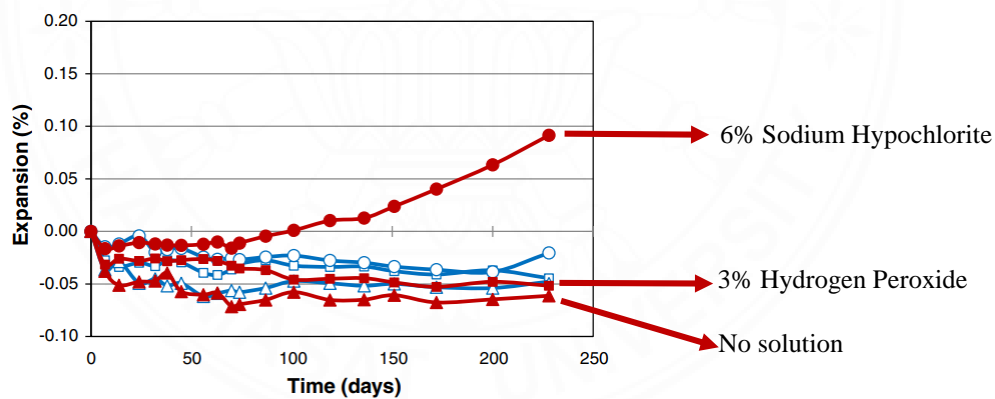
Figure 2.10 Effects of submerging solution on expansion (Sinlapasertsakulwong, 2019)

2.4.1.5 Effects of numbers of wet-dry cycles

To accelerate the mortar bar test, the numbers of wet-dry cycles can also be considered as one of the parameters. Therefore, Saengsoy, Yongchaitrakul, Sinlapasertsakulwong and Tangtermsirikul (2021) carried out the mortar bar test to study between two different numbers of wet-dry cycles; 4 cycles/ 2 weeks and 7 cycles/ 2 weeks. The test conditions were applied to mortar bars made using different types of

aggregates, which are iron sulfide-contaminated aggregates, reactive aggregates (Pyrite and Pyrrhotite minerals), and non-reactive aggregates. The results after 35 days showed that, for all types of aggregates, the same trend was shown. With 7 cycles/ 2 weeks, the expansion of the mortar bars was higher than the 4 cycles/ 2 weeks condition (Figure 2.11).
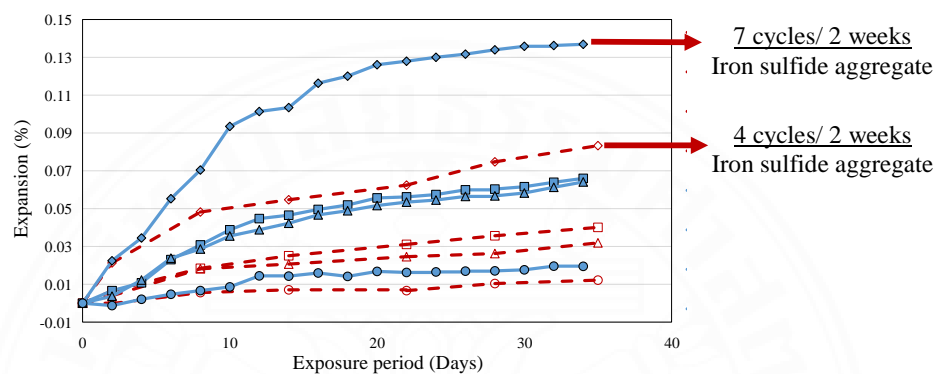
Figure 2.11 Effects of numbers of wet-dry cycles on expansion (Saengsoy et al., 2021)

2.4.1.6 Effects of types of iron sulfide minerals

As mentioned in the literature review of the iron sulfide minerals, there are many kinds of iron sulfide minerals in nature. Therefore, the rate of reaction of iron sulfide oxidation may be different according to types of iron sulfide. Sinlapasertsakulwong (2019) conducted accelerated mortar bar test to find the iron sulfide minerals that could accelerate the mortar bar test due to iron sulfide oxidation. The aggregates studied in the experiment were iron sulfide-containing aggregates, reactive aggregates (Pyrite and Pyrrhotite minerals), and non-reactive aggregates. All the mortar bars made using these different types of aggregates were subjected to the same test conditions. The non-reactive aggregate was used as the control specimen. After 35 days, the test results showed that mortar bars with Pyrrhotite expanded slightly higher than mortar bars with Pyrite (Figure 2.12). This is due to the reactivity of Pyrrhotite which is higher than Pyrite. Surprisingly, the iron sulfide-containing aggregates, which were the rocks contaminated with iron sulfide minerals showed the highest expansion, which was double the expansion of mortar bars with Pyrrhotite. The

assumption was made that it may be due to the scattered small particles of iron sulfide in the aggregates. This characteristic gave higher specific surface area for the iron sulfide oxidation to take place, therefore, it showed the maximum expansion among all types of aggregates.
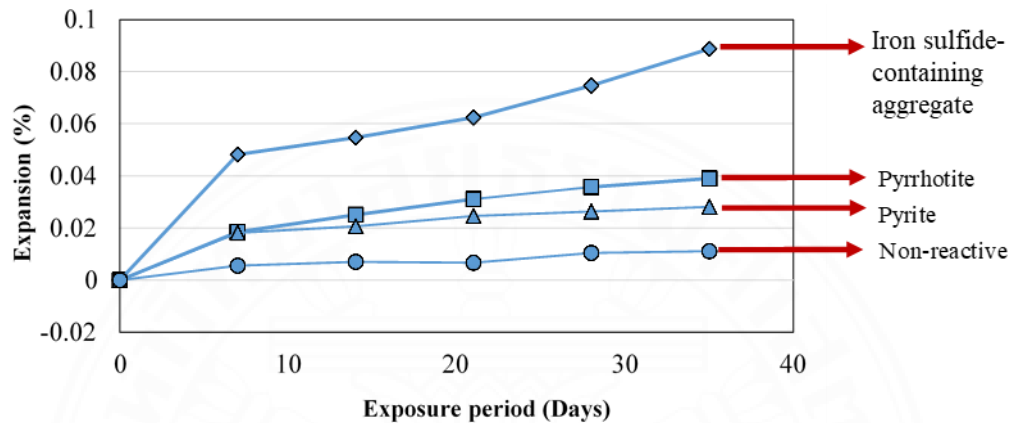
Figure 2.12 Effects of types of iron sulfide minerals on expansion

(Sinlapasertsakulwong, 2019)

2.5 Design of proper mix proportion

Guirguis et al. (2018) studied about the mix proportion that would reduce the damage caused by iron sulfide oxidation by using the accelerated mortar bar test proposed by Rodrigues, Duchesne and Fournier (2015). The test was done using different types of aggregates, both iron sulfide reactive and non-reactive aggregates. Many test conditions were varied such as the type of cements, type of cement replacing materials, water to cement ratio, and soaking period. Each of which has the effect on the properties of concrete.

2.5.1 Effects of types of cement

There are many cement types available in the construction industry for different purposes. From a study of Guirguis et al. (2018), when the cement type is changed from the GU Portland cement to low heat of hydration Portland cement (Figure 2.13), the expansion is reduced to half of its original expansion. And when compare the expansion of mortar bars made with ordinary Portland cement with high sulfate-resisting Portland cement, an even higher reduction of expansion is shown (Figure 2.14). Therefore, both

low heat and high sulfate-resisting Portland cement were able to reduce the expansion due to iron sulfide oxidation.
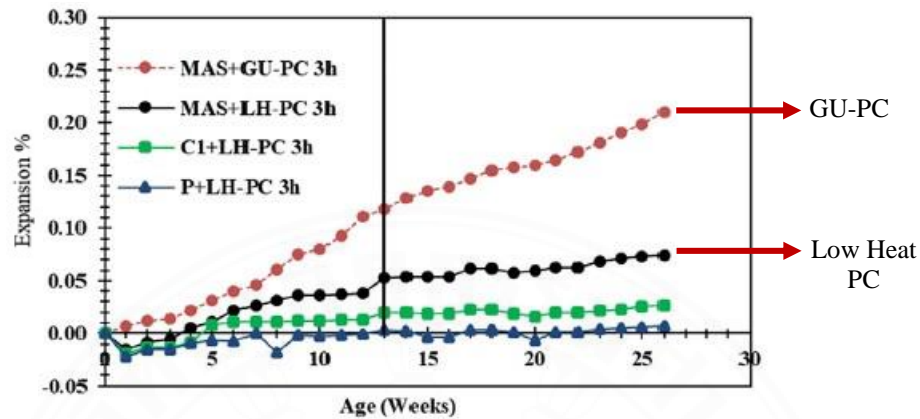
Figure 2.13 Effects of types of cement on expansion (low heat of hydration Portland cement) (Guirguis et al., 2018)
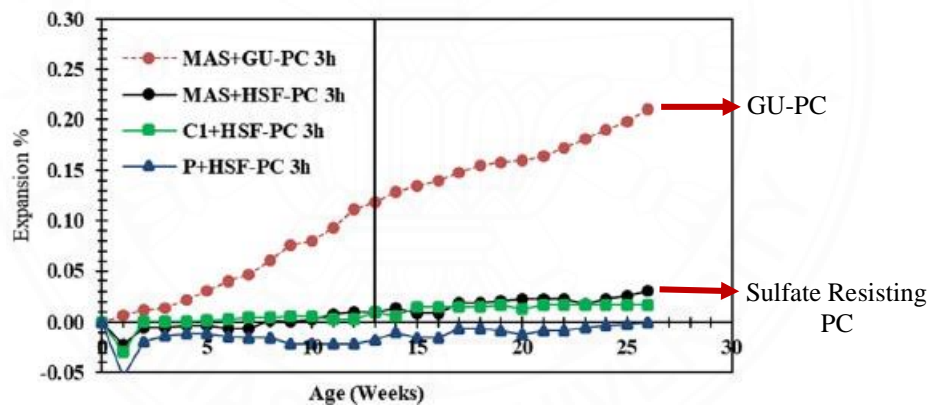
Figure 2.14 Effects of types of cement on expansion (high sulfate-resisting Portland cement) (Guirguis et al., 2018)

2.5.2 Effects of types of cement replacing materials

Many types of cement replacing materials are available in the construction industry. They are used to enhance the performance of the concrete. Each type provides different concrete properties. With specimens that were made using iron sulfide-containing aggregates, from the study of El-Mosallamy and Shehata (2020), when slag was added to the GU Portland cement, a great reduction of the expansion can be seen when compared to the mixture of GU Portland cement only (Figure 2.15). While adding

the low calcium fly ash to the cementing system, the more significant reduction of expansion is observed.

However, when metakaolin was used as a cement replacing materials in the study, the adverse expansion was observed. The slightly higher expansion than the GU Portland cement of mixture with metakaolin is shown (Figure 2.15).
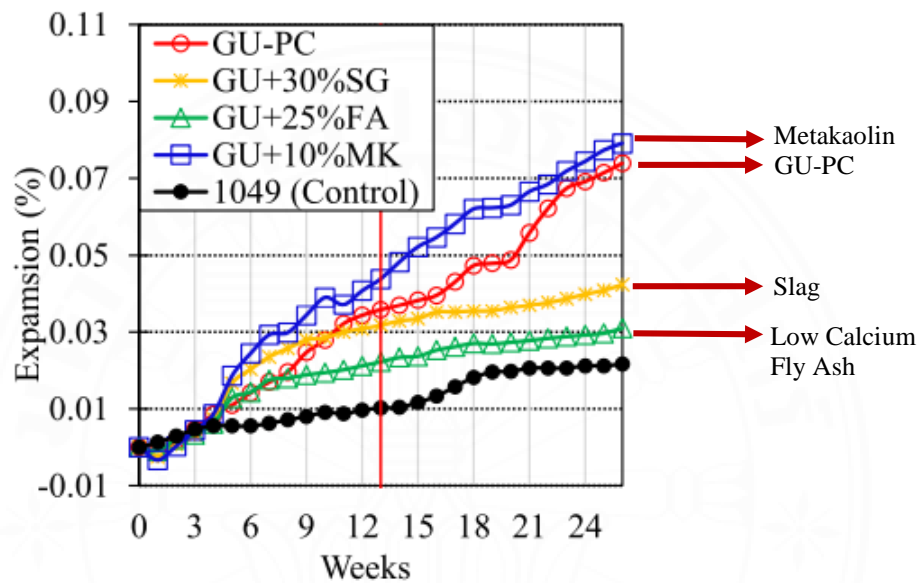
Figure 2.15 Effects of types of cement replacing materials on expansion due to iron sulfide oxidation (El-Mosallamy & Shehata, 2020)

According to Guirguis et al. (2018) and El-Mosallamy and Shehata (2020), it can be concluded that the 2 main factors that contribute to the reduction of the mortar bar expansion are the use of cement replacing materials and the cement types in cementitious systems. The expansion was reduced by up to 80% by adjusting these 2 factors. The mechanism behind this reduction is that the studied cement replacing materials minimize the pore structure of the mortars, therefore, the penetration of the oxidizing solution into the mortars is reduced. In other words, the cement replacing material makes the concrete denser, so it is harder to expand. Since oxygen and water, which are the main components for the iron sulfide oxidation cannot penetrate to inner part of the concrete. Another mechanism is the lower amount of $Ca(OH)_2$ in the system when cement replacing materials are used and the lower amount of C_3A in the system when low heat Portland cement is used. However, not every type of cement replacing

materials are able to reduce the expansion due to iron sulfide oxidation, for instance, metakaolin. This great expansion of metakaolin was due to the high amount of alumina presents in metakaolin. Refer to Eq. 1.6, alumina is a reactant in the production of secondary ettringite. Therefore, the higher amount of reactive alumina yields more amount of expansive secondary ettringite.

2.6 Cement replacing materials

The production of cement produces massive emission of CO_2. Recently, people have becoming aware of the environment and global warming. Many countries and sectors aim to reduce the CO_2 emission. Therefore, the use of substituting materials to partially replace Portland cement has been researched and studied over decades. The materials should be able to enhance or improve concrete performances in some ways, but not lowering the concrete performance when compared to the cement only mixture. These materials are called as cement replacing materials (CRMs) or supplementary cementitious materials (SCMs) in some studies. (For this thesis, the word cement replacing materials (CRMs) will be used for this definition throughout the entire thesis.) The term 'pozzolanic materials' is sometimes used. Pozzolanic materials are any materials that possess the ability to harden in water when they are mixed with calcium hydroxide (CH) or any substances that can release calcium hydroxide (such as Portland cement). Natural pozzolanic materials are the ones that can be used just after grinding. While artificial pozzolanic materials are the materials that require additional treatment for their chemical and/ or structural modification to obtain stronger pozzolanic properties. Some examples of artificial pozzolanic materials are fly ash, silica fume, calcined clay, blast furnace slag, etc. (McCarthy & Dyer, 2019).

2.6.1 Fly ash

Fly ash is a by-product from the burning of coal in power plants to generate electricity. When coal is being burnt, an extremely high temperature is used at 400-500℃. Most of the minerals from coal are melted. The by-product that is heavy sink to the bottom and is called bottom ash. While the one that is light is floated and being captured by the precipitator. The particles are then cooled down suddenly, results in

spherical and smooth-surface fly ash. Figure 2.16 illustrates the process of fly ash production in power plant.
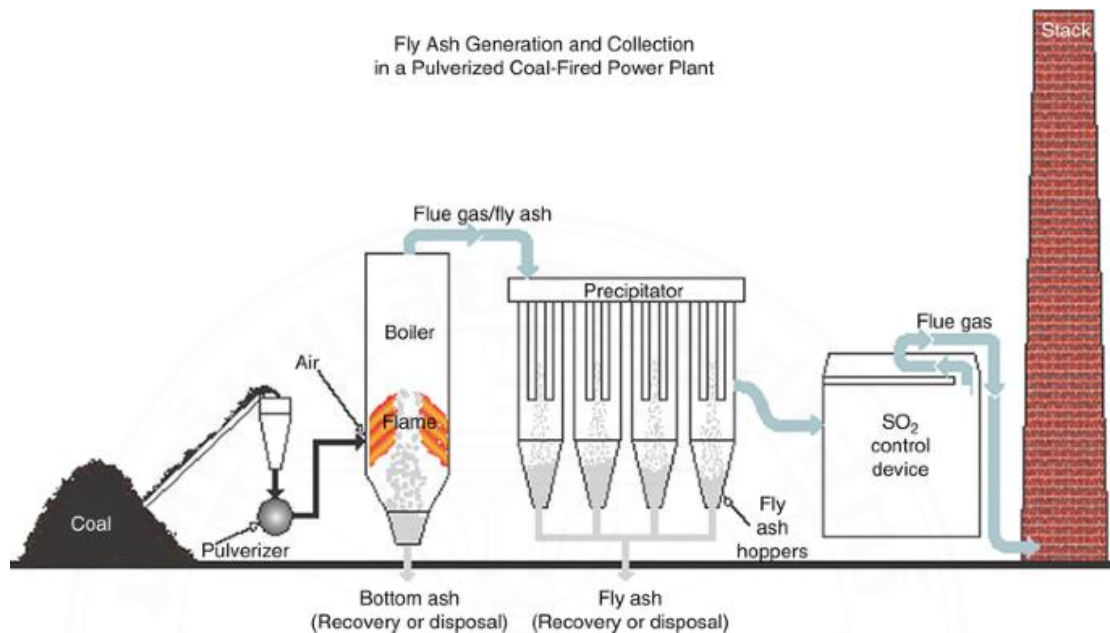
Figure 2.16 Fly ash production in coal thermal power plants (Chou, 2012)

Production of fly ash has been recognized for around 100 years in United States. The usage of fly ash is various such as landfill, blending in concrete, used as fine aggregates, etc. The chemical compositions of fly ash prescribes its application. Fly ash is categorized into two classes which are Class C and Class F fly ashes based on its chemical compositions according to ASTM C 618, which is a standard published in United States (ASTM, 2017). Type of coal that is used in power plants is also one of the factors that distinguish the class of fly ash since different types of coals contain different amount of major oxides. Other factors are the burning process and by-product collecting systems used in the power plants. Class F fly ash or siliceous fly ash is known to have high amount of Silica (SiO_2), Alumina (Al_2O_3), and Iron (Fe_2O_3), in which the summation of these three oxides is greater than 70%. On the other hand, Class C fly ash or calcareous fly ash contains the summation of the three oxides greater than 50% (McCarthy & Dyer, 2019). Class C fly ash contains high amount of calcium content (CaO), while Class F is low CaO fly ash (Nguyen et al., 2019). Europe also has its own standard for the types of fly ash as in BS EN 450-1: Fly ash for concrete (BS EN 450-

1:2012). These standard fly ashes are blended in concrete as pozzolanic materials (Ahmarazzanman, 2000; Nguyen et al., 2019; Poon et al., 2016; Rashad, 2015). The fly ash that does not meet the requirement is then used mainly for landfill and is rarely used in concrete production, such as fly ashes with high amount of calcium (CaO), free lime, and SO_3 contents (Kaewmanee et al., 2013; Nawaz et al., 2016; Nguyen et al., 2019).

In Thailand, TIS 2135 is used as a standard for fly ash. Fly ash is classified into Class 1, Class 2a and Class 2b, and Class 3. Class 2a fly ash contains low amount of CaO and Class 2b fly ash has high amount of CaO (Thai Industrial Standards, 2002). There are two main fly ash sources. First source is Mae Moh power plant in Lampang province (in the North of Thailand). The fly ash obtained from this source is found to have high content of SO_3 and CaO. Fly ash from in Mae Moh is the main source of fly ash used in Thailand, where it produces up to 80-85% of the available fly ash in Thailand. The other source is BLCP power plant in Rayong province (in the East of Thailand). The fly ash produced from here contains relatively lower amount of SO_3 and CaO than that of fly ash from Mae Moh power plant. BLCP power plant contributes about 15% of fly ash supplied in Thailand (Tangtermsirikul, 2005). Other fly ashes that does not meet the TIS 2135 standard are called as substandard fly ashes (Nguyen et al., 2019). There have been many studies carried out to study these substandard fly ashes behavior in concrete and to utilize them in concrete production (Kaewmanee et al., 2013; Nawaz et al., 2016)

Fly ash that is blended in cement is considered as one of the pozzolanic materials that possesses pozzolanic behavior. Fly ash has high amount of silica (40-60%) and alumina (20-30%) as it contains amorphous aluminosilicates that will later react with calcium hydroxide from cement hydration to form gel-like substance, calcium-silicate hydrate (CSH) (Kasaniya et al., 2021). As mentioned above, chemical compositions of fly ash depend on the coal and the techniques used to burn coal in power plants. Therefore, many studies have been done to explore the advantages and disadvantages of different types of fly ashes. Kaewmanee et al. (2013), Nawaz et al. (2016) and Visvalingam et al. (2022) studied fly ash with high amount of free lime (free CaO) content on durability properties. It was found that fly ash with high amount of free lime content showed faster setting and higher compressive strength. While expansions due to autoclave and alkali-aggregate reaction were higher than fly ash with

normal amount of free lime, but were better than cement-only mixture. Shrinkage was lower than cement-only mixture and normal consistency, water requirement of mixtures, carbonation depth, chloride and sulfate resistances show no significant differences from fly ash with normal amount of free lime (Kaewmanee et al., 2013). Fly ash with high free lime and/or SO_3 contents cause higher sulfate expansion than fly ash with normal free lime and SO_3 contents. The water-to-binder ratio (w/b) also plays a major role. As the w/b increases, the sulfate expansion increases (Visvalingam et al., 2022). Fly ash enhances the paste resistance against sulfuric acid attack, especially when fly ash with low amount of CaO is used (Wanna et al., 2021). In the research field of iron sulfide-contaminated aggregates, Guirguis et al. (2018) reported that fly ash with low amount of calcium enhances the resistance of expansion due to iron sulfide oxidation reaction. The expansion of low calcium fly ash was lower than GU Portland cement-only mixture. Same trend was found in the study of El-Mosallamy and Shehata (2020) that low calcium fly ash reduced the expansion due to iron sulfide-contaminated aggregates.

When fly ash is used as a fine aggregate replacement in concrete, it is found that fly ash improves the concrete density. The permeability resistance of the concrete increases. The voids between the cement particles are filled by the CSH gel which has been formed during the pozzolanic reaction and filler effect of fly ash. The reduction in pore size started after 7 days since the hydration products needed in pozzolanic reaction ($Ca(OH)_2$) is available after some times. The effective period for modification of pore structure is after 14 days. This result is fully exhibited after 28 days due to slow pozzolanic reaction of fly ash. The pozzolanic reaction can only take place after the hydration reaction of cement has started. With the use of fly ash in the mixture, it resulted in a denser concrete structure and finer concrete pore structure in which it inhibited the penetration of water and oxygen into inner part of the concrete. However, the modification of the pore refinement with the use of fly ash only occurs after early age of concrete. The addition of limestone powder in the fly ash concrete is also reported to able to aid the early age strength of concrete (Dhandapani et al., 2018).

2.6.2 Calcined clay

Calcined clay is known for its orange-brown color. The term calcination means an action of heating or the thermal treatment of solid materials. Therefore, calcined clay is a clay that has been heated before being used (in concrete production). The clay used to make calcined clay can be found easily and is abundant especially in the areas near the earth's equator (Scrivener et al., 2018). These clay contains clay minerals and is found to have high amount of silica and alumina. In order to use this material, the clay is burnt under a certain range of temperature, which is in between 600-900℃. This heating condition destroys the crystalline network of the clay mineral, making it becomes reactive and gains pozzolanic activity (Argin & Uzal, 2021; Scrivener et al., 2018). The pozzolanic activity of calcined clay depends on the clay minerals in original clay and the heating condition used. After clay is burnt, silica and alumina becomes unstable and is in amorphous state. After the thermal treatment, the calcined clay is ground into fine particles. The specific surface area of calcined clay particles also found to affect the performance of concrete. One of the common burnt clay being used in the concrete production is metakaolin. It was found to be used since 1990s. Metakaolin is made from burning kaolin at temperature in between 650 to 800℃. Clay with 85-90% of kaolin is known for providing improvement of concrete performance. The reactivity of produced metakaolin depends on the crystallinity of the mineral called kaolinite and degree of dihydroxylation gained. The more well-ordered the crystallinity is, the less reactive the clay will be (McCarthy & Dyer, 2019).

Many researchers have come up with the use of blending between calcined clay and limestone powder. It is commonly known as Limestone calcined clay (LC[3]). A study on concrete mixture containing limestone calcined clay showed that the pore structure of the concrete became significantly finer and smaller in diameter at early age. It even showed a finer pore structure than the use of fly ash replacement in concrete. This is due to the combination of the pozzolanic and filler effects of the limestone calcined clay. Calcined clay has smaller particle size than fly ash, so it reacts faster and gives higher mechanical performance at early age. It also has higher reactivity at early age than fly ash. The outstanding advantage of using limestone calcined clay in cementitious system is the high degree of pore refinement it gives. This strong point is

obtained due to the kaolinite content in the calcined clay. The higher content of kaolinite content, the higher degree of pore refinement of the concrete.
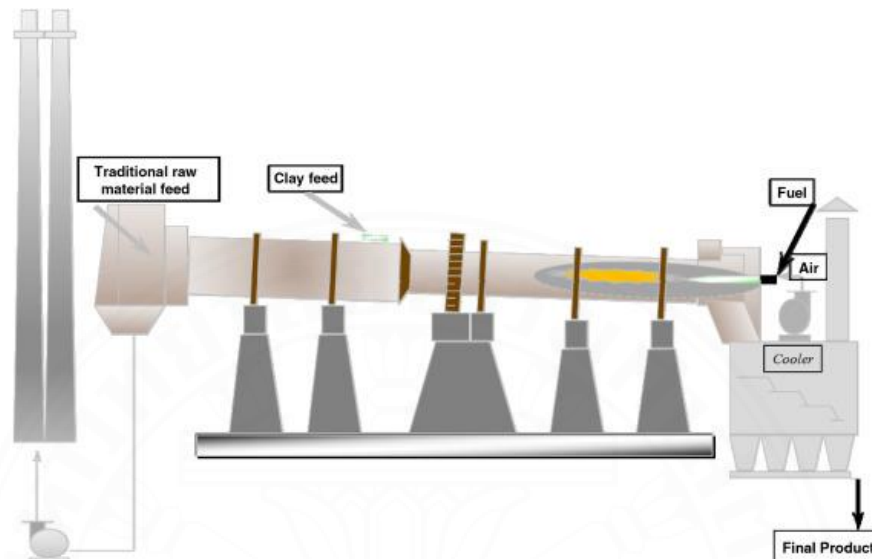
Figure 2.17 Calcined clay production (Almenares et al., 2017)

This kaolinite content also influence the mechanical properties of concrete. In contrast to fly ash system, the limestone calcined clay system has an earlier pore refinement which occurs in early age stage (Dhandapani & Santhanam, 2017).

2.6.3 Limestone powder

Limestone powder is used widely in many countries, such as Canada, China, United States, and Europe. It is widely available and low cost (McCarthy & Dyer, 2019). Limestone powder is a by-product obtained from limestone quarry. Bessey (1938) found that calcium carbonate ($CaCO_3$) can react with calcium aluminate hydrates (or alumina) in cement to form calcium carboaluminate. The American standard, ASTM C 595 (2012) allows the content of limestone up to 15% in Portland-limestone cement. Many research reported that limestone powder enhanced the concrete performance with its filling, cement dilution, and nucleation effects. This is mainly due to its particle size, dissolution rate, polymorphous structures, etc. (Wang et al., 2018). Limestone powder stands out for its filler effect that gives denser structure to concrete. Limestone powder improves concrete in various aspects either it is used as

cement replacing material or fine aggregate. Limestone powder reduces setting time and total shrinkage of concrete. It enhances concrete mechanical properties such as compressive strength, elastic modulus, and flexural strength. However, in order to obtain these results, the limestone powder has to be used in proper amount and particle size. It was reported that when coarse or too fine particles of limestone powder was used, the setting time of concrete is increased and less CSH and calcium hydroxide (CH) were formed. Limestone powder was reported causing good performance on sulfate resistance. This is due to the dilution effect by limestone powder replacement. With limestone powder replacement, the amount of C_3S, C_2S and C_3A decreased therefore, the produced gypsum and ettringite also reduced (Sezer, 2012).

2.6.4 Silica fume

Silica fume, another pozzolan, is commonly used to replace cement in concrete mixtures. Silica fume is also a by-product, the same as fly ash. It is obtained from production of silicon metal or ferrosilicon (FeSi) alloys or simply the process of melting silicon. When SiO_2 gas comes in contact with the air above the furnace in which the temperature is a lot lower, it rapidly oxidizes and condenses as amorphous SiO_2 and form silica smoke (Uzbas & Aydin, 2020; Yeginobali, 2009).

Silica fume is known to have extremely fine particles. This makes it a great filler in the concrete. With increase in surface area, it yields additional pozzolanic reaction. It can be used as a cement replacing material or additive for concrete. It has been commonly reported appropriate for producing high strength concrete. It also improves concrete properties including reducing shrinkage, increasing compressive, tensile and flexural strengths, and elastic modulus (Nochaiya et al., 2010). Shehata and Thomas (2002) reported that silica fume concrete showed low alkalinity in its pore solution at early age. During pozzolanic reaction, it also consumes more amount of calcium hydroxide than fly ash and produces calcium silicate hydrate (CSH). This is because it contains high silica content and has extremely fine particles. These fine particles were found to aid the refining of pore structures of the cement paste making its microstructure denser (Kurt et al., 2016; Muller et al., 2015; Uzbas & Aydin, 2020). Silica fume is commonly used to replace cement at the amount of 5-10% for good improvement of concrete performance.
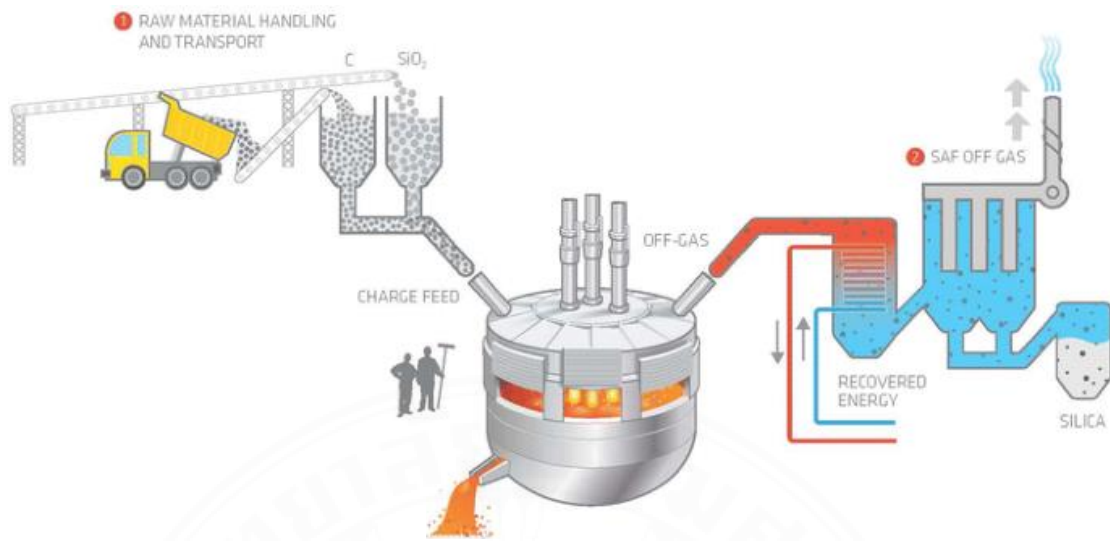
Figure 2.18 Silica fume production (Amin et al., 2022)

CHAPTER 3

METHODOLOGY

3.1 Materials

Materials that were used in this study are shown by the diagram in Figure 3.1. The experimental programs involve experimental tests and microstructural tests. Mortar bars were used for the experimental tests and microstructural tests including XRD and SEM, while microstructural tests of MIP and TGA/ DTG were performed using paste.
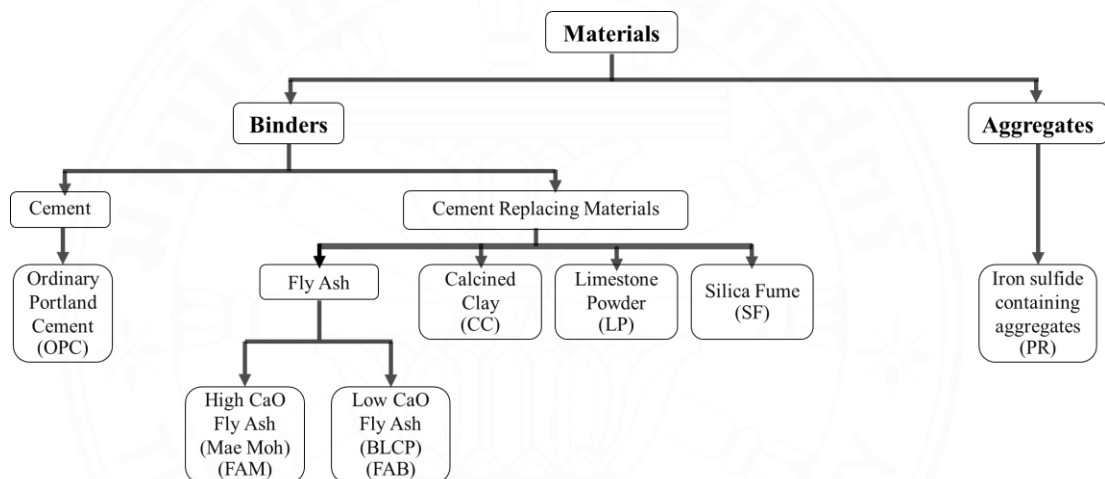
Figure 3.1 Diagram showing the materials used in the study

3.1.1 Binders

The binders that were used in the experiment are separated into 2 types; cement and cement replacing materials.

3.1.1.1 Cement

Ordinary Portland cement (OPC Type I) is the only type of cement that was used. The OPC was from Siam Cement Group (SCG) Public Company Limited of Thailand.

3.1.1.2 Cement replacing materials

Five types of cement replacing materials were used. The first type is Mae Moh fly ash (FAM) from Mae Moh power plant, Lampang province (in the North of Thailand), which has high CaO and SO_3 contents. The second type is BLCP fly ash (FAB) from BLCP power plant, Rayong province (in the East of Thailand), which has low CaO and SO_3 contents. The third type is calcined clay (CC). The fourth type is limestone powder (LP). Calcined clay and limestone powder were received from Siam Research and Innovation (SRI) of Siam Cement Group (SCG) Public Company Limited. The last type is silica fume (SF) from China. Particle morphology of all binders are shown in Figure 3.2(a-e). The chemical and mineral compositions and physical properties of all type of binders are presented in Table 3.1, Table 3.3 and Table 3.5, respectively.
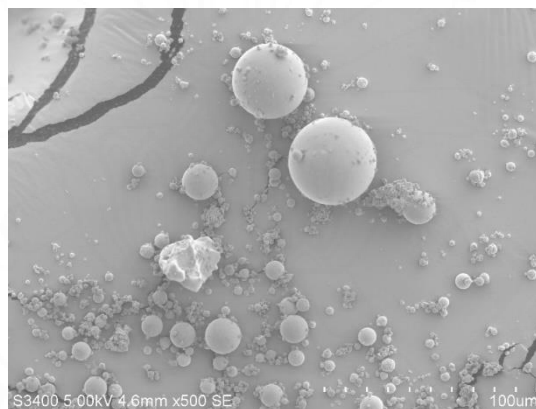
(a) Mae Moh Fly ash (FAM)
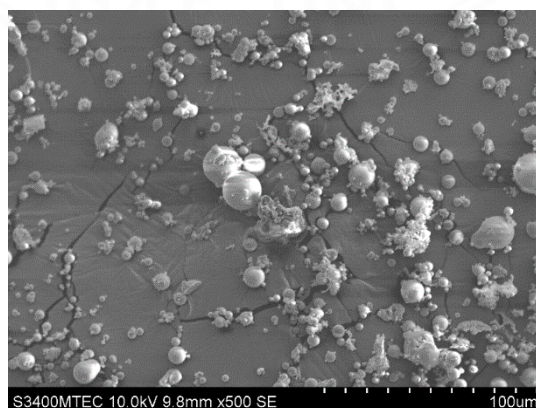
(b) BLCP Fly ash (FAB)
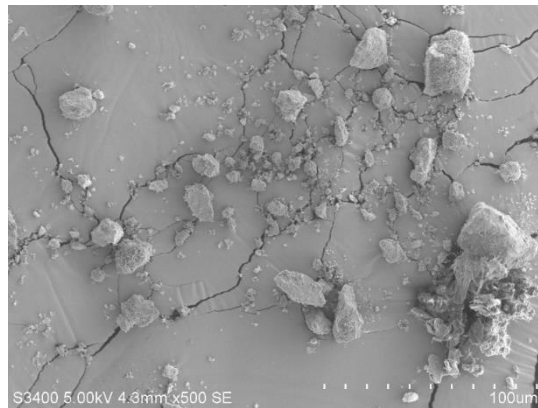
(c) Calcined clay (CC)
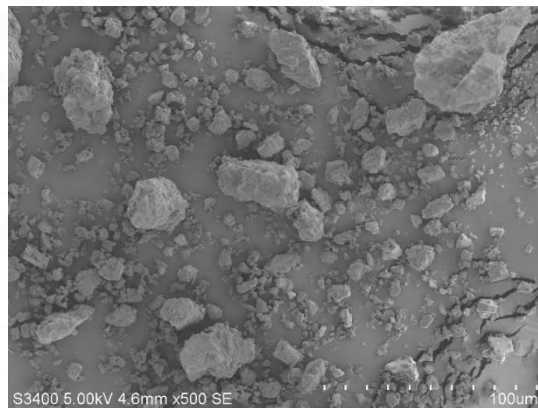
(d) Limestone powder (LP)
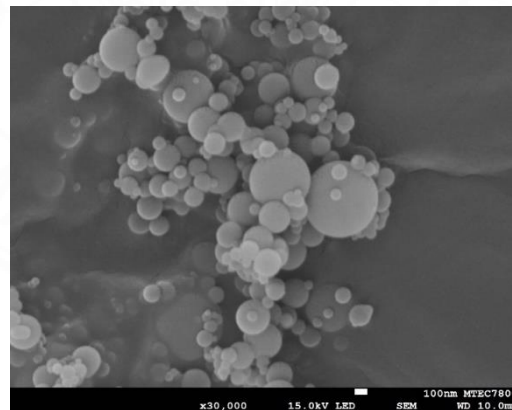
(e) Silica fume (SF)

Figure 3.2 Particle morphology of the binders used in the study

3.1.2 Aggregate

The iron sulfide-containing aggregates from China (Figure 3.3), which are the reactive aggregates were used. As seen from Table 3.2 the aggregates contain high amount of iron and sulfur; with Fe_2O_3 of 35.20% and SO_3 of 44.45%. Also the main

minerals found from XRD results of this iron sulfide-containing aggregates are Pyrite 22.56% and Pyrrhotite 2.15%. Only one range of aggregate's particle size was used, which is the size between 2.36 to 4.75 mm (passing through the sieve No.4 and retaining on the sieve No.8 – using sieves that follow ASTM and ISO standards). The oxide and mineral compositions of tested iron sulfide-containing aggregate are presented in Table 3.2 and Table 3.4, respectively.

Figure 3.3 Tested iron sulfide-containing aggregates (Saengsoy et al., 2021)

Table 3.1 Chemical compositions of the tested binders

Chemical Compositions (% by weight)	Binders					
	OPC	FAM	FAB	CC	LP	SF
SiO_2	18.93	32.94	61.46	46.75	0.79	93.81
Al_2O_3	5.51	16.68	20.27	24.97	0.42	0.24
Fe_2O_3	3.31	14.04	5.56	11.58	0.23	0.09
CaO	65.53	26.06	1.73	5.69	54.66	0.58
MgO	1.24	3.37	0.96	3.20	0.59	0.70
SO_3	2.88	2.67	0.28	0.04	0.00	0.37
Na_2O	0.15	1.78	0.73	1.25	0.02	-
K_2O	0.31	2.05	1.36	0.53	0.01	-
TiO_2	0.00	0.35	0.00	2.07	0.01	-
LOI	0.00	0.7	5.68	3.33	43.21	2.11
Free lime	1.60	2.36	0.07	-	-	-

Table 3.2 Chemical compositions of the tested iron sulfide-containing aggregate

Chemical Compositions (% by weight)	Iron sulfide-containing aggregate
SiO_2	10.40
Al_2O_3	2.28
Fe_2O_3	35.20
CaO	2.48
MgO	2.09
SO_3	44.45
MnO	0.02
Na_2O	0.87
K_2O	0.45
TiO_2	0.07
P_2O_3	0.02
CuO	0.05

Table 3.3 Mineral compositions of the tested binders

Mineral Compositions (% by weight)	Binders		
	FAM	FAB	CC
Quartz	2.07	15.47	1.43
Anhydrite	5.23	0.00	-
Albite	0.00	0.00	4.17
Lime	0.58	0.00	0.00
Portlandite	3.33	0.00	0.00
Periclase	0.33	0.00	0.00
Anatase	0.00	0.00	0.88
Diaoyudaoite	0.00	2.61	0.00
Hematite	1.29	0.32	13.29
Magnetite	2.21	1.04	0.00
Mullite	0.00	12.53	0.00
Anorthoclase	0.00	0.00	1.41
Amorphous	84.98	68.04	78.89

Table 3.4 Mineral compositions of the tested iron sulfide-containing aggregate

Mineral Compositions (% by weight)	Iron sulfide-containing aggregate
Quartz	1.87
Microcline	0.00
Albite	4.62
Muscovite	0.00
Gypsum	0.00
Calcite	2.80
Pyrite	22.56
Pyrrhotite	2.15
Siderite	2.92
Annite	3.03
Dolomite	0.00
Clinochlore	0.00
Phlogopite	0.00
Talc	0.00
Amorphous	60.06

Table 3.5 Physical properties of the tested binders

Physical Properties	Binders					
	OPC	FAM	FAB	CC	LP	SF
Specific Gravity	3.15	2.57	2.17	2.67	2.70	2.25
Blaine's Fineness (cm^2/g)	3054	2254	2723	3196	5270	17,000
Median Particle Size (μm)	18.21	37.62	15.70	17.65	10.00	-

Remark: (-) = No information

3.2 Mix proportions

3.2.1 Mortars for modified accelerated mortar bar test

The water-to-binder ratio was 0.45. The ratio of aggregate-to-binder was 2.25 (based on the standard ASTM C1260). The replacement percentages were varied as shown in Table 3.6. Four binder systems were studied, which were single, binary, ternary, and quaternary systems. For binary binder system, high and low CaO fly ashes

were both used at 30% and 45% replacement, calcined clay was used at 45% replacement, and limestone powder and silica fume were used at 10% replacement. For ternary binder system, high and low CaO fly ashes were used with limestone powder together at 30% replacement, low CaO fly ash was used with silica fume together at 30% replacement, and calcined clay was used with limestone powder together at 45% replacement. For quaternary binder system, high and low CaO fly ashes were used with calcined clay and limestone powder together at 45% replacement. Remark that if calcined clay and limestone powder are used together, the ratio of calcined clay to limestone powder is always 2 to 1.

3.2.2 Pastes for MIP and TGA/DTG tests

The binder systems and replacement percentages for paste mixtures were varied to be the same as those in the mortars in section 3.2.1 and are shown in Table 3.6. The differences were that there was no aggregates used since the tests were performed on paste, and water-to-binder ratio of 0.3 was used for all paste mixtures.

Table 3.6 Tested mix proportions

Binder Systems	% r	Mix ID	Binders					
			OPC	FAM	FAB	CC	LP	SF
Single	0	OPC	1.00	-	-	-	-	-
2 binders (Binary)	10	LP10	0.90	-	-	-	0.10	-
		SF10	0.90	-	-	-	-	0.10
	30	FAM30	0.70	0.30	-	-	-	-
		FAB30	0.70	-	0.30	-	-	-
	45	FAM45	0.55	0.45	-	-	-	-
		FAB45	0.55	-	0.45	-	-	-
		CC45	0.55	-	-	0.45	-	-
3 binders (Ternary)	30	FAM20LP10	0.70	0.20	-	-	0.10	-
		FAB20LP10	0.70	-	0.20	-	0.10	-
		FAB20SF10	0.70	-	0.20	-	-	0.10
	45	CC30LP15	0.55	-	-	0.30	0.15	-
4 binders (Quaternary)	45	CC20LP10FAM15	0.55	0.15	-	0.20	0.10	-
		CC20LP10FAB15	0.55	-	0.15	0.20	0.10	-

Remark: %r is replacement percentage of the CRMs

3.3 Methodology

3.3.1 Mortars for modified accelerated mortar bar test

3.3.1.1 Preparation of mortar bars

Mortar bars were prepared with a water-to-binder ratio of 0.45 and a binder-to-aggregate ratio of 1:2.25 following ASTM C 1260. The iron sulfide-containing fine aggregates were sieved to obtain the sizes in between 2.36 to 4.75 mm, and were oven-dried before mixing. The mold sizes were $25 \times 25 \times 285$ mm. After the specimens were demolded, they were cured in water for 24 hours at room temperature (25°C).

3.3.1.2 Wet-dry cycle

After demolding, the mortar bars were submersed in water for 24 hours and air-dried for 1 hour. The mortar bars then entered the first dry cycle by being stored at 60°C with 80% relative humidity (RH). The relative humidity was maintained by placing water in the container that is used to store the mortar bars with a caution not to drop mortar bars in water. The mortar bars then entered the first wet cycle by being submersed in bleach solution of 6% NaOCl (sodium hypochlorite) for 3 hours and air-dried for 1 hour before storing again at 60°C with 80% RH. During the wet cycles, additional air was pumped in the container filled with 6% NaOCl solution to increase rate of iron sulfide oxidation. Figure 3.4 presents the steps of modified accelerated mortar bar test. The volume ratio of the 6% NaOCl solution to one mortar bar is 4 ± 0.5 to 1. The volume of one mortar bar was used as 184 ml following ASTM C 1260. The mortar bars were subjected to 7 wet–dry cycles per two weeks for (at least) 30 days.

3.3.1.3 Expansion Measurement

The mortar bar's length was measured using the length comparator after it was air-dried for 1 hour after the 3-hour submersion in 6% NaOCl solution. This length was later used in the calculation for the % expansion (Eq. (3.1)) after the end of each wet-dry cycle. The % expansion is the percentage of length change with respect to the initial length which was taken after the mortar bar was demolded (before being cured in water).

Expansion (%) = ((L(t) - L_0)/ L_0) ×100 (3.1)

where L(t) is length after test at each exposure period (millimeter), t is exposure period (days), and L_0 is initial length before test (millimeter).
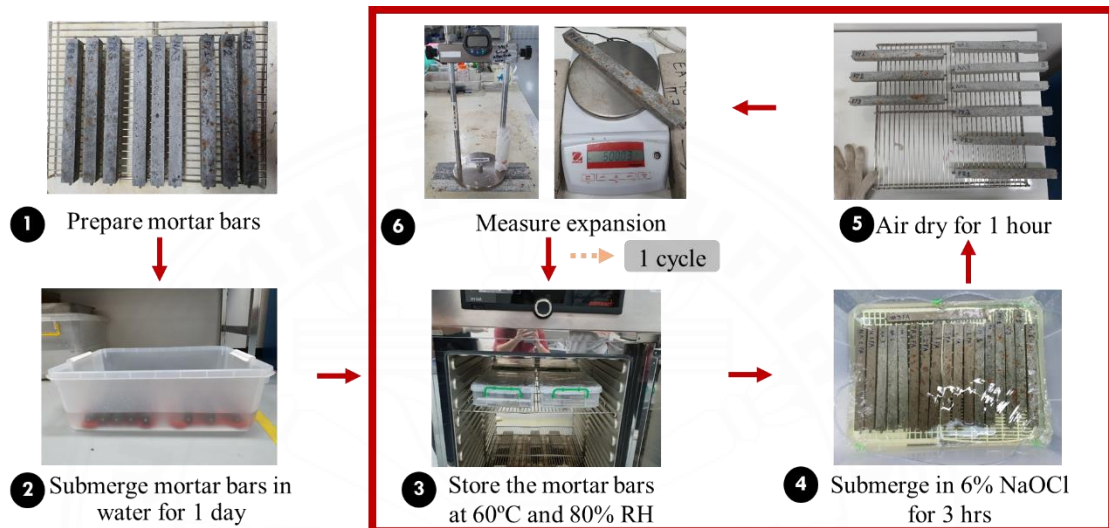
Figure 3.4 Steps of modified accelerated mortar bar test

Figure 3.5 Length comparator

3.3.1.4 Rust analysis

Due to iron sulfide that is present in the aggregates, the rust will be observed on the mortar bar surface. The images of rust stain were recorded using a digital camera. The images were taken after the mortar bars were subjected to 30 days of modified

accelerated mortar bar test (Figure 3.6). The surfaces on the two sides of each mortar bar were observed in the analysis. These two surfaces were considered to be best representing the rust staining from the experiment. Therefore, two surfaces were observed per one mortar bar. The final images of the mortar bar surfaces of all specimens were then analysed using an open-source software, ImageJ (Figure 3.7).

Figure 3.6 Image of mortar bar surface taken from the digital camera (32 days)

Firstly, the unit used in the analysis was set in the software. Then the area of rust stain on the surface was calculated. The total area of the mortar bar surface was also calculated and expressed as unit area (Figure 3.8). The degree of severity of rust occurred on the surface of each mix proportion was expressed in % rust area as shown in the below equation (Eq. 4.2). The results were then being compared using OPC mixture as reference.
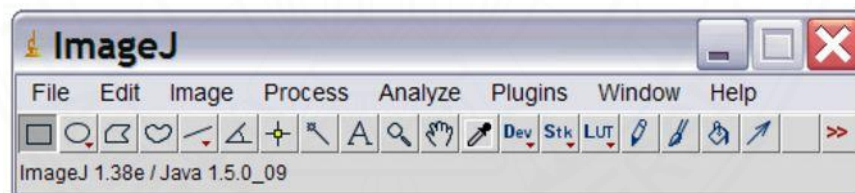
Figure 3.7 ImageJ software used for image analysis of rust
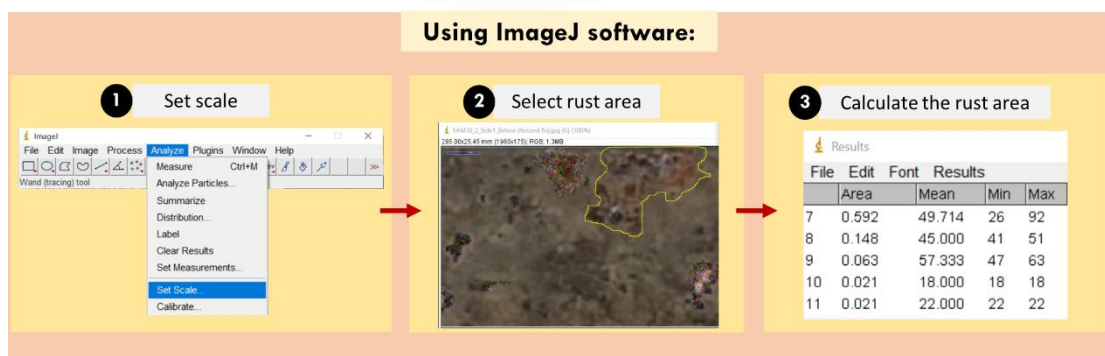
Figure 3.8 Steps of image analysis using ImageJ software

$$\text{Rust area (\%) of one mortar bar surface} = \frac{\text{Area of rust stain on the surface}}{\text{Total area of the mortar bar surface}} \times 100$$

(4.2)

3.3.2 Microstructural analysis

To understand the mechanisms of the effects of type of binders on the expansion and rust stain of mortar bars due to iron sulfide oxidation, microstructural analysis is necessary. The analysis provides both physical and chemical behavioral aspects of the studied mixtures. Four microstructural tests were done after the evaluations of expansion and rust stain had been done. They consisted of Scanning Electron Microscopy (SEM) and Energy Dispersive Spectroscopy (EDS), X-Ray Diffraction (XRD), Thermogravimetric Analysis (TGA), and Mercury Intrusion Porosimetry (MIP). SEM/EDS and XRD tests were conducted on mortar samples that had been exposed in modified accelerated mortar bar test. While MIP and TGA/DTG tests were done on water-cured paste mixtures at 28 days.

3.3.2.1 Preparation of Pastes

Pastes were prepared with a water-to-binder ratio of 0.30. (The mold sizes used were $50 \times 50 \times 50$ mm). After the specimens were demolded (Figure 3.9), they were cured in water at room temperature until reaching the satisfied sample age for microstructural tests. For TGA/ DTG and MIP tests, the test age of samples was 28 days.

Figure 3.9 Cement paste cube (after demolded) used for TGA/DTG and MIP tests

3.3.2.2 SEM (Scanning Electron Microscopy) and EDS (Energy Dispersive Spectroscopy)

SEM test was done to obtain the images of the hydrated products from the tested samples. With the mortar bars that had undergone the accelerated mortar bar test, they were cut into $1 \times 1 \times 1$ cm^3 cubes. After stopping hydration process, which included the submersion in acetone (C_3H_6O) for 24 hours and oven drying in an oven at 40 ℃ for another 24 hours. Remark that the stored temperature in the oven should not exceed 60 ℃ to prevent the disintegration of ettringite which is the substance that the study concerns. While the samples were waiting to be tested, they were kept in close containers away from moisture to prevent any possible further chemical reaction of the substances inside the samples. For secondary electron method, the cut samples were coated with gold before being put in the SEM machine. Along with the SEM test, with the same preparation of the tested samples, EDS test could also be done to obtain the chemical compositions of the hydrated products present in the samples. The EDS results were obtained using the EDAX software. Figure 3.10 shows SEM/EDS machine and the computer system used to display the results.
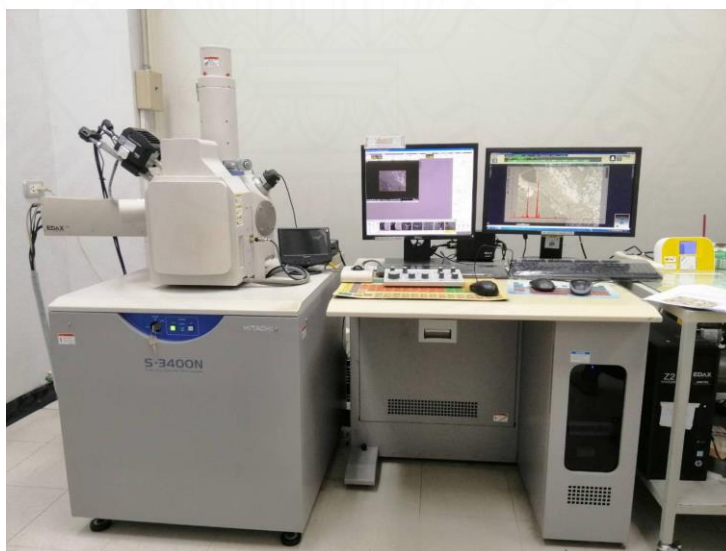
Figure 3.10 SEM/EDS machine and the computer system used to display the results

3.3.2.3 XRD (X-ray Diffraction)

XRD test was carried out to obtain the amount of mineral compounds of the hydrated products present in the samples. The mortar samples after having gone through modified accelerated mortar bar test were crushed into smaller pieces with the help of a hammer. Through sieving, the sample with a desired size range between 2.36 to 4.75 mm was used. The broken samples then underwent the hydration stopping process, which was done in the same way as mentioned in the section 3.3.2.2. The samples were ground using a grinding machine, Retsch Planetary ball mill PM 100, with a speed of 300 rpm (revolutions per minute) for 4 minutes and a pause of 20 seconds before reversing and ground with a the same speed for another 4 minutes. The final samples that were obtained was a very fine powder that passed sieve No. 100 (150 μm). The samples were then mixed with corundum and were tested.

After grinding the samples, they were tested using the Bruker D4 Endeavor machine. The Eva program was used for determining the composition of the compound, and Rietveld analysis implemented in TOPAS software was used for quantifying the amounts of the compounds. The measurement conditions were defined as 0.02 degrees for the step angle, 0.2 seconds for the count time, and 5 to 70 degrees for the range of 2θ. The tube voltage and current were 35 kV and 45 mA, respectively (Nguyen, 2018). When not being tested, the samples were kept in a zipper bag and put in a close container to keep away from moisture.

3.3.2.4 TGA (Thermogravimetric Analysis)

TGA test was also done to obtain the amount of the hydrated products present in the samples. When the paste cubes reached the age of 28 days, they were prepared for the test with exactly the same procedure as mentioned in section 3.3.2.2. When not being tested, the samples were kept in a zipper bag and put in a close container to keep away from moisture. TGA/DTG results were obtained by utilizing TGA Mettler Toledo machine as shown in Figure 3.11.

The derivative thermogravimetric (DTG) analysis was performed using about 10 mg of the powdered cement paste. The test temperature ranged from 30°C to 1000°C with a heating rate of 10°C/min. To measure the amount of the hydrated products of different binders, especially ettringite, portlandite and gypsum contents, the paste

samples were analyzed at the age of 28 days after the powders were mixed with water. The specific temperature intervals for decomposition of ettringite and portlandite in each mixture were determined from their DTG curves. In this study, the peak in the range of 65-120°C was used to estimate the amount of ettringite. The DTG analysis was used for the quantitative determination of ettringite. The peak in the range of 140-160°C was used to estimate the amount of gypsum. And the peak in the range of 450-500°C was used to estimate the amount of portlandite.

Figure 3.11 TGA Mettler Toledo machine (directindustry.com, n.d.)

3.3.2.5 MIP (Mercury Intrusion Porosimetry)

MIP tests were performed to obtain the total porosity and the pore size distribution along with average pore diameter and critical pore size of the tested samples. After being cured for 28 days in water, the paste cubes were wet-cut into $1 \times 1 \times 1$ cm small cubes with blades. The cut samples then underwent the hydration stopping process, which was done with the same process as mentioned in the section 3.3.2.2. The samples were later tested using Micromeritics AutoPore 9600 machine (Figure 3.12) with software MicroActive AutoPore V 9600 version 1.03.

Figure 3.12 Micromeritics AutoPore 9600 machine for MIP test (micromeritics.com, 2015)
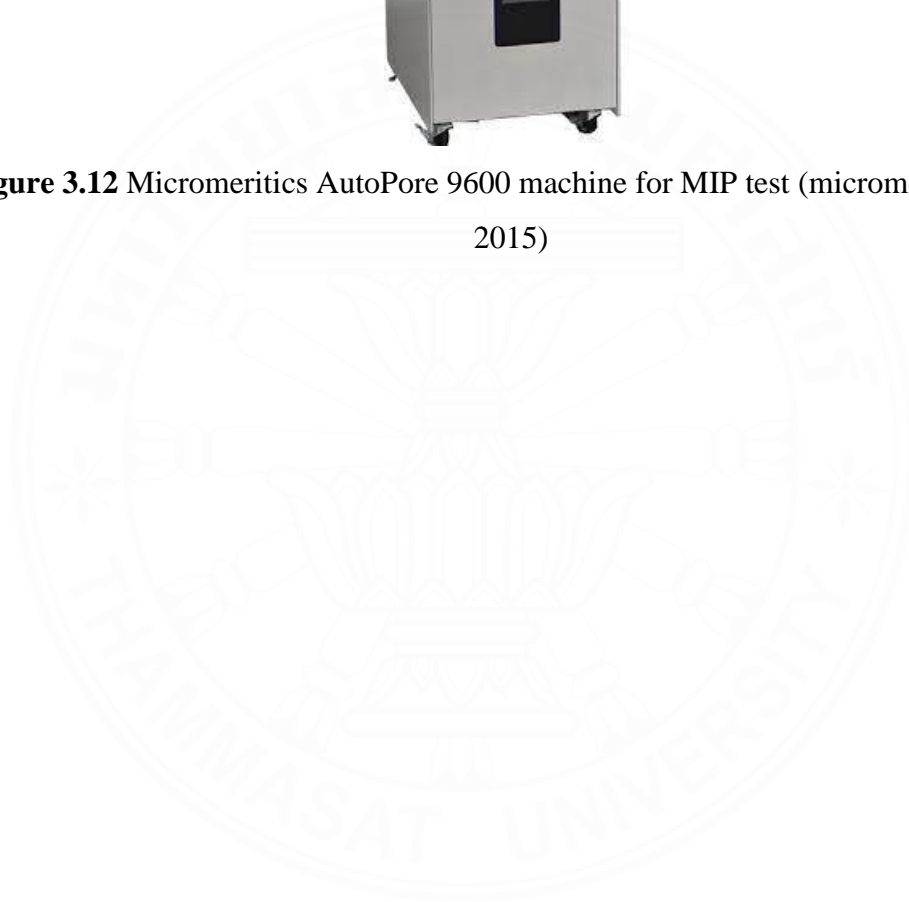
CHAPTER 4

EFFECTS OF TYPES OF BINDERS ON EXPANSION OF MORTAR BARS DUE TO IRON SULFIDE OXIDATION

To get an insight understanding of the effects of types of binders on expansion of mortar bars due to iron sulfide oxidation, the results are separated into different sections based on types of binders.

4.1 Effects of fly ash

From the results in Figure 4.1, Ordinary Portland cement shows rapid rise in expansion from 1 day to 6 days. After 6 days, the expansion increases moderately until 32 days. At 32 days, the expansion reaches almost 800 microns. Similarly, other mixtures also show rapid increases of expansion from 1 day to 6 days. While binary mixture with high CaO fly ash replacement shows sharp rise in expansion after 6 days, binary mixture with low CaO fly ash replacement shows gradual increases. It is obviously seen that mortar bars made with high CaO fly ash show higher expansion than the ones made from cement only. As expected, binary mixture containing low CaO fly ash shows lower expansion than OPC. When compare high CaO and low CaO fly ashes at the same replacement of 30%, FAM30 shows higher expansion from 1 day to 32 days than OPC. Inversely, FAB30 shows lower expansion from 1 day to 32 days than OPC. At 32 days, FAM30 shows 1.5 times greater expansion than OPC, while FAB30 shows around two-third of the OPC's expansion.

Commonly, when fly ash is used to replace cement in the mixtures, effects of cement dilution and pozzolanic reaction occur. With these two effects, the amount of cement hydrated $Ca(OH)_2$ in the system is reduced. Hence, less calcium hydroxide is available to further react with sulfate ions from iron sulfide oxidation to form gypsum and ettringite. From the above results, low CaO fly ash follows the principle in that it causes lower expansion, but not the high CaO fly ash. The fact that high CaO fly ash mixture shows higher expansion than OPC even though it contains lesser $Ca(OH)_2$ in the system can be explained by two aspects, chemical and physical properties.
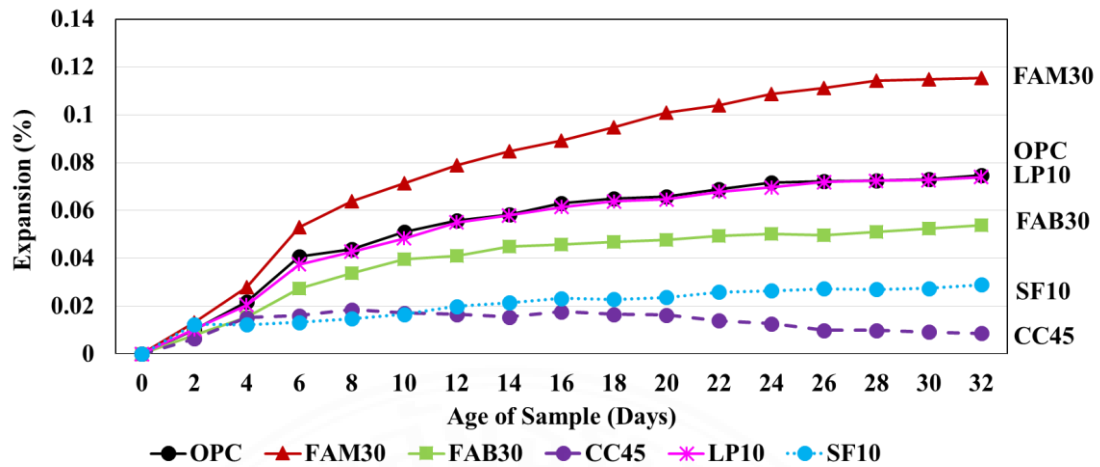
Figure 4.1 Effects of types of binders on expansion due to iron sulfide oxidation

High CaO fly ash possesses higher amount of sulfate (SO_3), magnesium oxide (MgO), and free lime contents than OPC. These three chemical compounds result in formation of expansive products which leads to expansion in concrete. Nawaz, Julnipitawong, Krammart and Tangtermsirikul (2016) reported in their study that higher amount of free lime in the mixtures resulted in higher expansion. In addition, although the OPC system is partially replaced with high CaO fly ash and effects of cement dilution and pozzolanic reaction take place, the system still contains high SO_3 amount and high amount of calcium due to the presence of high CaO and free lime contents from high CaO fly ash (according to Table 3.1, high CaO fly ash contains 2.67%, 26.06%, and 2.36% by weight of SO_3, CaO, and free lime contents, respectively, while low CaO fly ash has 0.28%, 1.73%, and 0.07% by weight, respectively). Consequently, there is high content of calcium available to react with sulfate ions in sulfuric acid (H_2SO_4). Finally, this yields high amount of gypsum, which means higher volume increase in the concrete matrix. Also, this will later cause the abundance of secondary ettringite in the system. Both gypsum and ettringite have higher volume than the original substances (Nawaz et al., 2016), in the orders of 1 to 2 times (Eglington, 1998) and 3 to 8 times (Tagnit-Hamou et al., 2005), respectively. As low CaO fly ash has the least amount of calcium when compared to both OPC and high CaO fly ash, the low CaO fly ash provides less amount of $Ca(OH)_2$ in the systems than high CaO fly ash. Therefore, lesser $Ca(OH)_2$ is available to react with sulfate ions, so it shows lower

expansion than mixtures of high CaO fly ash and cement only. Mardani-Aghabaglou, Sezer and Ramyar (2014) stated that low calcium fly ash tends to resist sulfate attack better than high calcium fly ash since it consumes more amount of Ca(OH)$_2$ in the system. Furthermore, it also forms more calcium silicate hydrates (CSH) and calcium aluminate silicate hydrates (CASH) in long term. Baghabra, Maslehuddin and Saadi (1995) hypothesized that the fly ash with CaO content less than 5% did not contain the reactive alumina to react with sulfates.

Table 4.1 shows portlandite content of paste mixtures obtained from the XRD test. These results represent available portlandite content in the mortar system. The available portlandite content in FAM30 mixture is higher than that in FAB30 mixture at 7.53% and 7.45%, respectively. These results correspond with the expansion results that FAM30 expands more than FAB30 mixture. However, when compared the portlandite content in OPC-only mixture, which is 13.84%, with FAM30 mixture, the OPC-only mixture has more available portlandite content in its system, but it expands less than the FAM30 mixture. This excessive expansion is due to the expansive products produced from high CaO fly ash itself as reported by Nawaz et al. (2016), Chatchawan (2017) and Nguyen et al. (2019). From XRD results of the tested mortar bars with iron sulfide-containing aggregates, the mineral compositions showing portlandite, gypsum, and ettringite contents are listed in Table 4.2. Portlandite content in Table 4.2 is the amount of remaining portlandite content after reaction of CH and sulfuric acid and pozzolanic reaction take place. It can be seen that low CaO fly ash or FAB30 mix yields 0.27% and 1.47% of portlandite and ettringite contents, respectively, which are both lower than high CaO fly ash binary mixture or FAM30 that are 0.31% and 1.86%, respectively. However, when take a closer look, the OPC-only mixture yields higher amounts of the three mentioned products than both high and low CaO fly ashes mixtures. This shows that expansive products from the iron sulfide oxidation and other chemical reactions are not the only factor influencing the expansion of mortar bars. The below paragraphs will discuss about the influence from physical aspect which involves pore structure of the system on expansion due to iron sulfide oxidation.

Table 4.1 Portlandite content results of paste mixtures at 28 days from XRD test

Mix ID	OPC	FAM30	FAB30	LP10	FAM20LP10	FAB20LP10
Portlandite (%)	13.84	7.53	7.45	13.49	9.75	9.60

Shehata, Thomas and Bleszynski (1999) reported that the alkalinity in the pore solution of the mixtures also plays a role in expansion. This can be seen from the Ca/Si ratio of fly ash. The high ratio of Ca/Si results in high alkalinity in pore solution. Specimens with fly ash that contains higher calcium and lower silica contents expands more than those with the opposite conditions. From Table 3.1 (in Chapter 3), high CaO fly ash possesses higher Ca/Si ratio than low CaO fly ash, hence it expands more.

Table 4.2 Portlandite, gypsum and ettringite contents of tested mortar bars with iron sulfide-containing aggregate after being exposed to modified AMBT from XRD test

Mix ID	Portlandite (%)	Gypsum (%)	Ettringite (%)
OPC	0.64	1.63	2.77
FAM30	0.31	1.43	1.86
FAB30	0.27	1.52	1.47
LP10	0.26	1.47	2.25
CC45	0.13	1.44	1.49
FAM20LP10	0.38	1.13	1.42
FAB20LP10	0.07	1.86	1.96

Aside from the chemical aspect, porosity of the mixture is considered. Figure 4.2 and Figure 4.3 show pore size distribution and cumulative pore volume of paste mixtures at 28 days, respectively from MIP test. Also, the average pore diameter and total porosity of paste mixtures at 28 days is displayed in Table 4.3. From Table 4.3, the mixtures with fly ash shows lower average pore size than the OPC-only mixture, which coincides with many researches (Dhandapani et al., 2018; Mullauer et al., 2013; Wanna et al., 2021). The lower pore size of fly ash mixtures than OPC-only mixture plays an important role in reducing expansion due to iron sulfide oxidation. This refinement of pore structure aids the resistance to penetration of water and moisture

into the concrete. This will later reduce the chance of iron sulfide oxidation occurrence, hence lower the amount of expansive products and expansion. While the total porosity from this study shows that OPC-only mixture has lower total porosity percentage than fly ash mixtures. Total porosity is related to the total pore volume. It means that fly ash mixtures contain more available space in its concrete system than OPC-only mixture to accommodate the expansive products. However, if ettringite is produced and high crystallization pressure is generated in pore system, cracking and expansion can occur (Shi et al., 2019). From the results of ettringite yielded from FAM30 and FAB30 and total porosity, it can be seen that for FAB30, the expansive products are less and there is more space available for the products to fill in. While in the mixture of FAM30, it produced expansive products at a greater amount, but the space availability is much lower, therefore, the expansive products tend to expand and cause greater expansion in FAM30 than FAB30. From Figure 4.2, FAB30 possesses pores with greater pore diameter than FAM30. Also, it has bigger critical pore size than FAM30. Figure 4.3 shows that FAB30 has higher pore volume at every pore size. The fact that FAB30 has larger pore size and volume than FAM30 is because high CaO fly ash is chemically more reactive than low CaO fly ash especially at early age.
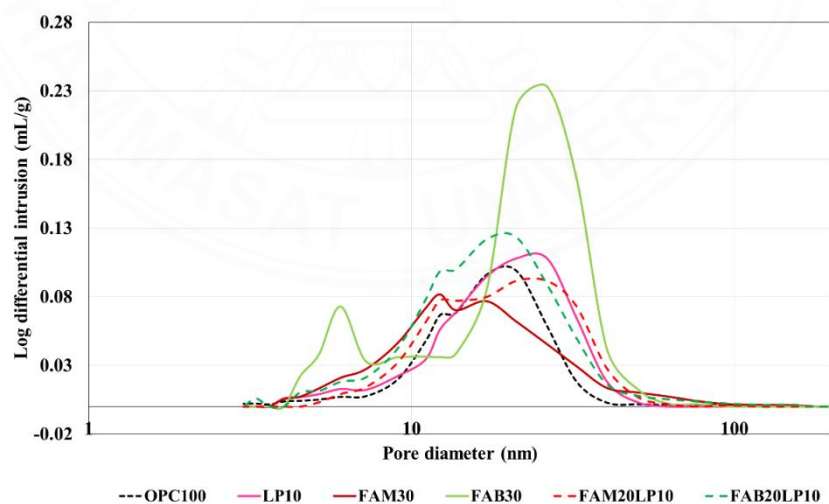
Figure 4.2 Pore size distribution of paste mixtures at 28 days
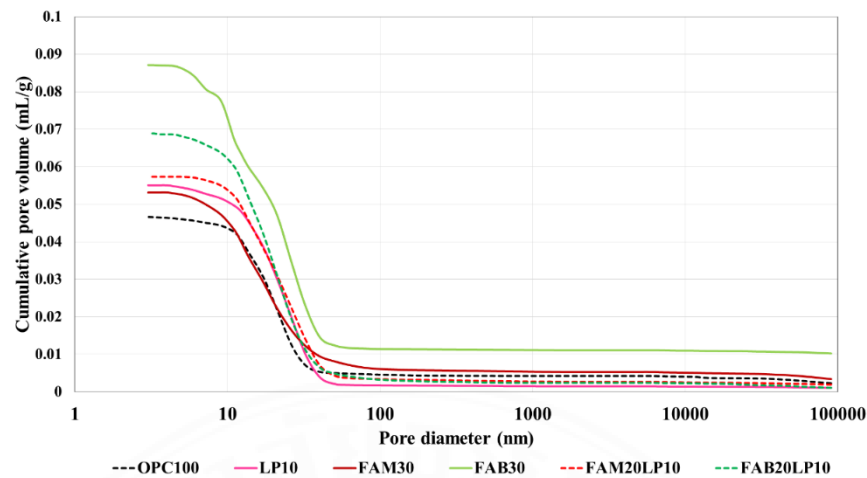
Figure 4.3 Cumulative pore volume of paste mixtures at 28 days

Table 4.3 Average pore diameter and total porosity of paste mixtures at 28 days from MIP test

Mix ID	OPC	FAM30	FAB30	LP10	FAM20LP10	FAB20LP10
Average pore diameter (nm)	20.10	16.78	13.88	19.22	19.71	16.89
Total porosity (%)	9.50	10.55	15.62	11.79	11.17	13.30

Specimens with high and low CaO fly ashes at 30% replacement in binary binder system were selected for SEM/EDS tests (FAM30 and FAB30). After the mortar bar specimens underwent the modified AMBT for 32 days, they have been kept in a closed container away from moisture (with minimum moisture entering the container) at room temperature. This is to prevent the samples from any further possible chemical reactions. From SEM/EDS tests, the results are shown in Figure 4.5 to Figure 4.9.

For both specimens, the SEM was done by scanning the paste around the iron sulfide-containing aggregates to search for any possible products from iron sulfide oxidation. Figure 4.4 shows the specimens of FAM30 mixture where the circled areas are the locations where the products are found. Figures 4.5 and 4.6 shows abundant amount of gypsum from FAM30 mixture, while Figure 4.7 shows ettringite, also from FAM30.

Figure 4.4 Cut mortar bar (FAM30) used to do SEM (before coated with gold)
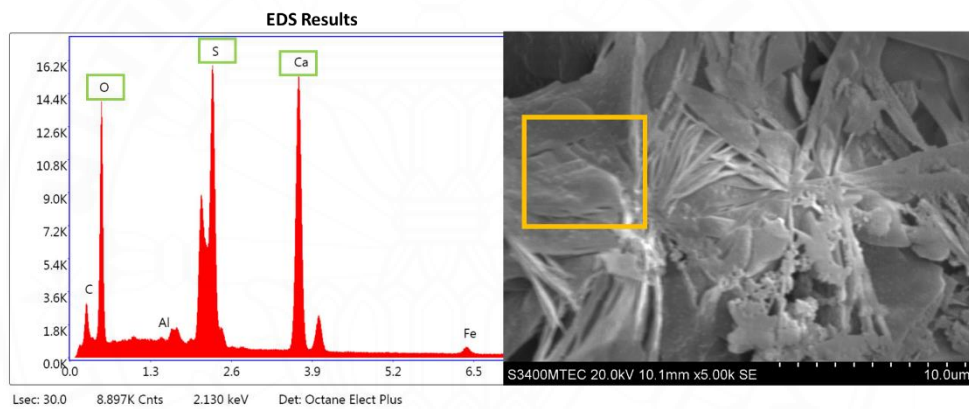
Figure 4.5 SEM and EDS results of FAM30 mixture showing gypsum
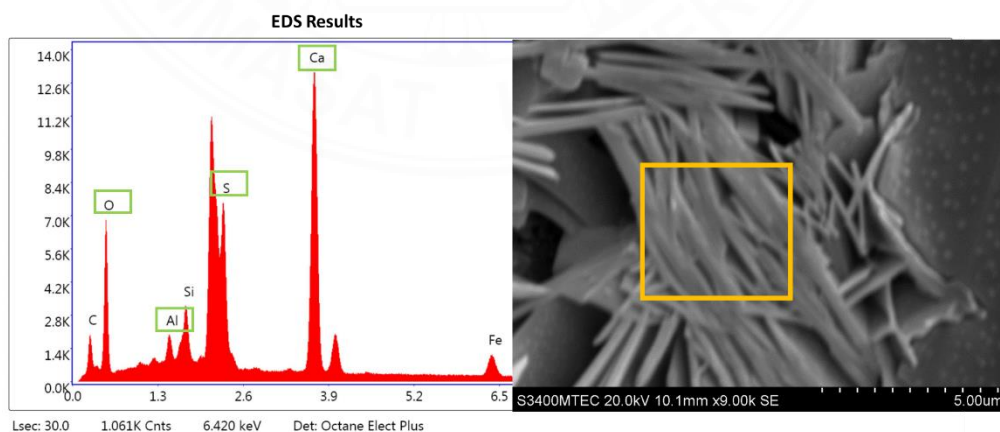
Figure 4.6 SEM and EDS results of FAM30 mixture showing gypsum
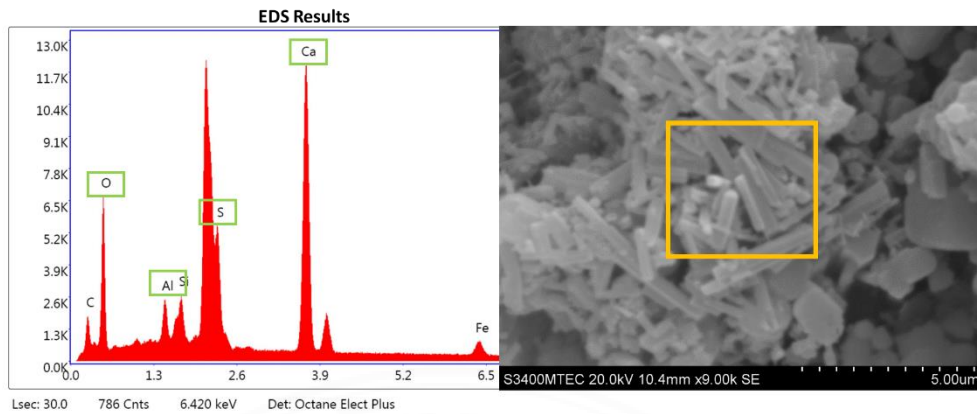
Figure 4.7 SEM and EDS results of FAM30 mixture showing ettringite

In FAB30, abundant gypsum was observed as can be seen from Figures 4.8 and 4.9. However, ettringite was not found as in the specimens of FAM30.
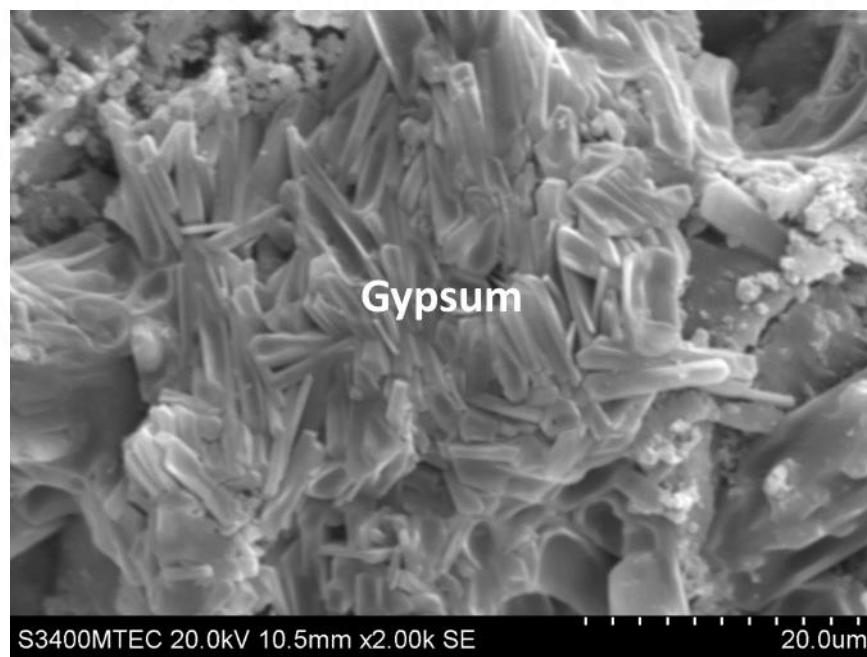
Figure 4.8 SEM result of FAB30 mixture showing gypsum
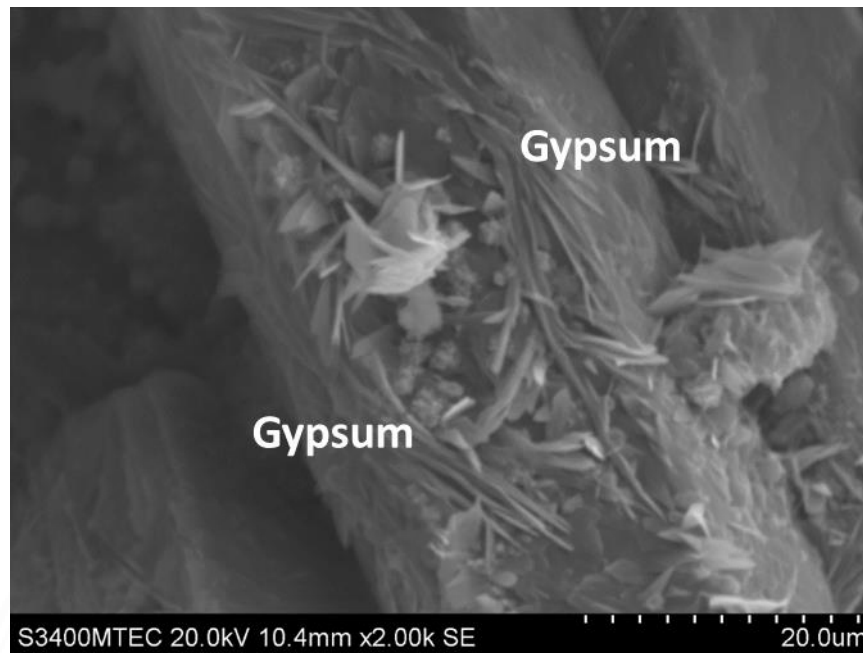
Figure 4.9 SEM result of FAB30 mixture showing gypsum

4.1.1 Effects of replacement percentage of fly ash

When different replacement percentages are considered, the expansion difference is also obvious when 30% and 45% replacement are compared (Figure 4.10). For high CaO fly ash, at 32 days and at 30% replacement, FAM30 shows around 400 microns higher expansion than OPC. However, when 45% replacement is used, FAM45 shows lower expansion than replacement at 30% (FAM30). FAM45 at 32 days shows around 200 microns higher than OPC in expansion. Similarly, when higher amount of low CaO fly ash is used to replace cement, the expansion is reduced. The reasons of this lower expansion when more amount of fly ash is used for both high and low CaO fly ashes are due to the cement dilution and pozzolanic reaction effects. When higher percentage of fly ash is used to replace cement, this means that lower amounts of tri-calcium-silicate (C_3S) and di-calcium-silicate (C_2S) are available for the production of $Ca(OH)_2$ during cement hydration. Also, this $Ca(OH)_2$ is later consumed by the fly ash during pozzolanic reaction, thus, less gypsum and ettringite will be produced. The same observation was also reported in the review of Elahi, Reza and Shearer (2021).
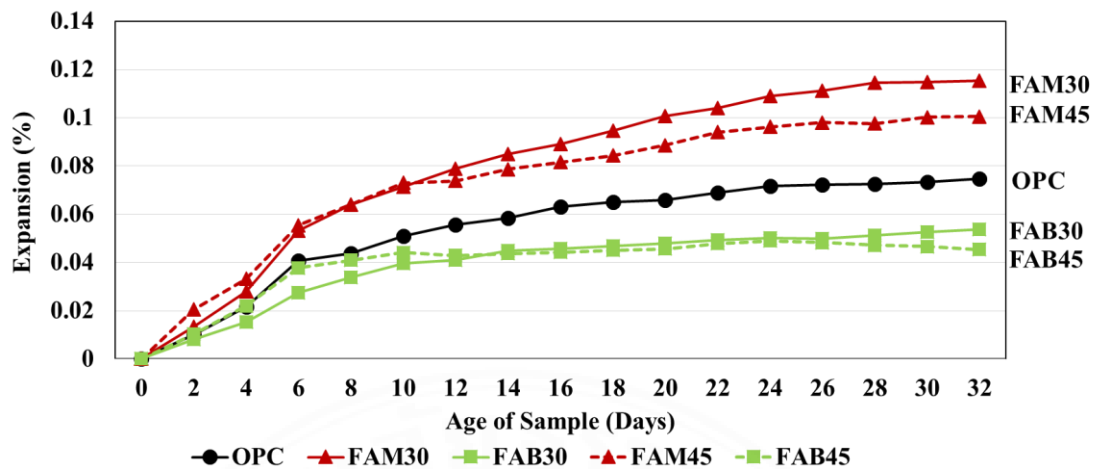
Figure 4.10 Effects of replacement percentage of fly ash on expansion due to iron sulfide oxidation

4.2 Effects of limestone powder

As can be seen in Figure 4.11, when cement is replaced with 10% limestone powder in binary system, it shows equivalent expansion results as OPC was observed from 1 day to 32 days. This is likely because limestone powder is an inert cement replacing material that does not enter the cement hydration (Kaewmanee & Tangtermsirikul, 2014). Sezer's study (2012) found that with the use of limestone powder in the mixture, due to the cement dilution, the amount of C_3A, C_3S and C_2S decrease, therefore, reduce the formation of ettringite and gypsum. Limestone powder is best known for its filler effect. This can be seen from MIP result in Table 4.2. The average pore diameter at 28 days of limestone powder binary mixture is slightly lower than that of OPC-only mixture. On the other hand, the total pore volume of paste mixture with limestone powder is more than paste of OPC-only. This results confirm the filler effect of limestone powder that it causes the system to have many pores with smaller pore size. Moreover, Table 4.1 shows that the portlandite content in LP10 mixture is slightly lower than that in OPC-only mixture. And from Table 4.2, the amount of gypsum and ettringite in the system of LP10 is slightly lower than that of OPC-only mixture.

4.2.1 Effects of limestone powder in ternary binder system of FA-LP-OPC

The expansion results when limestone powder was used with high CaO fly ash in ternary binder system are shown in Figure 4.11. From the previous discussion, it is now known that high CaO fly ash results in significantly higher expansion than OPC, while limestone powder shows equivalent expansion as OPC. When high CaO fly ash and limestone powder are used together to replace OPC at 30%, the expansion is lower than that of the binary mixture with high CaO fly ash. With the use of limestone powder, the expansion of high CaO fly ash-limestone powder mixture is reduced by almost 400 microns at 32 days when compared to high CaO fly ash binary mixture at the same replacement.

When limestone powder is used with low CaO fly ash (Figure 4.11), the contrast results from the ternary binder system with high CaO fly ash and limestone powder are obtained. Instead of aiding the fly ash in reducing the expansion as in the samples with high CaO fly ash, limestone powder when used with low CaO fly ash causes a higher expansion than when only low CaO fly ash is used in binary binder system. FAB20LP10 shows slightly higher expansion than FAB30 since 1 day up to 32 days. Even though FAB20LP10 shows higher expansion than FAB30, its expansion is still much lower than that of OPC. The expansion at 32 days is almost 200 microns lower than the expansion of OPC.
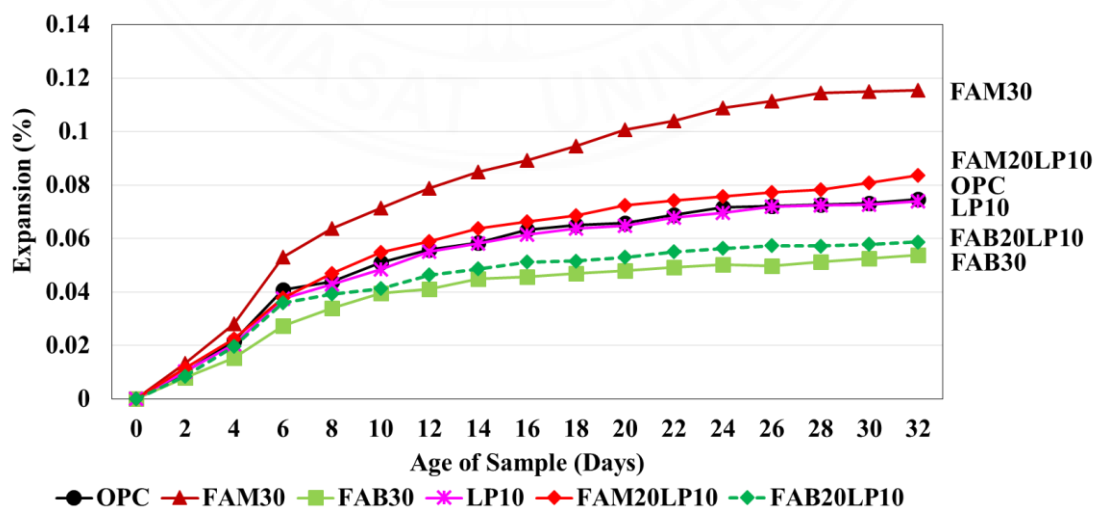
Figure 4.11 Effects of limestone powder in ternary binder system of FA-LP-OPC on expansion due to iron sulfide oxidation

Many studies mentioned the synergetic effect between limestone powder and fly ash that the mixture yielded calcium monocarboaluminate hydrate which provided strength to the concrete (De Weerdt et al., 2011), but they did not mention effects of different types of fly ashes with limestone powder. When limestone powder is introduced to the system of fly ash and cement in FAM20LP10 and FAB20LP10 mixtures, primarily, effect of cement dilution takes place (Kaewmanee & Tangtermsirikul, 2014). Comparing the expansion between the two types of fly ashes in ternary binder system, for high CaO fly ash, the ternary binder system contains less reactive compounds such as CaO, SO_3, and free lime than the binary binder system due to less amount of fly ash in the systems. So, the expansion was reduced. As fly ash content in ternary binder system is less than in binary binder system, pozzolanic reaction in ternary binder system also has less effect on the system which means $Ca(OH)_2$ is less consumed. However, the ternary binder system showed more reduction in expansion than binary binder system. Therefore, the less amount of fly ash is a dominant cause for this lower expansion. On the other hand, in the low CaO fly ash systems, the expansion of ternary systems is greater than binary binder system. For this circumstance, the effects of pozzolanic reaction plays the major role. Since less amount of low CaO fly ash was used in the ternary binder system, the effect of pozzolanic reaction is less. Therefore, more $Ca(OH)_2$ is present in the system to form gypsum. A study stated that the cement replacing materials with high silica content, such as fly ash, slag and silica fume, can improve the sulfate resistance of the system of limestone powder and cement (Shi et al., 2019).

4.3 Effects of Calcined Clay

The expansion of calcined clay mixture at 45% replacement of calcined clay (CC45) is shown in Figure 4.12. The expansion of CC45 is significantly low when compared to other types of binders. At 6 days, CC45 expands only half of the OPC-only mixture. CC45 expansion starts to be stable from 6 days onward with a magnitude around 180 microns. The expansion maintains its stability until 20 days. From 20 days onward, the expansion of CC45 drops continuously, which indicates that it starts to shrink gradually. This is because of the nature of calcined clay which possesses larger shrinkage behavior when compared to OPC. As was reported in the study of Sudsawong

(2022), the calcined clay at 30% replacement showed larger shrinkage over time than OPC-only mixture and even larger than the shrinkage of high CaO fly ash mixture. This total shrinkage involves all form of shrinkage which are chemical, autogenous and drying shrinkage. Chemical and autogenous shrinkage are mainly due to chemical reaction of cementitious materials, while drying shrinkage is due to the physical loss of water in pore systems of hardened concrete. The large shrinkage in CC system is due to the early reactivity of calcined clay and rapid development of dense pore structure, consequently increases the chemical shrinkage and autogenous shrinkage. The autogenous shrinkage occurs due to the early pore refinement of the system from the use of calcined clay (Afroz et al., 2023). Therefore, these behaviours are commonly encountered when calcined clay is used in the concrete mixture.

The testing condition of the modified accelerated mortar bar test in this study also enables the shrinkage environment as the samples went through the longer dry cycle at 60 ℃ than the wet cycle. Throughout the test period, CC45 shows the least expansion among all types of binder systems that use calcined clay (included CC30LP15, CC20LP10FAM15, and CC30LP10FAB15). It shows expansion value of around 100 microns at 32 days which is just half of its maximum expansion at 190 microns at 8 days. And it is 7 times less expansion than the OPC only mixture at 32 days.

Similar to fly ash, calcined clay possesses the pozzolanic behavior. Calcined clay contains high content of reactive silica and alumina. Due to its high reactivity, it consumes high amount of $Ca(OH)_2$ from cement hydration and used it during pozzolanic reaction. The amount of $Ca(OH)_2$ is then reduced, thus formation of gypsum and ettringite is reduced. The available $Ca(OH)_2$ is also reduced due to cement dilution effect from the replacement of calcined clay in cement. From Table 4.2, it is shown that the summation of expansive products, gypsum and ettringite, of CC45 mixture is close to FAB30, 2.99% and 2.93%, respectively, and both show low expansion. They are significantly lower than the expansive products found in OPC-only, FAM30, and LP10 mixtures.

Calcined clay is reported to be very reactive at early age (Bonen, 1993; Frías & Cabrera, 2000; Oriol & Pera, 1995) which is different from fly ash that shows its reactivity at later age. The reactivity of calcined clay not only results in great

consumption of Ca(OH)$_2$, but also yields the refinement and rapid modification of pore structure since early age, even faster than OPC-only mixtures. Some research also reported that the additional formation of CSH in pozzolanic reaction between metakaolin and Ca(OH)$_2$ from cement hydration fills in the pore structure making the systems denser. So, this phenomena can stop the penetration of water and oxygen into the concrete structure more effectively than other types of mixtures at early age. This is the reason for the very low expansion of CC45 mixture.

4.3.1 Effects of limestone powder in ternary binder system of CC-LP-OPC

Commonly, calcined clay is often used in combination with limestone powder as cement replacing materials. Many researchers referred to the combination of cement, calcined clay and limestone powder as LC^3 or limestone calcined clay cement. As seen from the promising expansion reduction result of CC45, in Figure 4.12, the expansion from the use of calcined clay and limestone powder at 45% replacement (CC30LP15) is significantly lower than the expansion from mixture of OPC-only throughout the test ages. With slightly higher expansion from 1 to 6 days (220 microns at 6 days), CC30LP15 mixture expands stably after 6 days. The expansion is plateau until 20 days. Then from 20 days onwards, the shrinkage starts (as also seen in CC45), but not as obvious as CC45. At 32 days, the expansion of CC30LP15 is 200 microns, which is twice the expansion of CC45. Therefore, for the expansion results, CC30LP15 does not show effective reduction in expansion as CC45.
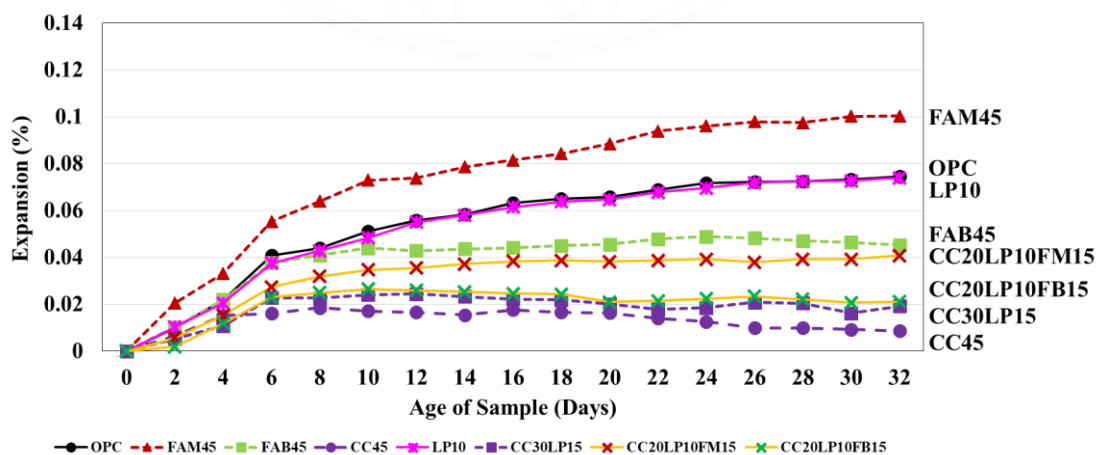
Figure 4.12 Effects of calcined clay on expansion due to iron sulfide oxidation

The shrinkage in CC30LP15 from 20 days is due to the behaviour of calcined clay that it is very reactive since early age, so it causes shrinkage as explained in section 4.3. And the proportion of calcined clay used in CC30LP15 is only 30% replacement which is less than CC45 mixtures that uses 45% replacement of calcined clay, so the shrinkage is milder than CC45.

Shi et al. (2019) stated that mixtures with the ratio of calcined clay to summation of calcined clay and limestone powder of more than or equal to 0.5, CC/(CC+LP) ≥ 0.5, is considered to be well resistant to sulfate. When calcined clay and limestone powder are used together, they promote the synergetic effect which enhances one another without any loss in compressive strength. This synergetic effect is also found in the ternary mixture of cement with fly ash and limestone powder. The product of calcium monocarboaluminate (Mc) and hemicarboaluminate (Hc) can be found in the mixture of calcined clay and limestone powder from the reaction of metakaolin (in calcined clay) and limestone powder. This Mc and Hc provide dense microstructure for the concrete system at early age (Franco & Karen, 2021). However, in this study, both Mc and Hc were not detected from XRD test. This is because the samples in this experiment was stored under high pH condition (in the solution of sodium hypochlorite) during its wet cycle. Mc and Hc are not stable in high pH environment. To detect Mc and Hc, the compounds must have been stored in other conditions.

The fact that calcined clay itself consumes high amount of calcium hydroxide from the cement hydration plays major role in this explanation. When compared to OPC-only mixture, CC30LP15 expands less due to firstly, the effect of cement dilution from the replacement with calcined clay and limestone powder. Therefore, there is less $Ca(OH)_2$ produced from cement hydration reaction. Additionally, high reactivity of calcined clay at early age consumes $Ca(OH)_2$ fast, so there is less calcium hydroxide availability in the system for further iron sulfide oxidation. However due to fewer percent replacement used in CC30LP15 than CC45, the effects from pozzolanic reaction is less than in CC45. While LC^3 mixture was found to have ettringite formed due to presence of excess calcite in the systems. This calcite prevents the ettringite from converting to monosulphate (Ms).

Besides the chemical effect from pozzolanic reactivity of calcined clay, its high

reactivity is also shown in the pore size reduction of the concrete system. Along with the filler effect by limestone powder, both cement replacing materials collaborate each other in producing dense concrete structure. Dhandapani and Santhanam (2017) reported that the mixture of LC^3 or limestone calcined clay showed reduction in pore size at early age (from 3 days). This is due not only to the fineness and packing effect of LC^3, but also the higher pozzolanic reactivity of the calcined clay in the mixture. In their study, it is stated that LC^3 consumes a lot of portlandite since 3 days, while fly ash slowly starts the consumption from 14 days to 28 days. This mechanisms help to explain the low expansion of CC45 and CC30LP15 mixtures that use calcined clay. When the concrete structure is dense, it means that the penetration of water and moisture to reach iron sulfide particles inside the mortar samples is low. Therefore, lower rate of iron sulfide oxidation can be expected.

4.3.2 Effects of quaternary binder system of FA-CC-LP-OPC

From section 4.3.1, CC30LP15 shows a very low expansion of 200 microns at 32 days, which is only one-fourth of the OPC only mixture's expansion. However, in reality, the mixture of CC and LP does not overcome all the durability problems and properties of concrete. Many researchers have been searching for mixtures that might solve this problem. One of the solutions is to add fly ash in the systems of CC and LP. Therefore, the quaternary binder system of calcined clay, limestone powder, and fly ash is also investigated in this study.

Figure 4.12 shows the expansion of quaternary binder system of calcined clay, limestone powder and low CaO fly ash. As discussed in previous sections, both mixtures of ternary binder systems of CC with LP, and binary binder system of FAB at both 30 and 45% replacements have great performance in reducing expansion due to iron sulfide oxidation. As expected, the expansion of CC20LP10FAB15 is dramatically lower than the OPC only mixture. CC20LP10FAB15 expands similarly to CC30LP15 at all ages throughout the test period with a very slightly higher magnitude. But it is still not as good in reducing expansion as the CC45 mixture. At 32 days, the expansion of CC20LP10FAB15 is 200 microns which is one-fourth of the expansion of OPC only mixture. The same as other mixtures that use calcined clay (except CC20LP10FAM15), CC20LP10FAB15 expansion rises from 0 to 6 days, and then shows a stable expansion

until 18 days. Later, it shows slight shrinkage from 18 days and remains stable until 32 days.

CC20LP10FAM15 expands sharply from 0 to 6 days. Then it shows gradual expansion until 32 days without any sign of shrinkage (as seen from the mixtures of CC45 and CC20LP15). At 32 days, the expansion reaches 400 microns which is half of the expansion of the OPC-only mixture at the same age. CC20LP10FAM15 shows a different trend from 20 days to 32 days from other mixtures that incorporate calcined clay. While other mixtures show shrinkage (at different degree), CC20LP10FAM15 shows a stable expansion. Throughout the test period, CC20LP10FAM15 shows the highest expansion among all the mixtures that contain calcined clay. But it still significantly reduces the expansion problem when compared to the OPC-only system. Unlike the mixture of CC20LP10FAB15, CC20LP10FAM15 does not show shrinkage. This should be due to the expansive products of high CaO fly ash that it counteracts with the shrinkage from calcined clay. The expansion from high CaO fly ash compensates the shrinkage from calcined clay.

4.4 Effects of silica fume

From Figure 4.13, silica fume in binary binder system at 10% replacement (SF10) shows lower expansion than OPC-only mixture. From 0 to 32 days, SF10 expands gradually and reached 300 microns at 32 days which is approximate half of the expansion of OPC-only mixture. When comparing different types of binders in binary binder system, SF10 shows good performance in reducing expansion and it is the second best binary binder system just after the CC45 mixture. It also shows no shrinkage throughout the test period. When comparing between the mixtures at the same percent replacement, SF10 shows obvious lower expansion than LP10 with a difference of almost 500 microns at 32 days.

According to Lilkov, Petrov, Tzvetanova and Savov (2012), a concrete mixture with silica fume showed great pozzolanic activity when compared to fly ash. The mixture with silica fume showed its pore refinement at 15 days which is comparable to pore structure of fly ash mixture at 30 days. This great pozzolanic behavior is found to be due to the amorphous silicon dioxide (SiO_2) or the silica content of silica fume which reacts well with the calcium hydroxide from cement hydration

over time. Its fineness which is extra fine when compared to fly ash and cement particles increases the surface area of the silica fume for pozzolanic reaction. Besides the effect from cement dilution, these 2 factors enables silica fume to consume more calcium hydroxide than other tested cement replacing materials in this study. With only 10% replacement of silica fume in cement, the expansion is almost as low as the mixture with 45% replacement of calcined clay. Additionally, Shehata and Thomas (2002) reported in their study that silica fume showed low alkalinity in its pore solution at early age. This low alkalinity also contributes to the low expansion of mortar system. It also keeps the alkalinity in pore solution of mortar system low over time.

4.4.1 Effects of silica fume in ternary binder system of FA-SF-OPC

The expansion of low CaO fly ash mixtures due to iron sulfide oxidation is low when compared to the OPC-only mixture. When silica fume is introduced in the system of low CaO fly ash, the expansion is even more reduced as shown in Figure 4.13. When silica fume is used in ternary binder system with low CAO fly ash and OPC, the mixture reduces the expansion satisfactorily. From 0 to 8 days, it shows a gradual expansion, which is different from other mixtures that show sharp increase in expansion. The expansion then remains stable until the end of the test program. At 32 days, the expansion is around 200 microns. It is one fourth of the expansion of OPC only mixture at the same age. The ternary binder of FAB20SF10 shows obvious results in enhancing reduction in expansion than the ternary binder systems of FAB20LP10 and FAM20LP10.

As explained in section 4.4, silica fume exhibits active pozzolanic behavior at early age. Due to its chemical minerals and its extra fine particles. Similar to silica fume, fly ash is another pozzolanic material which is aluminosilicates. With reactive alumina and silica, fly ash shows great pozzolanic behavior. However, its pozzolanic reaction starts at later age. From a study of Afroz, Zhang, Nguyen, Kim and Castel (2016), the TGA results showed that calcium hydroxide consumption of fly ash started from 14 days onward and the calcium hydroxide content continued to decrease over time. As seen in section 4.1 (Effects of fly ash), the expansion is based on types of fly ash, low CaO fly ash causes lower expansion than high CaO fly ash, and lower than the control sample throughout the experimental period. Therefore, to observe the effects of

ternary binder system with silica fume, low CaO fly ash was selected with an expectation that both types of cement replacing materials would enhance the expansion resistance in concrete. The low expansion of FAB20SF10 is due to the synergistic effect of silica fume and low CaO fly ash. Chemically, silica fume contributes its pozzolanic behavior at early age excellently which can be seen from 1 day. Most of the calcium hydroxide from hydration is consumed by silica fume. Low CaO fly ash then carried on with its pozzolanic behavior at later age. Therefore, the mixture with both silica fume and low CaO fly ash shows low expansion and maintains low expansion throughout the experimental period. The mixture also shows greater reduction in expansion than the binary mixture of silica fume alone. The effect of cement dilution should also be mentioned since the cement was replaced at higher percentage in FAB20SF10 than in SF10. Lesser calcium hydroxide is produced from ternary mixture with combined silica fume and low CaO fly ash.

The pozzolanic behavior of both silica fume and low CaO fly ash also contributes to the refinement of pore structure as experienced in the binary mixture of each binder. While physically, silica fume's ultra-fineness gives the mixture dense microstructure. This characteristic reduces the moisture and oxygen permeability. Therefore, less moisture and oxygen are able to penetrate inside the structure. Also, the ion diffusion is decreased hence the rate of iron sulfide oxidation decreases.
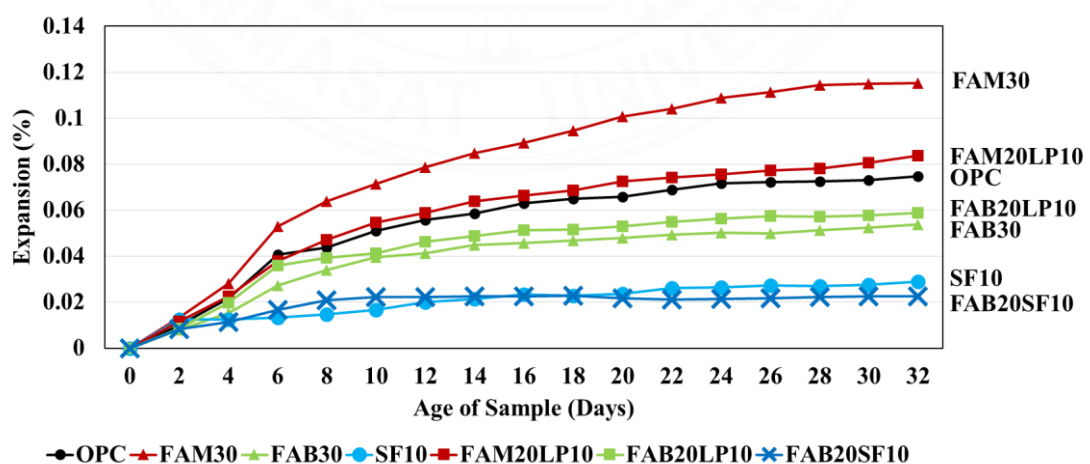
Figure 4.13 Effects of silica fume in ternary binder system of FA-SF-OPC on expansion due to iron sulfide oxidation

4.5 Summary of expansion results

Among all the types of binders used in the study of expansion due to iron sulfide oxidation, the mixture of calcined clay at 45% replacement shows the best performance in reducing the expansion. However, it also shows shrinkage after 20 days of test.

When the replacement at 10% is considered, the binary binder mixture of silica fume shows a great reduction in expansion, whereas limestone powder shows no difference from the OPC only mixture.

At 30% replacement, the ternary binder system of low CaO fly ash and silica fume shows the best reduction in expansion, followed by the binary binder system of low CaO fly ash in which it shows 2 times higher expansion than FAB20SF10, but is still almost half lower than OPC-only mixture. Both ternary and binary binder mixtures of high CaO fly ash show higher expansion than OPC-only mixture.

Lastly, at 45% replacement, the binary binder system of calcined clay show the lowest expansion at all ages, followed by ternary mixture of CC and LP, then the quaternary mixture of CC and LP and low CaO fly ash. However, all of these three mixtures show shrinkage from 20 days onward. If shrinkage is to be considered, the best system that reduce expansion without shrinkage is quaternary mixture of CC and LP and high CaO fly ash.

CHAPTER 5

EFFECTS OF TYPES OF BINDERS ON RUST STAIN ON SURFACE OF MORTAR BARS DUE TO IRON SULFIDE OXIDATION

Apart from the expansion, another obvious damage due to iron sulfide oxidation is the rust stain on the concrete surface. The area of rust stain appeared on the specimen surfaces at 32 days is used for the analysis of severity of the rust stain. Figure 5.1 shows mortar bar samples of different mixtures at 32 days with rust stain on their surface. Figure 5.2 shows images of mortar bar surfaces after they have been analysed by using image analysis software. To get an insight understanding of the effects of types of binders on rusting of mortar bars due to iron sulfide oxidation, the results are separated into different sections based on types of binders and types of binder systems. Also, it is noted that in this study, the samples were stored under high pH condition during their wet cycles, therefore, the formation of rust may not be at its full extent due to this restricted environment.

It can be seen in Figure 5.1 that it is difficult to distinguish the amount of rusting occurs on the surface of different mixtures. Therefore, a quantitative analysis is necessary.
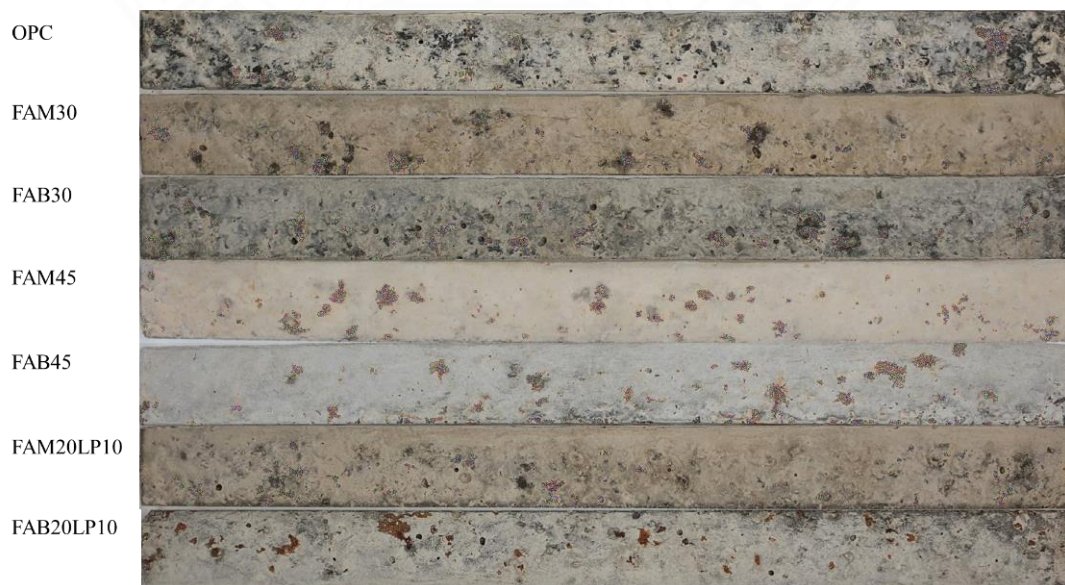
Figure 5.1 Surface of mortar bars of different mixtures at 32 days
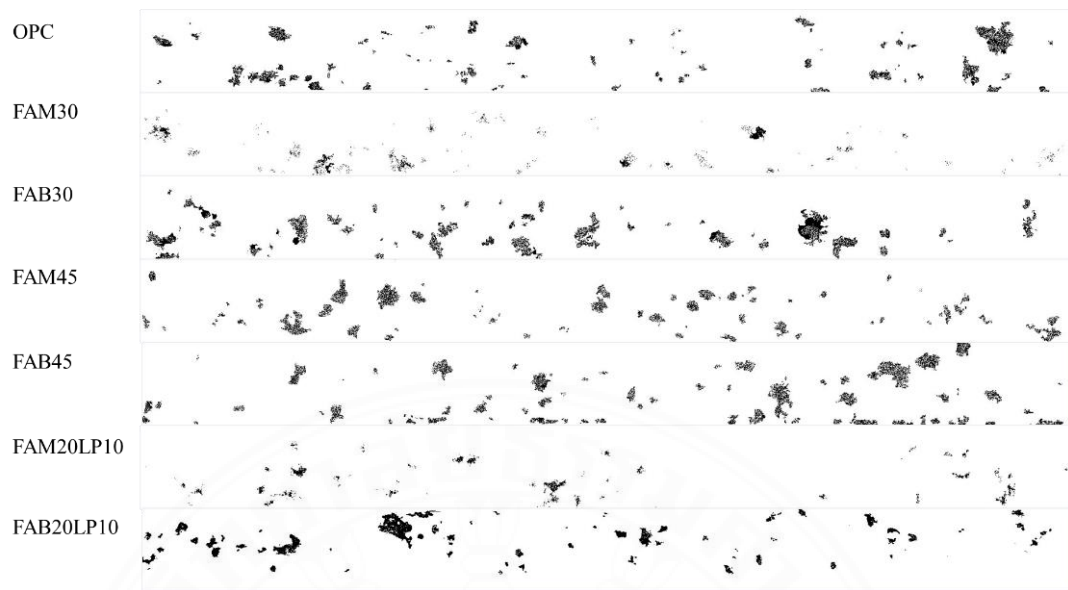
Figure 5.2 Rust area on mortar bar's surface of different mixtures at 32 days (after render)

The rust staining found in the mortar bar was also confirmed from the SEM-EDS analysis of a cut mortar bar of FAM30 mixture that the observed staining was a rust product. The SEM picture is shown in Figure 5.3. The rust staining composed of Iron (Fe) and Oxygen (O) elements as shown in Figure 5.4.
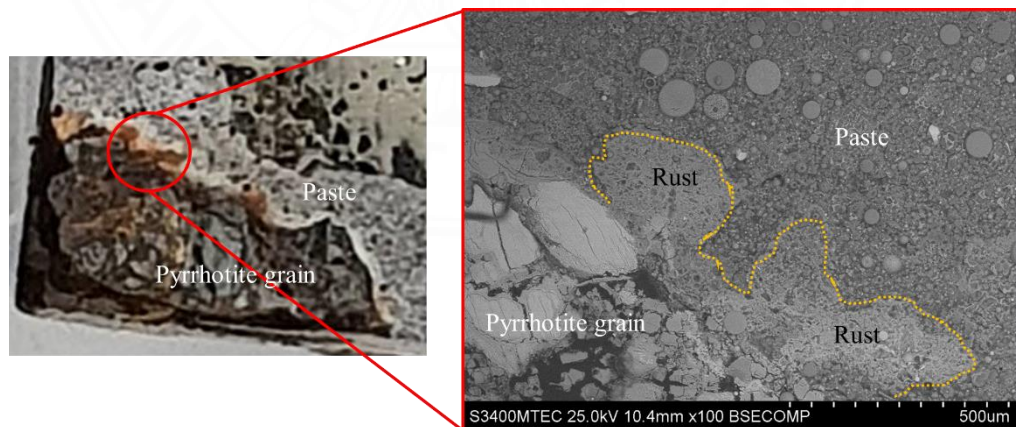
Figure 5.3 SEM picture showing rust staining from the Pyrrhotite grain in a cut FAM30 mortar bar
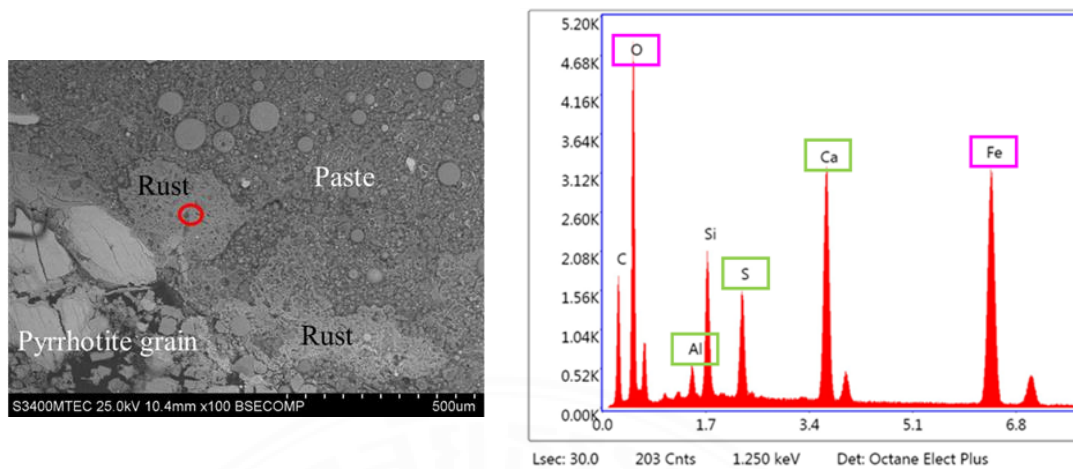
Figure 5.4 EDS results of rust staining from the Pyrrhotite grain in a cut FAM30
mortar bar

5.1 Effects of fly ash

From Figure 5.5, OPC shows rust area of around 5.5% of the total area. At 30%
fly ash replacement in binary binder system, the two types of fly ashes show different
results when compared to OPC-only mixture. High CaO fly ash specimens show less
rust area than OPC, while low CaO fly ash specimens show more rust area than OPC.
This rust area results are quite contrary to the expansion results. Recall that in expansion
results (section 4.1), the high CaO fly ash causes dramatically higher expansion than
low CaO fly ash in binary binder system.

This points out that the mechanisms that govern the expansion and rust stain are
different. As it is known that low pH level or low alkalinity condition favors formation
of rust. High CaO fly ash has higher alkalinity than the low CaO fly ash (Wanna et al.,
2021). It is mainly due to the higher Portlandite content in the mixture with high CaO
fly ash. In this study, calcium hydroxide or portlandite phase is investigated as it implies
the alkalinity level of the mortars. Table 4.1 (in Chapter 4) shows the amount of
portlandite content in paste mixtures at 28 days obtained from XRD test. These values
represent the available portlandite content in the paste system that is ready for further
chemical reactions such as pozzolanic reaction or reaction of CH with sulfuric acid as
seen in mortar system with iron sulfide. From Table 4.1, FAM30 has more available
portlandite content in its system than FAB30 mixture (7.53% and 7.45%, respectively).
This confirms the higher alkalinity level in FAM30 mixture which is one reason for its

less rust area. From Table 5.1, the Portlandite contents obtained from XRD test of the tested mortar bars with iron sulfide-containing aggregates with high and low CaO fly ashes (FAM30 and FAB30) are shown. FAM30 possesses higher Portlandite content than FAB30, 0.31% and 0.27%, respectively. This indicates that FAM30 still has higher alkalinity than FAB30 even after the iron sulfide oxidation takes place, which coincides with the rust area results, in which FAM30 has less rust than FAB30 at 32 days. Mixture with either type of fly ash has lower Portlandite content and so alkalinity level than OPC-only mixture. It is certainly due to the effects of cement dilution since less amount of cement was used in the FAM30 and FAB30 mixtures, and pozzolanic reaction of fly ash.

Furthermore, the rust stain due to the iron sulfide oxidation that damages the structure's aesthetics occurs on the surface of the concrete, which is different from the mechanisms of steel corrosion that the rust occurs inside the concrete structures. Therefore, the refinement of pore structure which is one of the main mechanisms that reduce the expansion may not be a dominant cause in reducing surface rusting. However, to compare OPC-only mixture with FAM30, it is interesting to point out that OPC-only mixture has higher portlandite content than mixture with high CaO fly ash, but it still shows more rust stain than FAM30. In this case, the pore structure may partially play a part. From the results of average pore diameter and total porosity in Table 4.3 (in Chapter 4), OPC-only mixture has the largest average pore diameter, even though it has lower total porosity than fly ash mixtures (as can also be seen from the graphs of cumulative pore volume in Figure 4.3 in Chapter 4). So, this may enable more water and moisture to interact with the iron sulfide-containing aggregates placed near the surface of the mortar samples, resulting in more rust staining. FAM30 mixture contains more pores of smaller diameter than OPC-only mixture. From Figure 4.2 (in Chapter 4), the pore size distributions of paste mixtures depict that FAM30 mixture has smaller critical pore size than OPC-only mixture. This smaller pore structure of FAM30 mixture than OPC-only mixture allows less water and oxygen molecules to penetrate into the concrete with FAM30 mixture than OPC-only mixture. On the other hand, FAB30 mixture has lower portlandite content than FAM30 and OPC-only mixtures. FAB30 mixture has smaller average pore diameter than OPC-only mixture with much higher total porosity than OPC-only mixture. Refinement of pore structure occurs due

to effect of pozzolanic reaction from the use of fly ash in the mixtures (as also seen in binary mixture with high CaO fly ash). However, FAB30 mixture shows more rust stain than OPC-only mixture. In this case, the alkalinity level of the mixture is dominant over pore structure in governing the rust staining on the surface of the mortar bar.
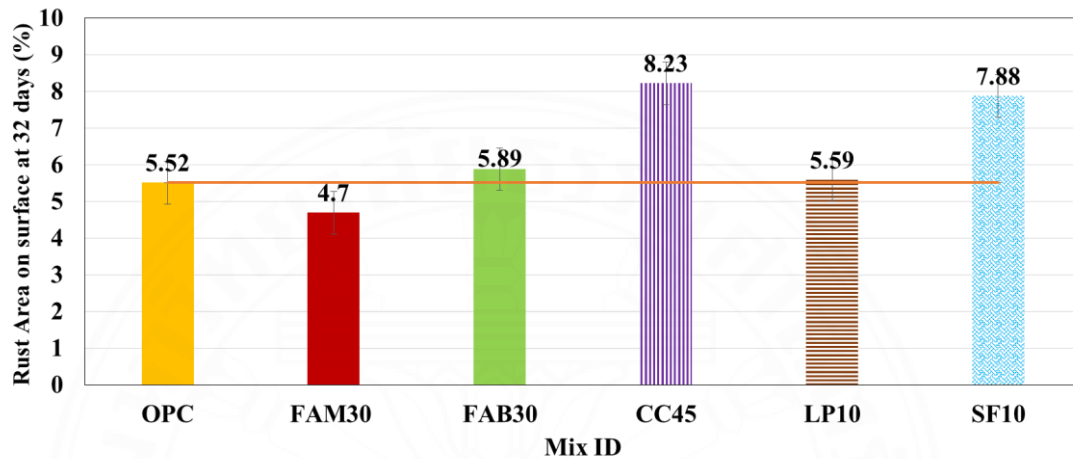
Figure 5.5 Effects of types of binders on rust staining due to iron sulfide oxidation

Table 5.1 Portlandite content results of tested mortar samples from XRD test

Mix ID	OPC	FAM30	FAB30	LP10	CC45	FAM20LP10	FAB20LP10
Portlandite (%)	0.64	0.31	0.27	0.26	0.13	0.38	0.07

The amount of portlandite in cement paste with no aggregate at 28 days from TGA/ DTG tests was also investigated to compare the portlandite content in the system without iron sulfide-containing aggregates as shown in the Table 5.2 and Figure 5.6. The trends of the portlandite content from TGA/DTG tests of paste mixtures coincide and support the explanation in the above section. From the results, FAM30 typically has higher alkalinity level than FAB30, but not as high as in OPC-only mixture. The amount of portlandite from TGA/ DTG tests is calculated from Eq. 5.1.

$$\text{Amount of CH (\%)} = \frac{M_{Ca(OH)_2}}{M_{H_2O}} \times \frac{W_{450} - W_{500}}{W_{Total}} \times 100\% \qquad (5.1)$$

where $M_{Ca(OH)_2} = 74$ (g/mol) and $M_{H_2O} = 18$ (g/mol)
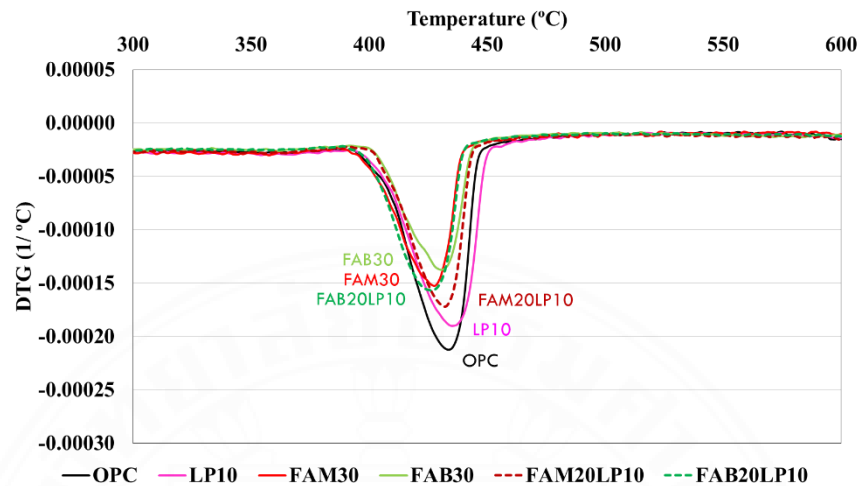
Figure 5.6 TGA/ DTG test results showing portlandite content of paste mixtures at 28 days

Table 5.2 Portlandite content results of paste mixtures from TGA/ DTG analysis

Mix ID	OPC	FAM30	FAB30	LP10	FAM20LP10	FAB20LP10
Portlandite (%)	1.75	1.56	1.39	1.89	1.61	1.47

5.1.1 Effects of replacement percentage of fly ash

From Figure 5.7, at 30% fly ash replacement in binary binder system, high CaO fly ash specimens show less rust area than OPC, while low CaO fly ash specimens show slightly higher rust area than OPC. When higher percentage of fly ash is added to the system to replace cement, the specimens show more rust area and are observed in both types of fly ashes. In high CaO fly ash-binding system with 45% fly ash replacement, the rust area increases and show slightly higher rust area than OPC. While, in low CaO fly ash-binding system, the rust area increases significantly from 5.89% to 6.8%. From 30 to 45 percent replacement of fly ashes in the mixtures for both types of fly ashes, the rust area increases by about 1%.

This increase in rust area when higher replacement of fly ash was used should be due to the cement dilution and pozzolanic reaction effects which reduce the amount

of $Ca(OH)_2$ in the mixtures, and so lower the alkalinity. Since $Ca(OH)_2$ is one of the hydroxide that gives alkalinity to the concrete system, when less $Ca(OH)_2$ is present, less alkalinity is obtained. In addition, low CaO fly ash is worse than high CaO fly ash in reducing rust area because it leads to lower $Ca(OH)_2$ content than high CaO fly ash.
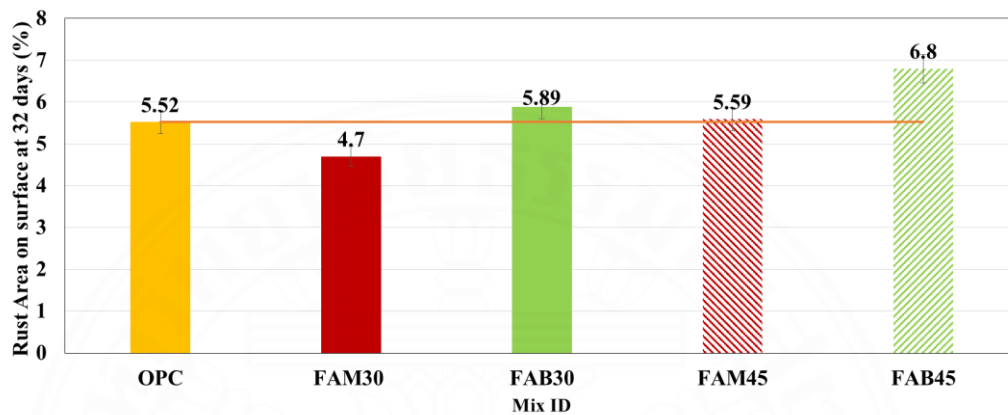
Figure 5.7 Effects of replacement percentage of fly ash on rust staining due to iron sulfide oxidation

5.2 Effects of limestone powder

When limestone powder is used at 10% replacement in binary binder system, negligible higher rust area at 32 days than OPC only mixture is obtained (Figure 5.5). The difference is not significant with 0.07% difference. Limestone powder shows significantly higher rust area when compared to binary mixture of FAM30, but the rust area is still less than FAB30 by 0.3%. When LP10 is compared to the binary binder system of SF10 at the same percent replacement, the difference in rust area results is obvious. LP10 specimens show almost 2.3% less rust area than SF10 specimens (Figure 5.5). This rust analysis demonstrates a similar trend with the expansion results in which limestone powder shows equivalent expansion to OPC.

As known that limestone powder is a cement replacing material that is very little reactive. When it is used alone in the mixture as CRM, it does not involve in any chemical reactions. Therefore, LP10 system certainly has lower alkalinity than OPC-only mixture from the effect of cement dilution. This corresponds with the portlandite amount found in the paste and mortar systems as shown in Tables 4.1 (in Chapter 4)

and 5.1, respectively. And it is the reason for slightly higher rust area observed from LP10 than from OPC-only mixture. For physical aspect, LP10 mixture has higher total porosity, but a slightly smaller average pore diameter than OPC-only mixture (Table 4.3 in Chapter 4). It has higher pore volume with smaller size than OPC-only mixture (Figure 4.3 in Chapter 4). From Figure 4.2 (in Chapter 4), LP10 mixture shows larger critical pore size than OPC-only mixture. This pore structure characteristic of LP10 mixture may be another supporting factor that allows more moisture and oxygen to get into the concrete and reacts with iron sulfide aggregate. Therefore, specimens of LP10 mixture shows slightly higher rust area than OPC-only mixture.

5.2.1 Effects of limestone powder in ternary binder system of FA-LP-OPC

Recall that from the expansion results, high CaO fly ash showed great reduction in expansion when used with limestone powder at 30% replacement than being used alone in the mixture, but still worse than OPC-only mixture. However, low CaO fly ash showed slightly higher expansion when was used with limestone powder than being used alone in FAB30 mixture, but still significantly better than OPC-only mixture. Here, the rust staining from ternary binder systems of high CaO and low CaO fly ashes with limestone powder are being investigated. When limestone powder and high CaO fly ash are used to replace 30% of cement, it shows remarkable reduction in rust stain (Figure 5.8). Comparing at the same replacement of 30%, the ternary binder system renders around 1% reduction of rust area from the binary binder system of FAM30. Since limestone powder is an inert cement replacing material, it does not consume $Ca(OH)_2$. Therefore, when limestone powder is used with 20% fly ash in ternary binder system, there are more amount of $Ca(OH)_2$ in the system than in the binary binder system of 30% fly ash, thus higher alkalinity is achieved in the system of FAM20LP10 (Kaewmanee & Tangtermsirikul, 2014). From XRD test results in Table 4.1 (in Chapter 4), the available Portlandite content obtained from paste mixture of FAM20LP10 is higher than that of FAM30, 9.75% and 7.53%, respectively. After the iron sulfide oxidation takes place in the tested mortar bars, the portlandite content of the tested mortar bars with iron sulfide-containing aggregates of FAM20LP10 mixture is still higher than the portlandite content of FAM30 mixtures, 0.38% and 0.31%, respectively

(Table 5.1). This explains the rust area results that FAM20LP10 has less rust area than FAM30.

In regard of pore structure, the ternary binder mixtures of both types of fly ashes have smaller average pore diameter than OPC-only mixture, but they have higher total porosity than OPC-only mixture. The average pore diameter indicates the pore size that the mortar systems contain. The pore size of any mortar systems is strongly related to the diffusion of water and oxygen into the mortar. The average pore diameter of FAM20LP10 is lower than OPC-only mixture. From Figures 4.2 and 4.3 (in Chapter 4), even though FAM20LP10 mixture has larger critical pore size than OPC-only mixture, it has more pores with smaller size (less than 10 nm) than OPC-only mixture. With both high alkalinity level in the system and many pores with small size of FAM20LP10 mixture, it shows less rust area than OPC-only mixture. The less rust area observed in FAM20LP10 mixture when compared to FAM30 mixture may be the contribution from the alkalinity level of the system since the average pore diameter of FAM20LP10 mixture is larger than FAM30 mixture, and the total porosity of both mixtures is similar.

On the other hand, when low CaO fly ash is used with limestone powder at 30% replacement in ternary binder system, the rusting problem is enhanced minimally from OPC-only mixture (Figure 5.8). Table 4.1 (in Chapter 4) shows that FAB20LP10 mixture provides more available portlandite content than FAB30 mixture. This is because FAB20LP10 is replaced with less amount of low CaO fly ash than FAB30 mixture. Hence, FAB20LP10 mixture shows less rust area than FAB30, though after iron sulfide oxidation occurs, portlandite content of FAB20LP10 mixture becomes lower than that of FAB30 mixture as seen in Table 5.1. On the other hand, FAB20LP10 mixture has smaller average pore size than OPC-only mixture (Table 4.3 in Chapter 4), hence it shows slightly less rust area than OPC-only mixture despite the lower portlandite content of FAB20LP10 mixture than OPC-only mixture.

It can be observed that with the addition of limestone powder to both systems of fly ashes (FAM20LP10 and FAB20LP10), the rust area on the mortar bar's surface is reduced. Furthermore, the reduction in rust area is more visible in the ternary system of high CaO fly ash than low CaO fly ash. This is mainly credited to the higher alkalinity level presents in FAM20LP10 mixture than in FAB20LP10 mixture.
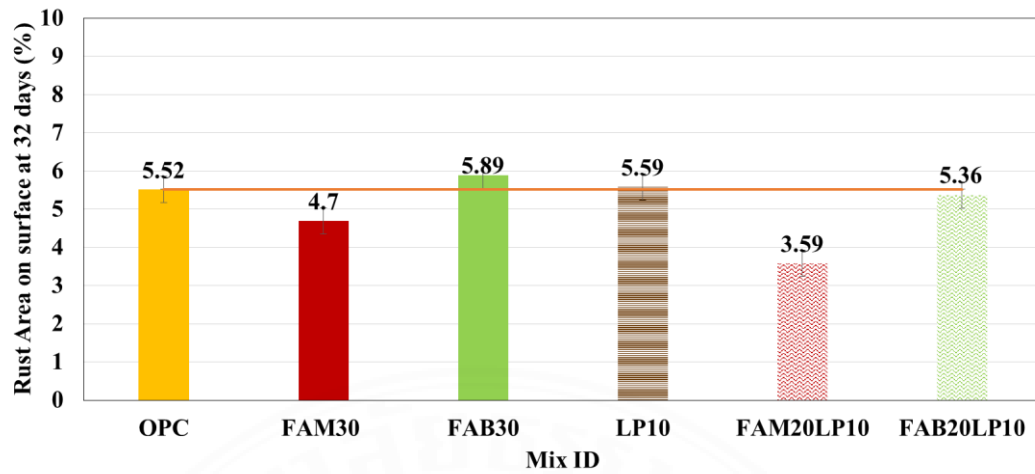
Figure 5.8 Effects of limestone powder in ternary binder system of FA-LP-OPC

5.3 Effects of calcined clay

Among all the binders that are used in binary binder system, the mixture of calcined clay at 45% replacement (CC45) shows the highest rust area on the surface of specimens (Figure 5.5). When compared to OPC, the rust area of CC45 is almost 3% more than OPC-only mixture. In contrast to the test result of expansion, recall that CC45 has the least expansion among all types of binders in binary binder system at all ages throughout the experimental test period. The differences between rust area of CC45 and FAB45 is 1.4% and between CC45 and FAM45 is 2.6%. From the MIP test results, it can be said that porosity of the mortar system is not the main reason for the large rust area occurred. According to many research (Bonen, 1993; Frías & Cabrera, 2000; Oriol & Pera, 1995), system with calcined clay shows great pore refinement since 3 days. And this porosity is reduced at early age which is earlier than systems with fly ash or limestone powder. From the chemical reactions, iron sulfide oxidation initiates when sufficient water and moisture come into contact with the iron sulfide particles. With respect to this, the system with calcined clay would be one of the excellent mixtures to reduce rust staining since the penetration of water and moisture is restricted. However, regarding the results in Figure 5.5, it is not. Therefore, the main mechanism is likely the alkalinity level of the mortar system.

From Table 5.1, portlandite content from CC45 mortar mixture is shown to be 0.13%, which is lower than that of OPC-only mixture and mixtures with fly ashes. This

is due to the highly reactive pozzolanic action of calcined clay which consumes large amount of calcium hydroxide since early age (as explained in section 4.3). Therefore, the amount of calcium hydroxide available in the system is less. Additionally, the amount of calcium in the system is reduced due to cement dilution effect as well. This condition is very favourable for the system in reducing expansion, but it makes the system likely vulnerable to gaining more rust stain. The same trend is also observed from the study of Sudsawong (2022). They found that available portlandite content of mortar mixtures with non-reactive aggregate in binary mixture of CC45 was lower than OPC-only mixture (1.52% and 13.92%, respectively).

5.3.1 Effects of limestone powder in ternary binder system of CC-LP-OPC

When limestone powder is used together in the mixture with calcined clay at 45% replacement (CC30LP15), the rust area on the specimens slightly drops by almost 0.25% from CC45 binary binder mixture (Figure 5.9). However, it is still considered having a significantly high magnitude. CC30LP15 has much higher rust area than OPC-only mixture and higher than binary mixtures containing the high or low CaO fly ash at the same replacement percentage of 45%. This drop in value of rust area observed in CC30LP15 mixture shall be due to the less amount of calcined clay used in CC30LP15 system than in CC45 system. In consequence, more calcium hydroxide is present in the mortar and higher alkalinity level in the system.

In addition, the study of Dhandapani and Santhanam (2017) found that the system of calcined clay and limestone powder shows reduction in pore size from 3 days. This is additionally due to the filler effect and fineness of limestone powder. With this expected smaller pore diameter and higher alkalinity level in CC30LP15 system than in CC45 mixture, the rust area shown in CC30LP15 mixture is lower than in CC45 mixture. Also, according to the study of Sudsawong (2022). Their results also showed that the mortar mixture with non-reactive aggregate of CC30LP15 had more portlandite content than CC45 mixture (2.78% and 1.52%, respectively). These results support the results of less rust area shown on mortar bar surface of CC30LP15 than is shown on mortar bar surface of CC45 mixture.

5.3.2 Effects of quaternary binder system of FA-CC-LP-OPC

When high CaO fly ash is added to the system of calcined clay and limestone powder, the magnitude of rust area is lower than CC45 and CC30LP15 mixtures (Figure 5.9). The difference between CC30LP15 and CC20LP10FAM15 is 0.8%, which is not significant, but still better than the mixture of low CaO fly ash and CCLP at 45% replacement. From Figure 5.9, CC20LP10FAB15 shows rust area at 32 days equal to 8.06% while CC30LP15 shows 8%. Using quaternary binder system of high CaO fly ash, calcined clay, and limestone powder does enhance the reduction in rust staining. Less rust area is obtained than CC30LP15 and CC45. But the rust area on this quaternary binder mixture is still considered high when compared to OPC-only mixture. Low CaO fly ash does not aid the rusting problem as much as high CaO fly ash does, which is opposite to the expansion results that low CaO fly ash reduces expansion more efficiently than high CaO fly ash. Following the above explanation in this chapter, this difference must come from the amount of $Ca(OH)_2$ available in the system that implies the alkalinity level of the mortar system. As known that high CaO fly ash contains more CaO content and free lime than low CaO fly ash. When high CaO fly ash is used with CC and LP, the system obtains more calcium hydroxide than the system that is replaced with low CaO fly ash. Consequently, CC20LP10FAM15 yields more calcium hydroxide, hence higher alkalinity level in mortar system than CC20LP10FAB15, and so lower area of rust. Similarly, the study of Sudsawong (2022) showed that the mortar mixture with non-reactive aggregate of CC20LP10FAM15 had more portlandite content than CC30LP15 and CC45 mixtures (3.32%, 2.78% and 1.52%, respectively). These results support the results of less rust area shown on mortar bar surface of CC20LP10FAM15, when high CaO fly ash is used to replace calcined clay and limestone powder in the system, than CC30LP15 and CC45 mixtures. The alkalinity level in CC20LP10FAM15 mixture is slightly higher than in the system of CC20LP10FAB15 due to the higher amount of $Ca(OH)_2$ in system when high CaO fly ash is used when compared to system with low CaO fly ash. Therefore, CC20LP10FAM15 mixture shows slightly less rust area than CC20LP10FAB15 mixture.

In aspect of pore structure, both calcined clay and fly ash exhibit active pozzolanic reaction. Calcined clay reduced porosity at early age from 3 days. Fly ash

reduced porosity from 14 days and continue into later age. Also, limestone powder contributes to the filler effect that would give the system smaller pore size. When used together, these three cement replacing materials tend to reduce porosity of the mortar system. Therefore, CC20LP10FAM15 and CC20LP10FAB15 show less rust area than CC45 mixture, and show equivalent rust area to CC30LP15 mixture. Pore refinement can be considered as supporting mechanism that may reduce amount of water and oxygen penetration into the mortar system which later reduce chance of iron sulfide oxidation.
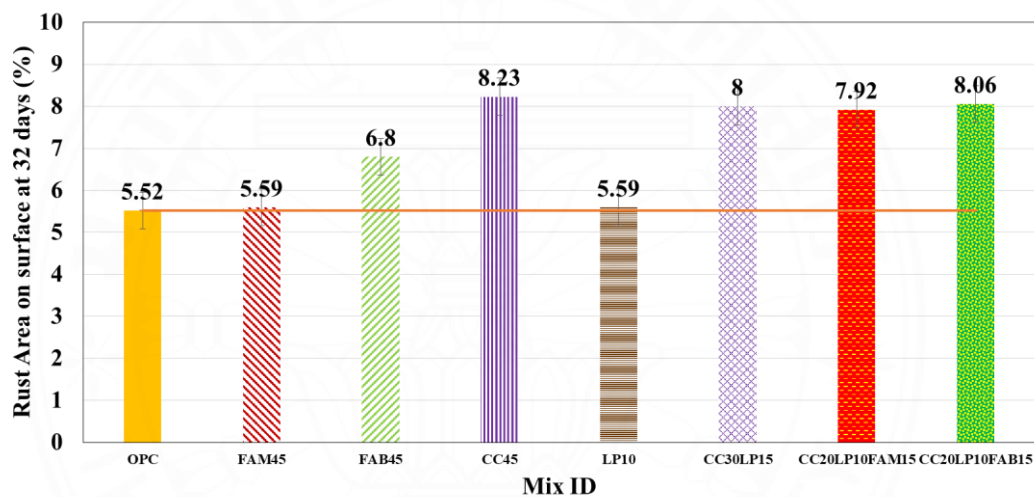
Figure 5.9 Effects of calcined clay on rust staining due to iron sulfide oxidation

5.4 Effects of silica fume

The effect of silica fume on rusting due to iron sulfide oxidation when it is used at 10% replacement does not give promising results. With silica fume in the mixture, the rust area at 32 days of the specimens is 7.88% which is significantly higher than OPC-only mixture (Figure 5.5). The percentage difference is almost 2.5%. SF10 specimens show the second highest rust area when comparing among binary binder systems. SF10 is second only to binary binder mixture of calcined clay, CC45 by about 0.4%.

Similar to calcined clay, silica fume is another cement replacing material that is reactive since early age. Therefore, with replacement of silica fume in mortar system, in terms of alkalinity level, the system exhibits low level of Portlandite content. Silica

fume also known for its ultra-fine particles which acts as filler. But in another way these ultra-fine particles also performs in increasing rate of reaction by its large surface area. This is another supportive reason for its high consumption of calcium hydroxide in the system, even though less amount of silica fume is being used. In addition, high reactivity of silica fume since early age also results in refinement of pore structure. Even though the porosity is refined, the mixture of SF10 still shows high rust area than binary mixtures of both types of fly ash. Therefore, the low alkalinity level should be a major reason for this large rust area of SF10 mixture since there is a high consumption of calcium hydroxide in the system, and this indicates that alkalinity seems to be more important than the pore structure in reducing rusting.

5.4.1 Effects of silica fume in ternary binder system of FA-SF-OPC

As can be seen from the effects of the binary binder system on rusting, both low CaO fly ash and silica fume cause more rust area than OPC-only mixture. While low CaO causes slightly higher rust area, silica fume results in an obvious higher rust area. When silica fume and low CaO fly ash are combined to observe their performances in ternary binder system, the results as shown in Figure 5.10 are unsurprising. The rust area amount of FAB20SF10 lies in between the rust area from binary binder systems of silica fume at 10% replacement and low CaO fly ash at 30% replacement. When compared to other ternary binder systems such as FAM20LP10 and FAB20LP10, the rust area yielded in FAB20SF10 is the largest. This mechanism is certainly manipulated by the alkalinity level of the mortar system. Among the binary and ternary binder systems with fly ash, FAM20LP10 has the highest amount of calcium hydroxide due to the use of high CaO fly ash. When low CaO fly ash is replaced, the calcium hydroxide content would be less than the system with high CaO fly ash at the same replacement percentage. Moreover, when replacing limestone powder which possesses low reactivity with silica fume which is highly reactive, the calcium hydroxide depletion in the system is noticeable. Consequently, low alkalinity level is observed in the system of FAB20SF10.
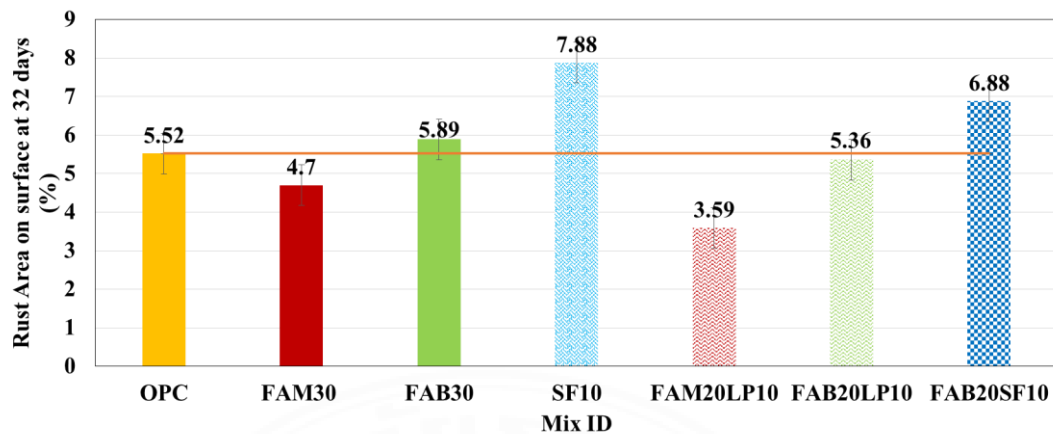
Figure 5.10 Effects of silica fume in ternary binder system of FA-SF-OPC on rust staining due to iron sulfide oxidation

5.5 Summary of rust area results

Among all the tested systems of binders used in the study regarding the evaluation of rusting due to iron sulfide oxidation, the ternary binder mixture of high CaO fly ash and limestone powder at 30% replacement (FAB20LP10) shows the lowest magnitude of rust area, which is also lower than OPC-only mixture. Binary mixture of calcined clay with cement (CC45) shows the highest magnitude of rust area. The results of rust and expansion due to iron sulfide oxidation is totally opposite.

When the replacement at 10% is considered, the binary binder mixture of limestone powder shows significantly lower rust area than silica fume mixture, but is still not much lower than OPC only mixture.

At 30% replacement, the ternary binder system of high CaO fly ash and limestone powder shows the lowest rust area. It is followed by the binary binder system of high CaO fly ash, and then, the ternary binder system of low CaO fly ash and limestone powder. These 3 mixtures show lower rust area than OPC-only mixture. While the binary binder system of low CaO fly ash only shows a little more rust area than OPC-only mixture. And the worst mixture among the mixtures at 30% replacement is the ternary binder mixture of low CaO fly ash and silica fume that shows obviously more rust area than OPC-only mixture.

Finally, at 45% replacement, the binary binder system of high CaO fly ash shows the lowest rust area which is close to the rust area results of OPC-only mixture,

followed by binary binder system of low CaO fly ash, but with much more rust area than OPC-only mixture. In addition, all the mixtures with 45% replacement and contain calcined clay shows significantly higher magnitude of rust area than OPC-only mixture.

The summary of both expansion and rust area results is shown in Table 5.3. All the tested mortar mixtures are compared with OPC-only mixture.

Table 5.3 Summary of both expansion and rust area results using OPC-only mixture as the benchmark for comparison

Binder Systems	Mix ID	Expansion Results	Rust Area Results	Remark
2 binders (binary)	LP10	(=)	(=)	
	SF10	✓✓	✗✗	
	FAM30	✗✗	✓✓	
	FAB30	✓	✗	
	FAM45	✗	✗	
	FAB45	✓	✗	
	CC45	✓✓*	✗✗	*shows shrinkage
3 binders (ternary)	FAM20LP10	✗	✓✓	
	FAB20LP10	✓	✓	
	FAB20SF10	✓✓	✗	
	CC30LP15	✓*	✗✗	*shows shrinkage
4 binders (quaternary)	CC20LP10FAM15	✓	✗✗	
	CC20LP10FAB15	✓✓	✗✗	

Remark: ✓✓ = best; ✓ = better; (=) = equivalent; ✗ = worse; ✗✗ = worst

5.6 Correlation between expansion results and rust area

The correlation was made between the results obtained from the two performance evaluations carried throughout this study, which are expansion of mortar bars and rust area on the mortar bars' surface. The plot of the expansion results versus rust area, both at 32 days, of the mortar bars is shown in Figure 5.11. The correlation shows that though being a little scattered, the expansion results and rust area tend to

have a reversed relationship. For the mortar mixtures that expand massively, they demonstrate low rust area, while, the mixtures that expand merely low show high rust area. This indicates that both problems (expansion and rust staining) are governed by different mechanisms.
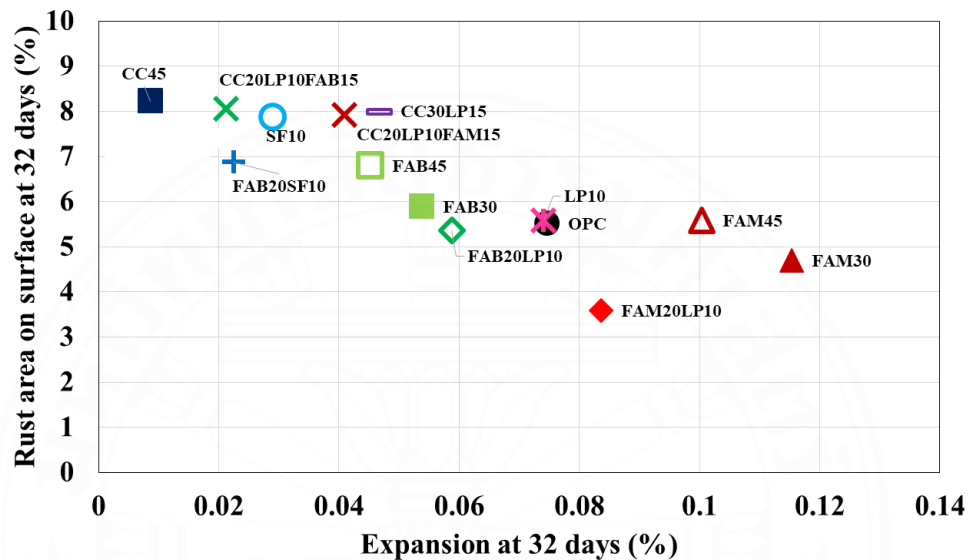
Figure 5.11 Correlation between expansion results and rust area

From the explanations in Chapters 4 and 5, the correlation can be drawn. Firstly, the expansion due to iron sulfide oxidation can be reduced by lowering the amount of $Ca(OH)_2$ of the mortar system. In order to obtain this sequence, first means, the use of cement replacing materials can provide an effect of cement dilution. With the use of CRM, the amount of cement is reduced, hence the amount of calcium hydroxide produced from cement hydration is reduced. Second means, choosing the CRMs that possess high pozzolanic reactivity in order to earn benefit from pozzolanic reaction. During pozzolanic reaction, the pozzolanic materials consume more calcium hydroxide, then less amount of calcium hydroxide is left to react with sulfuric acid. Therefore, less chance of production of gypsum and ettringite to occur. This is the reason that mixtures with fly ash, calcined clay, and silica fume show less expansion in the study than OPC-only mixture. However, from the study, it is now known that the chemical composition of the cement replacing materials should also be taken into consideration. As can see that even fly ash is a good CRM in many durability

performances of concrete, but fly ash with high CaO and SO_3 amount can further accelerate the expansion due to iron sulfide oxidation. Besides these chemical aspect, physical properties of the CRMs are also important. CRMs with high fineness greatly yield more surface area for better chemical reactions they participate in, later yields more effective pozzolanic reactivity.

Pore structure may portray one important role in term of expansion due to iron sulfide oxidation. The pore structure can be the transportation paths for water and moisture from the environment into the concrete, referring the mechanism of iron sulfide oxidation that the reaction starts when iron sulfide comes into contact with enough moisture and oxygen. In this aspect, the refined pore structure is definitely reducing the chance for iron sulfide oxidation to get initiated. On the other hand, for the rust staining on mortar's surfaces, refinement of pore structure seems to be a secondary supporting mechanism that benefits the rust prevention on the concrete surface.

The other mechanism that is dominant is the alkalinity or pH level of the mixtures. The main mechanism for reducing rust stain is the alkalinity of the concrete matrix. With the use of cement replacing materials in the mixture, the alkalinity is reduced when compared to the OPC-only mixture in which the alkalinity level is around 13. This is due to less amount of calcium hydroxide in the system which provides alkalinity to the concrete pore solution. Now, the different role of calcium hydroxide content is seen, with high amount of calcium hydroxide, high expansion is achieved, but lower rust staining is yielded, and vice versa.

Practically, the main thing that has to be considered to answer which mix proportion is the best to overcome the deterioration due to iron sulfide oxidation lies on the practical usage of the mixtures whether which member of the structure they are used for. Figure 5.12 shows the same results of correlation between expansion results and rust area as those shown in Figure 5.11, but with additional zoning to categorize the results into applicable groups for real practice, Zone I, II, III, and IV. The mixture of OPC-only is used here as the benchmark for comparison. Zone I is categorized as the mixtures that showed unfavourable performance in both reducing expansion and rust staining on the structure's surface. Zone II is the mixtures that showed less rust area, but does not reduce expansion such as the binary binder system with high CaO fly ash.

Zone III consists of only one mixture that is FAB20LP10 where it performs greatly in reducing both expansion and rust staining. Lastly, Zone IV, where most of the mixtures are collected here. They are the mixtures that showed a range of great to outstanding results in reducing expansion, however, they are poor in reducing rust staining, such as those mixtures with calcined clay, silica fume, and binary mixtures of low CaO fly ash. Suppose that a foundation is to be constructed, since the foundation is the important member that should carry and transfer load of the whole structure and it is underground so the surface appearance can be neglected. However, the mixture should be designed to reduce expansion due to iron sulfide oxidation. On the other hand, for wall members above ground, appearance is more important and strength is slightly overlook, so the mixture such as FAM20LP10 can be used. In this scenario, pop-out can be possibly generated from expansion due to iron sulfide oxidation. Therefore, in real practice, additional approach such as protective coating of the concrete structure should be considered.
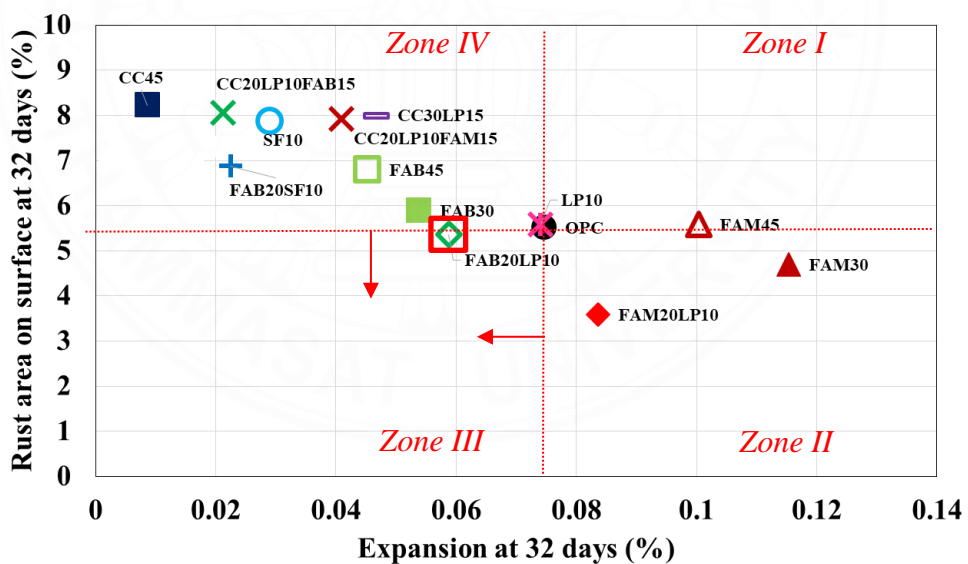

Figure 5.12 Correlation of expansion results and rust area with different zones indication

CHAPTER 6

VERIFICATION FOR MECHANISMS OF EFFECTS OF TYPES OF BINDERS ON EXPANSION AND RUSTING OF MORTAR BARS DUE TO IRON SULFIDE OXIDATION

To explain the mechanisms of expansion and rust staining due to iron sulfide oxidation, other than the microstructural tests, the modified iron sulfide oxidation was also repeated with the samples of OPC only mixture incorporating an iron sulfide-containing aggregate with addition of free lime and adjustment of water to binder ratio.

Nawaz, Julnipitawong, Krammart and Tangtermsirikul (2016) reported the effects of free lime content in fly ash on properties of mixtures with high free lime fly ash. From the test of alkali aggregate reaction, it was reported that with the increase in free lime content in concrete mixture, the expansion increases. The research found the increase in alkalinity in concrete system that is due to the additional calcium hydroxide from the free lime, which causes the expansion. Therefore, the additional free lime is added to the mortar mixtures to observe the effects of calcium hydroxide content on expansion and rust staining due to iron sulfide oxidation.

6.1 Verification of expansion mechanisms due to iron sulfide oxidation

Figure 6.1 demonstrates the expansion results due to iron sulfide oxidation to observe the hypothesis that whether or not the decrease in calcium hydroxide content will reduce the expansion due to iron sulfide oxidation. The results show that with the addition of free lime in the concrete system, the expansion increases. The OPC-only mixture has 1.6% free lime content in cement and is considered here as the control sample. When the free lime content in the cement is increased to 5%, the expansion increases 100 microns. Further, when the free lime in the cement is 10% in the cement, the expansion is almost 400 microns higher than the control sample. This test results support the fact that the increase in calcium hydroxide in the concrete system increases the expansion of the samples due to iron sulfide oxidation.
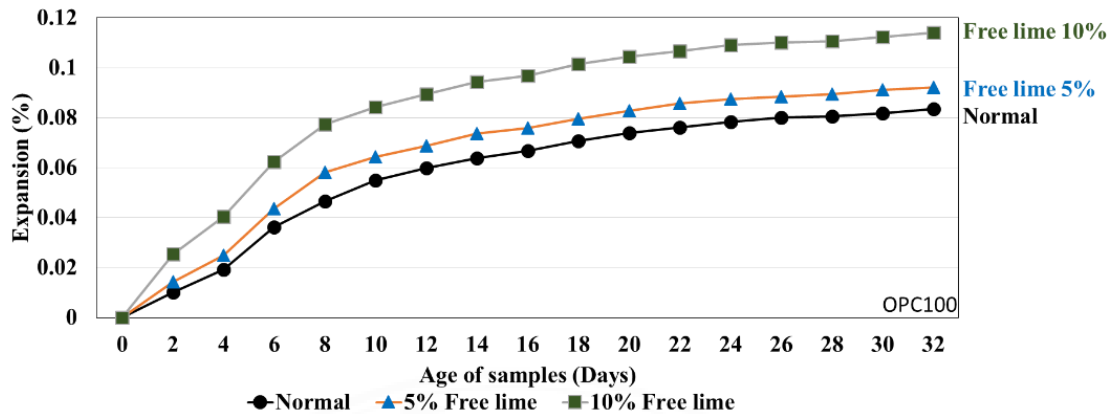
Figure 6.1 Expansion of mortar bars due to iron sulfide oxidation with the variation of free lime content in cement

Here, correlations between expansion results at 32 days of tested mixtures including fly ash, limestone powder, calcined clay and OPC-only mixtures and portlandite content are drawn. Firstly, the expansion results at 32 days and portlandite contents (from XRD test as shown in Tables 4.1 and 4.2) are plotted in Figures 6.2 and 6.3 (remark: portlandite contents of FAM45, CC45, CC30LP15 and CC20LP10FAM15 in Figure 6.2 are obtained from the study of Sudsawong, 2022). Figure 6.2 demonstrates the expansion results at 32 days and portlandite contents at 28 days in paste mixtures without iron sulfide-containing aggregates. While, Figure 6.3 demonstrates the expansion results at 32 days and portlandite contents in the tested mortar bars after the modified AMBT. Portlandite content in Figure 6.2 represents the available portlandite content in the mixture systems. It can be seen a good trend can be obtained that the mixtures with high available portlandite content shows high expansion due to iron sulfide oxidation. However, the mixtures with high CaO fly ash show a deviated trend that their expansions are away from and higher than other mixtures. This high expansion is basically due to the high CaO fly ash itself that it can produce expansive products such as ettringite and gypsum even without iron sulfide in the system (Chatchawan, 2017; Nguyen et al., 2019). So, when the iron sulfide-containing aggregate is used in the mixtures, the mixtures using high CaO fly ash show aggressively high expansion. On the other hand Figure 6.3 represents the portlandite content that is left after being consumed by the reaction of calcium hydroxide with sulfuric acid from iron sulfide oxidation and pozzolanic reaction of the mixtures. The

similar trend with Figure 6.2 is still observed in Figure 6.3 that the effects of cement dilution and pozzolanic reaction aid the problem of expansion due to iron sulfide oxidation. Therefore, there is a relationship between amount of calcium hydroxide in the mixtures and expansion of mixtures due to iron sulfide oxidation. In order to reduce the expansion due to iron sulfide oxidation, the amount of calcium hydroxide in the system should be maintained low.
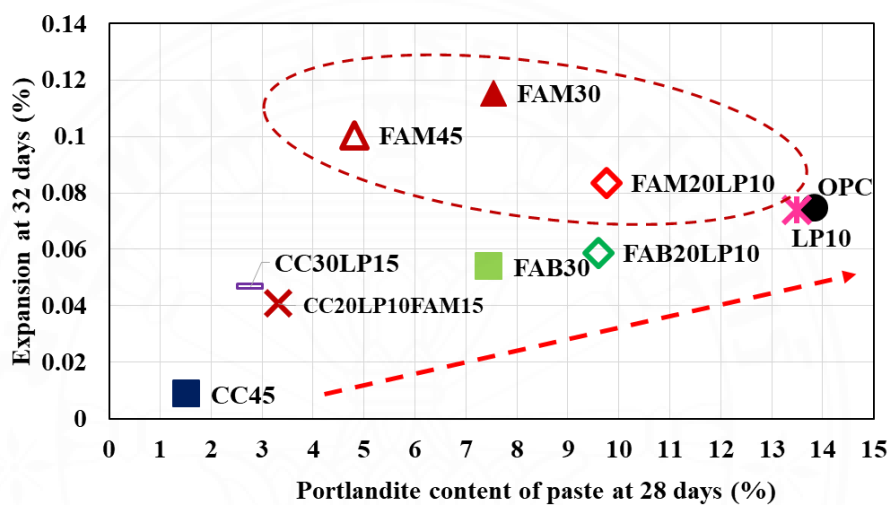

Figure 6.2 Correlation between expansion results at 32 days and portlandite content of paste mixtures at 28 days
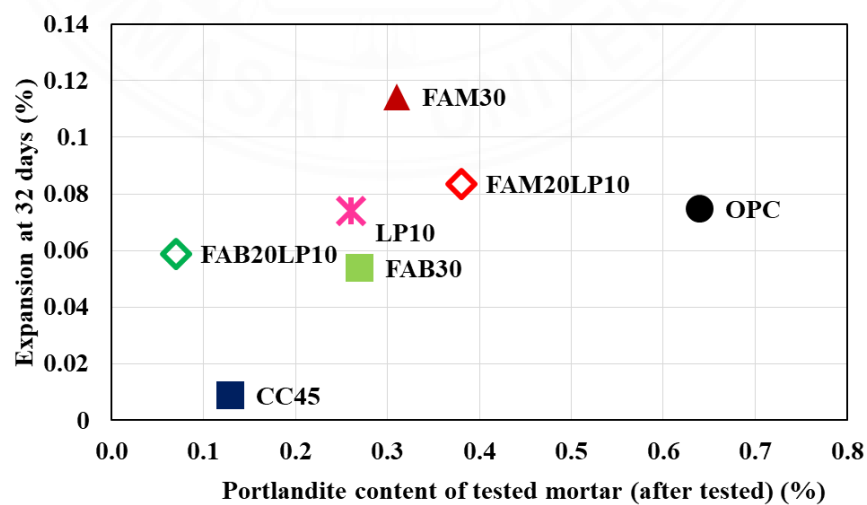

Figure 6.3 Correlation between expansion results at 32 days and portlandite content of tested mortar

Moreover, Figure 6.4 shows the correlation between expansion results at 32 days and amount of ettringite found in the tested mortar bars after they underwent the modified AMBT (according to Table 4.2). The figure shows that the mixture with high expansion has more amount of ettringite than the mixtures with low expansion, or vice versa. However, when the amount of gypsum (according to Table 4.2) is considered as shown in Figure 6.5, no good correlation can be found. This is because gypsum is an intermediate product which will later react with alumina phase in mortar system to produce ettringite. Therefore, the gypsum amount is not the main factor to explain the mechanism of expansion due to iron sulfide oxidation in this study. However, from Figure 6.4, it can be observed that even though the amount of ettringite found in FAM30 mixture is lower than OPC-only mixture, FAM30 mixture shows higher expansion than OPC-only mixture. This shows that the mechanisms of expansion due to iron sulfide oxidation should be further explained with the physical aspects of the mortar system such as the pore structure of mortar system.
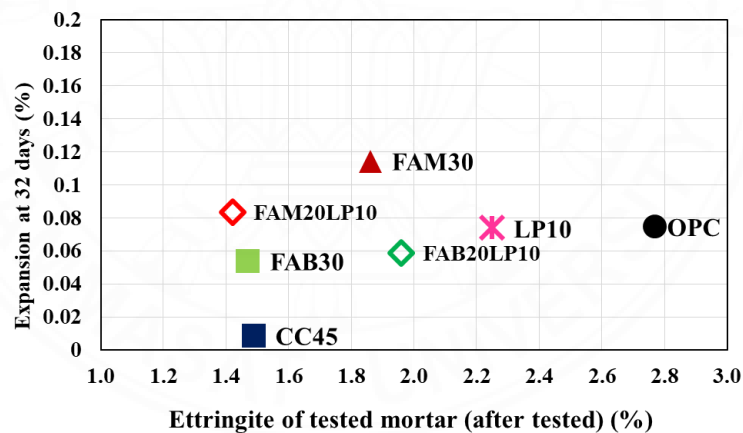

Figure 6.4 Correlation between expansion results at 32 days and ettringite content of tested mortar after modified AMBT
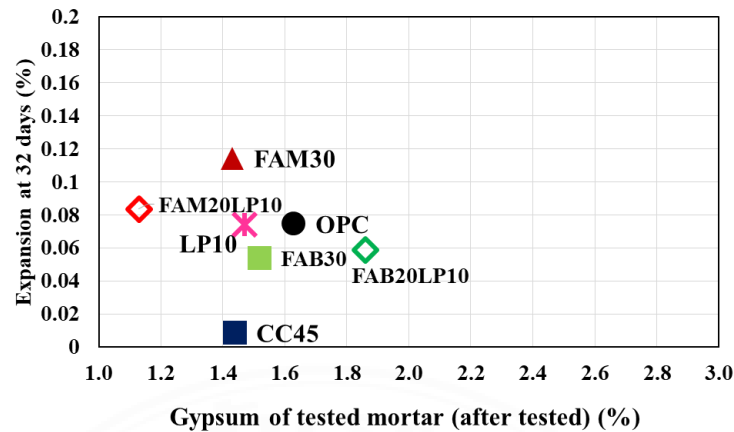
Figure 6.5 Correlation between expansion results at 32 days and gypsum content of tested mortar after modified AMBT

The modified accelerated mortar bar test was also conducted for the OPC-only mixtures that contain iron sulfide-containing aggregates where the water-to-binder ratio is varied. This test is done to observe the influence of the dense structure which can be implied to the lower penetration to the inner concrete system and the expansion due to iron sulfide oxidation. Figure 6.6 shows the expansion of the OPC-only mixture that incorporates iron sulfide-containing aggregate, where the only parameter varied is the w/b ratio. The control sample is the mixture of OPC-only with w/b equals to 0.45 which is the same w/b that is used for the main study. It is seen that when w/b increases, the expansion slightly increases though lower w/b is supposed to have higher alkalinity. This can support the assumption that the dense concrete structure can decrease the penetration of water and oxygen, therefore reduces the occurrence of iron sulfide oxidation.

Figure 6.6 Expansion of mortar bars due to iron sulfide oxidation with the variation of water-to-binder ratio

According to the results of average pore diameter and total porosity obtained from MIP test as shown in Table 4.3, correlations of expansion results at 32 days and aver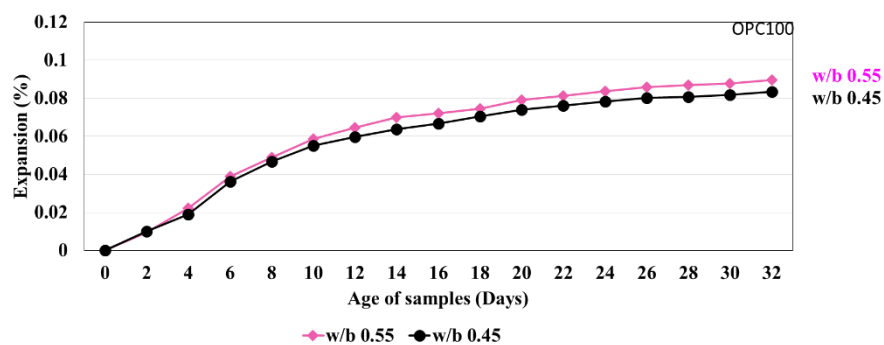age pore size and total porosity of paste mixtures are shown in Figures 6.7 and 6.8, respectively. In Figure 6.7, the mixtures with large expansion have larger average pore diameter than the mixtures with low expansion. This average pore diameter is basically the pore size of the mortar system. It means that the pore size of the mortar systems which dominates the diffusion of water and oxygen into the system has an important role in expansion due to iron sulfide oxidation. Mixtures with larger pore size tend to get more penetration of water and oxygen into the mortar system than mixtures with smaller pore size, therefore, there is more chance of iron sulfide oxidation to occur. In regard of total porosity, Figure 6.8 shows relationship between expansion at 32 days and total porosity. The mixtures with higher total porosity show lower expansion than mixtures with lower total porosity. This portrays that total porosity is also involved in the mechanisms of iron sulfide oxidation. With higher total porosity, more spaces are available in the mortar system to accommodate expansive products, producing lower expansive pressure. Therefore, the mixture with higher total porosity shows lower expansion than the mixture with lower total porosity. It is also noted that the mixtures with FAM show higher expansion above the trends in Figures 6.7 and 6.8 due to the same reason as mentioned earlier.
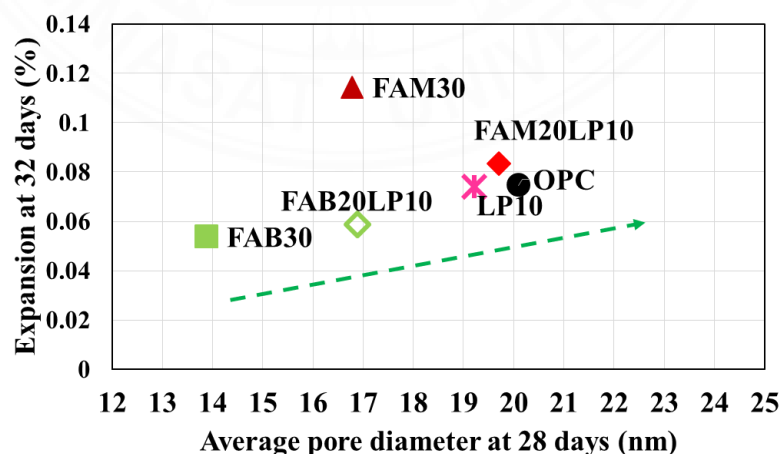
Figure 6.7 Correlation between expansion results at 32 days and average pore diameter of paste mixtures at 28 days
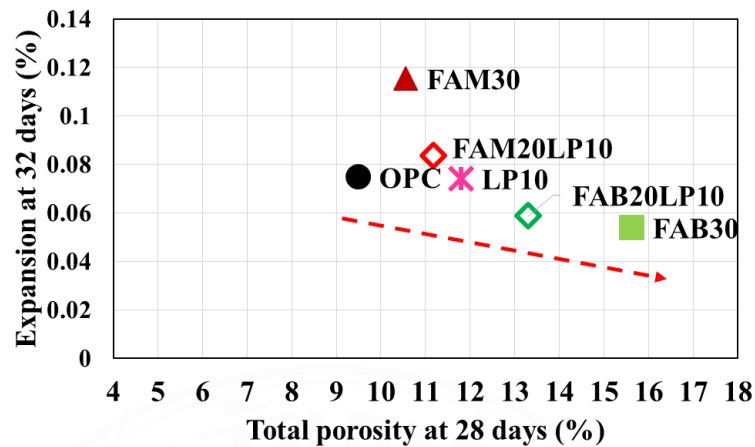
Figure 6.8 Correlation between expansion results at 32 days and total porosity of
paste mixtures at 28 days

6.2 Verification of rust staining mechanisms due to iron sulfide oxidation

The mortar bars that are added with additional free lime are also used in the
analysis for the rust area after they underwent the modified accelerated mortar bar test
for 32 days. The hypothesis is that with additional of free lime to the OPC-only mixture,
the alkalinity level of the concrete matrix increases, therefore, the rusting due to iron
sulfide oxidation should decrease. Figure 6.9 shows the test results. As expected, as the
free lime content increases, the rust area on the surface at 32 days becomes less. With
10% of free lime content in cement, the rust area is 3.24% which is almost 1.5% less
than that of the control OPC-only mixture with original free lime content in the cement.
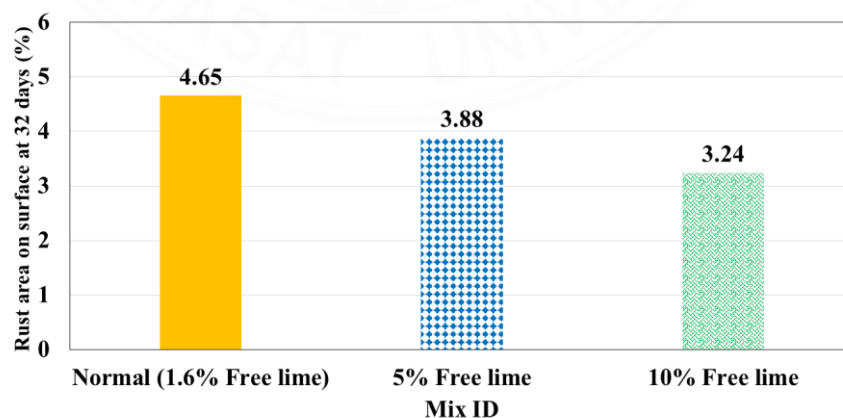
Figure 6.9 Rust area on surface of mortar bar due to iron sulfide oxidation with the
variation of free lime content in cement

Similarly, correlations between rust area results and portlandite content are made. Figure 6.10 depicts the correlation between rust area results and available portlandite content from paste mixtures at 28 days. The mixtures that contain high amount of portlandite content such as mixtures with high CaO fly ash show less rust area than mixtures that contain low portlandite content, and vice versa. As portlandite represents the alkalinity level of the mortar system, the mixtures with high portlandite contents yield high alkalinity level of the pore solution, thus, they show less rust area. And in Figure 6.11, the graph of amount of portlandite content of mortar bars that have underwent modified AMBT versus rust area results at 32 days is shown. The figure shows the remaining portlandite content after it is partially consumed by the pozzolanic reaction and the chemical reaction with sulfuric acid. It can be seen that the mixtures with high CaO fly ash still maintains high amount of portlandite content.

Figure 6.10 Correlation between rust area results at 32 days and portlandite content of paste mixtures at 28 days
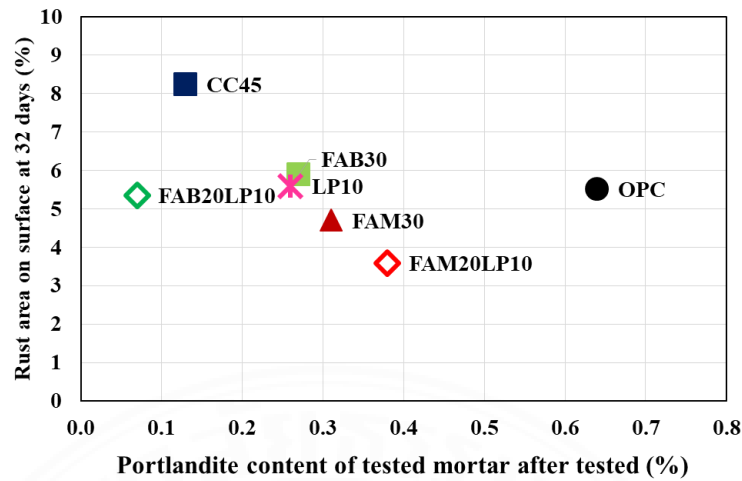
Figure 6.11 Correlation between rust area results at 32 days and portlandite content of tested mortar after modified AMBT

The mortar bars with varied w/b ratio that underwent the modified accelerated mortar bar test are also used to analyse the rust area on the mortar surface at 32 days. Figure 6.12 shows the rust area result at 32 days of the mixture with w/b of 0.45 and 0.55. With lower w/b ratio, the rusting is higher. As the hypothesis was that dense concrete structures might be able to reduce the chance of occurrence of iron sulfide oxidation (even though, the dense structure cannot be perfectly represented only by the w/b of mixtures, it can still be used to observe the trend of the results). However, as the results show that the mixture with w/b of 0.45 demonstrates more rust staining than that with w/b of 0.55. So this results can support the assumption made before that the pore structure is not the main factor that govern rust staining due to iron sulfide oxidation.
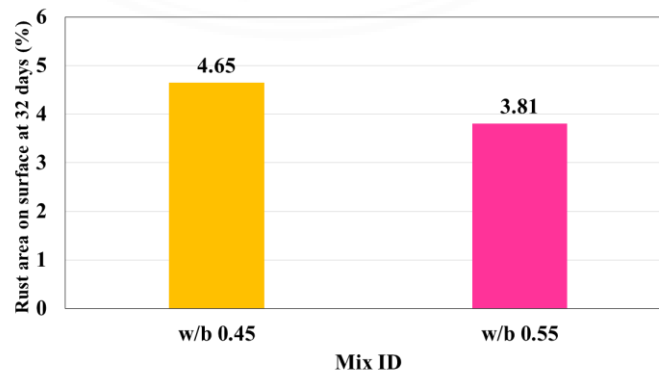
Figure 6.12 Rust area results on surface of mortar bar due to iron sulfide oxidation with the variation of water-to-binder ratio

Lastly, the results of average pore diameter and total porosity from MIP test are analysed to explain the rust area results. Figure 6.13 is a graph showing a relationship between rust area results at 32 days and average pore diameter of paste mixtures at 28 days. The figure shows that there is no relationship between the rust area and average pore diameter. Also, Figure 6.14 shows a graph of rust area plotted against total porosity of paste mixtures at 28 days. Figure 6.14 also shows that there is no correlation between the rust area results and total porosity of the mixtures. Therefore, the conclusion can be drawn that regarding mechanisms of rust staining due to iron sulfide oxidation, pore structure may act as a path for diffusion of water and oxygen into the mortar system. However, pore structure is merely a supporting mechanism for amount of rust area staining on mortar surface. The main mechanism that governs the rust staining due to iron sulfide oxidation is the alkalinity level of the mortar system. The alkalinity level of the mortar system should be maintained high in order to reduce rust staining on mortar surface.
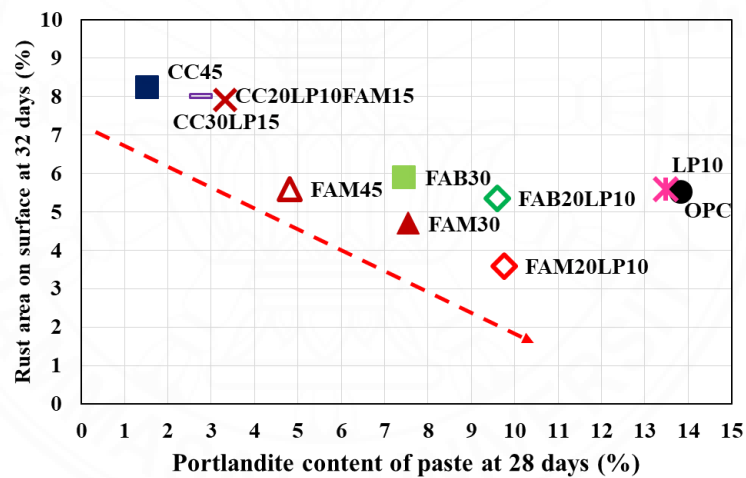

Figure 6.13 Correlation between rust area results at 32 days and average pore diameter of paste mixtures at 28 days

Figure 6.14 Correlation between rust area results at 32 days and total porosity of

paste mixtures at 28 days

CHAPTER 7

CONCLUSIONS AND RECOMMENDATIONS FOR FURTHER STUDIES

7.1 Conclusions

This study aims to find the proper mix proportion to reduce the damages caused by iron sulfide oxidation which include both expansion and rust staining, using cement replacing materials. From the test results, the following conclusions can be drawn:
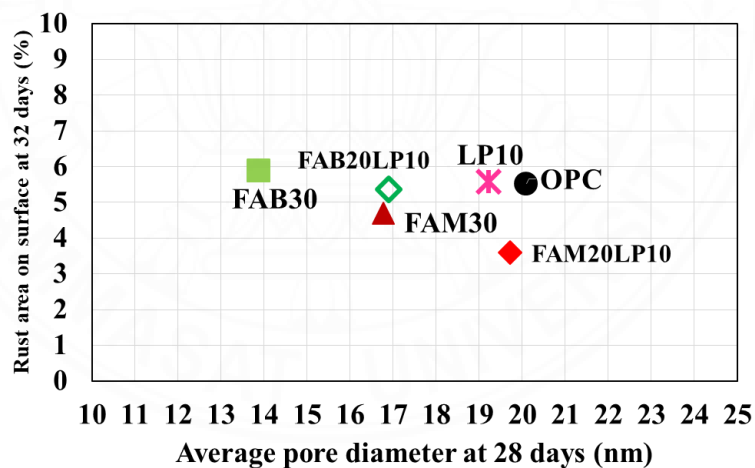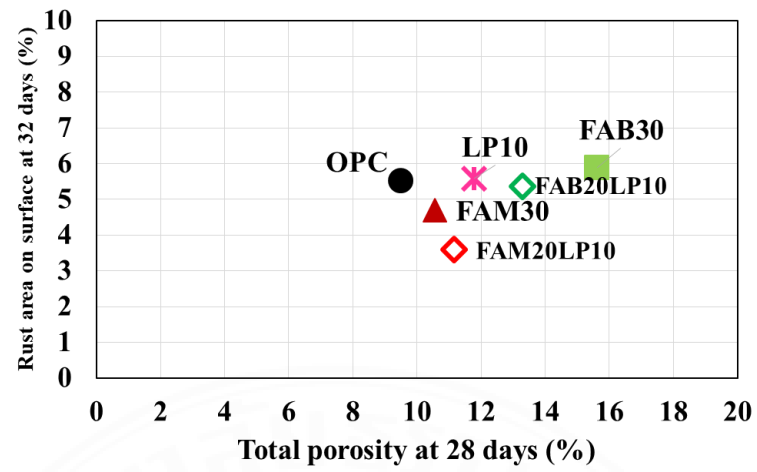
1) Calcined clay shows the best performance in reducing expansion. All the mixtures that contain calcined clay show promising low expansion. All these mixtures, except for the quaternary binder system of calcined clay, limestone powder and high CaO fly ash, show small shrinkage at 20 days.

2) Adversely, when considering rusting, calcined clay binary mixture shows the highest amount of rust area, also higher than OPC-only mixture. All the mixtures that contain calcined clay in the mixtures also show high rusting area.

3) Low CaO fly ash shows good result in reduction of expansion, and it reduces expansion obviously better than high CaO fly ash. In contrast to the result of expansion, the performance in rust area reduction of low CaO fly ash is worse than the OPC.

4) Contradicting to the performance of low CaO fly ash, high CaO fly ash causes remarkably higher expansion than OPC. However, it results in less rust stain than low CaO fly ash and much less than OPC.

5) When replacement percentage of fly ash is considered, 45% replacement of fly ash causes more reduction in expansion than 30% replacement. This characteristic is obtained for both types of fly ashes. For rust area, using fly ash at a higher replacement results in more rust staining and is not better than OPC-only mixture.

6) Limestone powder, when using in binary binder mixture, shows equivalent expansion results to OPC mixture. However, it shows negative effects for rust staining with a slightly more rust than OPC.

7) Limestone powder works jointly with both types of fly ashes in rust area reduction. While showing better performance in reducing expansion with high CaO fly ash, it shows not as good expansion reduction as in binary binder system of low CaO fly ash.

8) Silica fume causes very low expansion similar to calcined clay, but without shrinkage. However, it is still not as good as calcined clay in reducing expansion. On the other hand, for rusting, it shows unpleasant high rust area, but is still better than calcined clay binary binder mixture.

9) According to the study, both expansion and rust staining are governed by different main mechanisms. To reduce expansion, the amount of $Ca(OH)_2$ in the system and pore size should be reduced. While, to reduce rust staining, the alkalinity of the concrete should be maintained high.

10) In conclusion, the only tested mixture that can overcome both problems of iron sulfide oxidation which are expansion and rusting, is the ternary binder system of low CaO fly ash and limestone powder. It is the only mixture that shows better performance than OPC with regard to both expansion and rusting.

7.2 Recommendations for further studies

Problems due to iron sulfide oxidation is becoming vivid in many regions all over the world. Recently, many areas worldwide have encountered this issue including Thailand. However, the means to solve the problem is still unclear. As mentioned in Chapter 1, the solution consisting of three parts is proposed. With the design of proper mix proportion only does not entirely solve the problems. It has to be done in corporate with the last part of the solution which is the protection of the concrete structures. This protection is basically the coating technique. Further study should be done to study the effects of proper mix proportion and the coating together to solve both expansion and rusting due to iron sulfide oxidation. Moreover, the study can be done with different types of cement with coating as well to observe the effects of cement types with coating.

This study just focus on short term effects of the types of cement replacing materials due to iron sulfide oxidation. Longer exposure of specimens in modified accelerated mortar bar test should be considered. Also, to better reproduce the condition that enables the rust production, the samples made with different types of cement

replacing materials can also be stored in water to observe rust production at a higher degree. Also, further investigation on pore structure of each tested mixtures should be carried out to truly understand the mechanisms of iron sulfide oxidation involving both expansion and rust staining.

After knowing more about the mechanisms of iron sulfide oxidation from effects of cement replacing materials from this study, better mix design to solve both expansion and rust staining problems from iron sulfide oxidation can be expected. From the study, the alkalinity solution of the concrete system should be high to reduce rust staining on the surface of concrete. On the other hand, the amount of calcium hydroxide in the concrete system should be low to reduce the expansion due to iron sulfide oxidation. Therefore, the alkalinity of the concrete system should be raised high. It can be done by introducing other alkaline sources into the mixture, but not the calcium hydroxide since it will react with sulfuric acid from iron sulfide oxidation and cause expansion. Additionally, the pore size of the concrete system should be minimized to reduce the diffusion of moisture and oxygen into the concrete. Coating of the concrete structure at the product level can be done to reduce the deterioration from iron sulfide oxidation.

REFERENCES

Afroz, S., Zhang, Y., Nguyen, Q. D., Kim, T., & Castel, A. (2023). Shrinkage of blended cement concrete with fly ash or limestone calcined clay. *Materials and Structures*, *56*(1), 15. Retrieved from https://doi.org/10.1617/s11527-023-02099-8.

Almenares, R. S., Vizcaíno, L. M., Damas, S., Mathieu, A., Alujas, A., & Martirena, F. (2017). Industrial calcination of kaolinitic clays to make reactive pozzolans. *Case studies in construction materials*, *6*, 225-232. doi: 10.1016/j.cscm.2017.03.005.

Amin, M., Zeyad, A. M., Tayeh, B. A., & Agwa, I. S. (2022). Effect of ferrosilicon and silica fume on mechanical, durability, and microstructure characteristics of ultra high-performance concrete. *Construction and Building Materials*, *320*, 126233. doi: 10.1016/j.conbuildmat.2021.126233.

Argın, G., & Uzal, B. (2021). Enhancement of pozzolanic activity of calcined clays by limestone powder addition. *Construction and Building Materials*, *284*, 122789. doi: 10.1016/j.conbuildmat.2021.122789.

ASSOCIATION FRANÇAISE DE NORMALISATION (1997). AFNOR NF P 18-540. *Granulats—Définitions*, conformite´, spe´cifications. Paris

ASTM, C 1260 (2014). Standard Test Method for Potential Alkali Reactivity of Aggregates (Mortar-Bar Method). *ASTM International*, West Conshohocken, PA. doi: 10.1520/C1260-07.

ASTM, D 516 (2016). Standard Test Method for Sulfate Ion in Water. *ASTM International*, West Conshohocken, PA. doi: 10.1520/D0516-16.

ASTM, C 595 (2012). Standard Specification for Blended Hydraulic Cements. *ASTM International*, West Conshohocken, PA. doi: 10.1520/C0595-08A.

ASTM, C 618 (2022). Standard Specification for Coal Fly Ash and Raw or Calcined Natural Pozzolan for Use in Concrete. *ASTM International*, West Conshohocken, PA. doi: 10.1520/C0618-22.

Baghabra, O. S., Maslehuddin, M., & Saadi, M. M. (1995). Effect of magnesium sulfate and sodium sulfate on the durability performance of plain and blended cements. *Materials Journal*, *92*(1), 15-24. doi: 10.14359/1173.

Banchong, N., Saengsoy, W., & Tangtermsirikul, S. (2020). Study on mechanical and durability properties of mixtures with fly ash from Hongsa power plant. *ASEAN Engineering Journal*, *10*(1), 9-24. doi: 10.11113/aej.v10.15535.

Bonen, D. (1993). A microstructural study of the effect produced by magnesium sulfate on plain and silica fume-bearing Portland cement mortars. *Cement and concrete research*, *23*(3), 541-553. doi: 10.1016/0008-8846(93)90004-S.

Chanachon Sudswong (2022). *Effects of calcined clay on properties of mortar and concrete*. Thammasat University. doi: 10.14457/TU.the.2022.172.

Chou, MI.M. (2012). Fly Ash. In: Meyers, R.A. (eds) *Encyclopedia of Sustainability Science and Technology*. New York, NY: Springer. doi: 10.1007/978-1-4419-0851-3_121.

Daniele Di Stefano. (2021). Cement: The Most Destructuve Mateial in the World or a Driver of Progress? Retrieved January 17, 2023 from https://www.renewablematter.eu/articles/article/cement-the-most-destructive-material-in-the-world-or-a-driver-of-progress#:~:text=Concrete%20is%20the%20most%20consumed,on%20the%20entirety%20of%20Iraq).

De Weerdt, K., Kjellsen, K. O., Sellevold, E., & Justnes, H. (2011). Synergy between fly ash and limestone powder in ternary cements. *Cement and concrete composites*, *33*(1), 30-38. doi: 10.1016/j.cemconcomp.2010.09.006.

Dhandapani, Y., & Santhanam, M. (2017). Assessment of pore structure evolution in the limestone calcined clay cementitious system and its implications for performance. *Cement and Concrete Composites*, *84*, 36-47. doi: 10.1016/j.cemconcomp.2017.08.012.

Dhandapani, Y., Sakthivel, T., Santhanam, M., Gettu, R., & Pillai, R. G. (2018). Mechanical properties and durability performance of concretes with Limestone Calcined Clay Cement (LC^3). *Cement and Concrete Research*, *107*, 136-151. doi: 10.1016/j.cemconres.2018.02.005.

Direct Industry. Liquid analyzer TGA 2 (SF). Retrieved February 7, 2023, from https://www.directindustry.com/prod/mettler-toledo/product-122171-2308617.html

Elahi, M. M. A., Reza, A. N. R., & Shearer, C. R. (2021). Controlling aluminate phase hydration for sulfate resistance of Portland–limestone cements. *Proceedings of the Institution of Civil Engineers-Construction Materials*, *174*(1), 34-46. doi: 10.1680/jcoma.19.00099.

El-Mosallamy, M., & Shehata, M. H. (2020). Sulphide oxidation mortar tests for evaluation of the oxidation potential of sulphide-bearing aggregate. *Construction and Building Materials*, *264*, 120627. doi: 10.1016/j.conbuildmat.2020.120627.

Frank Ruehlicke. Pyrite. Retrieved February 5, 2023, from https://www.mindat.org/min-3314.html

Frías, M., & Cabrera, J. (2000). Pore size distribution and degree of hydration of metakaolin–cement pastes. *Cement and Concrete Research*, *30*(4), 561-569. doi: 10.1016/S0008-8846(00)00203-9.

Fridrichová, M., Dvořák, K., Gazdič, D., Mokrá, J., & Kulísek, K. (2016). Thermodynamic Stability of Ettringite Formed by Hydration of Ye'elimite Clinker. *Advances in Materials Science and Engineering*, *2016*. doi: 10.1155/2016/9280131.

Guirguis, B., & Shehata, M. H. (2017). A new screening test to evaluate the presence of oxidizable sulphide minerals in coarse aggregates. *Construction and Building Materials*, *154*, 1096-1104. doi: 10.1016/j.conbuildmat.2017.07.198.

Guirguis, B., Shehata, M. H., Duchesne, J., Fournier, B., Durand, B., & Rivard, P. (2018). The application of a new oxidation mortar bar test to mixtures containing different cementing systems. *Construction and Building Materials*, *173*, 775-785. doi: 10.1016/j.conbuildmat.2018.04.026.

Jana, D. (2020). Pyrrhotite epidemic in Eastern Connecticut: diagnosis and prevention. *ACI Materials Journal*, *117*(1), 1-20. doi: 10.14359/51718059.

Jeyakaran, T., Pornsiri, N., Saengsoy, W., & Tangtermsirikul, S. (2023). Test methods for performance-based evaluation of concrete containing iron sulfide-bearing aggregates: Development and application. *Results in Engineering*, *18*, 101068. doi: 10.1016/j.rineng.2023.101068.

Kaewmanee, K., Krammart, P., Sumranwanich, T., Choktaweekarn, P., & Tangtermsirikul, S. (2013). Effect of free lime content on properties of cement–fly ash mixtures. *Construction and Building Materials*, *38*, 829-836. doi: 10.1016/j.conbuildmat.2012.09.035.

Kaewmanee, K., & Tangtermsirikul, S. (2014). Properies of binder systems containing cement, fly ash, and limestone powder. *Songklanakarin Journal of Science & Technology*, *36*(5). Retrieved from https://www.researchgate.net/publication/286798906_Properies_of_bin der_systems_containing_cement_fly_ash_and_limestone_powder.

Kasaniya, M., Thomas, M. D., & Moffatt, E. G. (2021). Pozzolanic reactivity of natural pozzolans, ground glasses and coal bottom ashes and implication of their incorporation on the chloride permeability of concrete. *Cement and Concrete Research*, *139*, 106259. doi: 10.1016/j.cemconres.2020.106259.

Lilkov, V., Petrov, O., Tzvetanova, Y., & Savov, P. (2012). Mössbauer, DTA and XRD study of Portland cement blended with fly ash and silica fume. *Construction and Building Materials*, *29*, 33-41. doi: 10.1016/j.conbuildmat.2011.10.030.

Mardani-Aghabaglou, A., Sezer, G. İ., & Ramyar, K. (2014). Comparison of fly ash, silica fume and metakaolin from mechanical properties and durability performance of mortar mixtures view point. *Construction and Building Materials*, *70*, 17-25. doi: 10.1016/j.conbuildmat.2014.07.089.

Mark Kucera. Pyrrhotite. Retrieved February 5, 2023, from https://www.mindat.org/min-3328.html

McCarthy, M. J., & Dyer, T. D. (2019). Pozzolanas and pozzolanic materials. *Lea's Chemistry of Cement and Concrete*, *5*, 363-467. doi: 10.1016/B978-0-08-100773-0.00009-5.

Micromeritics (2015, February). *AUTOPORE V SERIES MERCURY INTRUSION POROSIMETER OPERATOR MANUAL*. 962-42800-01 (Rev B). Retrieved February 7, 2023, from https://www.micromeritics.com/Repository/Files/AutoPore_V_Series_ Operator_Manual_-_Rev_B_0.pdf

Midgley, H. (1958). The Staining of Concrete by Pyrite. *Magazine of Concrete Research*, *10*(29), 75-78. doi: 10.1680/macr.1958.10.29.75.

Müllauer, W., Beddoe, R. E., & Heinz, D. (2013). Sulfate attack expansion mechanisms. *Cement and concrete research*, *52*, 208-215. doi: 10.1016/j.cemconres.2013.07.005.

Muller, A. C. A., Scrivener, K. L., Skibsted, J., Gajewicz, A. M., & McDonald, P. J. (2015). Influence of silica fume on the microstructure of cement pastes: New insights from 1H NMR relaxometry. *Cement and Concrete Research*, *74*, 116-125. doi: 10.1016/j.cemconres.2015.04.005.

Nawaz, A., Julnipitawong, P., Krammart, P., & Tangtermsirikul, S. (2016). Effect and limitation of free lime content in cement-fly ash mixtures. *Construction and Building Materials*, *102*, 515-530. doi: 10.1016/j.conbuildmat.2015.10.174.

Nguyen, Thuy Bich Thi (2018). *Use of fly ash and bottom ash to enhance performance of expansive concrete*. Thammasat University. doi: 10.14457/TU.the.2018.934.

Nguyen, T. B. T., Chatchawan, R., Saengsoy, W., Tangtermsirikul, S., & Sugiyama, T. (2019). Influences of different types of fly ash and confinement on performances of expansive mortars and concretes. *Construction and Building Materials*, *209*, 176-186. doi: 10.1016/j.conbuildmat.2019.03.032.

Nochaiya, T., Wongkeo, W., & Chaipanich, A. (2010). Utilization of fly ash with silica fume and properties of Portland cement–fly ash–silica fume concrete. *Fuel*, *89*(3), 768-774. doi: 10.1016/j.fuel.2009.10.003.

Oliveira da Silva, I., Pialarissi Cavalaro, S. H., & Aguado de Cea, A. (2014). Evolution of pyrrhotite oxidation in aggregates for concrete. *Materiales de construcción (Madrid)*, *64*(316). doi: 10.3989/mc.2014.08413.

Oriol, M., & Pera, J. (1995). Pozzolanic activity of metakaolin under microwave treatment. *Cement and Concrete Research*, *25*(2), 265-270. doi: 10.1016/0008-8846(95)00007-0.

Pawee Sinlapasertsakulwong (2019). *Detection of iron sulfide-bearing aggregates by chemical tests and accelerated mortar bar method.* Thammasat University. doi: 10.14457/TU.the.2019.46.

Rachot Chatchawan (2017). *Use of fly ash to enhance performance of expansive concrete*. Thammasat University. doi: 10.14457/TU.the.2017.334.

Ramos, V., Rodrigues, A., Fournier, B., & Duchesne, J. (2016). Development of a quick screening staining test for detecting the oxidation potential of iron sulfide-bearing aggregates for use in concrete. *Cement and Concrete Research*, *81*, 49-58. doi: 10.1016/j.cemconres.2015.11.011.

Rashad, A. M. (2015). A brief on high-volume Class F fly ash as cement replacement–A guide for Civil Engineer. *International journal of sustainable built environment*, *4*(2), 278-306. doi: 10.1016/j.ijsbe.2015.10.002.

Rodrigues, A., Duchesne, J., & Fournier, B. (2015). A new accelerated mortar bar test to assess the potential deleterious effect of sulfide-bearing aggregate in concrete. *Cement and Concrete Research*, *73*, 96-110. doi: 10.1016/j.cemconres.2015.02.012.

Rodrigues, A., Duchesne, J., Fournier, B., Durand, B., Shehata, M. H., & Rivard, P. (2016). Evaluation Protocol for Concrete Aggregates Containing Iron Sulfide Minerals. *ACI Materials Journal*, *113*(3). doi: 10.14359/51688828.

Saengsoy, W., Yongchaitrakul, L., Sinlapasertsakulwong, P., & Tangtermsirikul, S. (2021). Identification of iron sulfide minerals in aggregates by accelerated mortar bar test. *In Bridge Maintenance, Safety, Management, Life-Cycle Sustainability and Innovations* (pp. 2664-2669). CRC Press. doi: 10.1201/9780429279119-364.

Schmidt, T., Leemann, A., Gallucci, E., & Scrivener, K. (2011). Physical and microstructural aspects of iron sulfide degradation in concrete. *Cement and Concrete Research*, *41*(3), 263-269. doi: 10.1016/j.cemconres.2010.11.011.

Scrivener, K., Martirena, F., Bishnoi, S., & Maity, S. (2018). Calcined clay limestone cements (LC^3). *Cement and Concrete Research*, *114*, 49-56. doi: 10.1016/j.cemconres.2017.08.017.

Sezer, G. İ. (2012). Compressive strength and sulfate resistance of limestone and/or silica fume mortars. *Construction and Building Materials*, *26*(1), 613-618. doi: 10.1016/j.conbuildmat.2011.06.064.

Shayan, A. (1988). Deterioration of a concrete surface due to the oxidation of pyrite contained in pyritic aggregates. *Cement and Concrete Research*, *18*(5), 723-730. doi: 10.1016/0008-8846(88)90095-6.

Shehata, M. H., Thomas, M. D., & Bleszynski, R. F. (1999). The effects of fly ash composition on the chemistry of pore solution in hydrated cement pastes. *Cement and Concrete Research*, *29*(12), 1915-1920. doi: 10.1016/S0008-8846(99)00190-8.

Shehata, M. H., & Thomas, M. D. (2002). Use of ternary blends containing silica fume and fly ash to suppress expansion due to alkali–silica reaction in concrete. *Cement and Concrete Research*, *32*(3), 341-349. doi: 10.1016/S0008-8846(01)00680-9.

Shi, Z., Ferreiro, S., Lothenbach, B., Geiker, M. R., Kunther, W., Kaufmann, J., Herfort, D., & Skibsted, J. (2019). Sulfate resistance of calcined clay–Limestone–Portland cements. *Cement and Concrete Research*, *116*, 238-251. doi: 10.1016/j.cemconres.2018.11.003.

Tagnit-Hamou, A., Saric-Coric, M., & Rivard, P. (2005). Internal deterioration of concrete by the oxidation of pyrrhotitic aggregates. *Cement and concrete research*, *35*(1), 99-107. doi: 10.1016/j.cemconres.2004.06.030.

Tangtermsirikul, S. (2005). Development of Fly Ash Usage in Thailand. *Society for Social Management Systems Internet Journal*, *1*(1). Retrieved from https://kutarr.kochi-tech.ac.jp/records/786.

Uzbas, B., & Aydin, A. C. (2020). Microstructural analysis of silica fume concrete with scanning electron microscopy and X-ray diffraction. *Engineering, Technology & Applied Science Research*, *10*(3), 5845-5850. doi: 10.48084/etasr.3288.

Visvalingam, S., Saengsoy, W., & Tangtermsirikul, S. (2022). Effects of free lime content in fly ash on sulfate expansion of cement–fly ash mixtures. *Journal of Material Cycles and Waste Management*, *24*(5), 2002-2014. doi: 10.1007/s10163-022-01460-3.

Wang, D., Shi, C., Farzadnia, N., Shi, Z., & Jia, H. (2018). A review on effects of limestone powder on the properties of concrete. *Construction and building materials*, *192*, 153-166. doi: 10.1016/j.conbuildmat.2018.10.119.

Wang, D., Shi, C., Farzadnia, N., Shi, Z., Jia, H., & Ou, Z. (2018). A review on use of limestone powder in cement-based materials: Mechanism, hydration and microstructures. *Construction and Building Materials*, *181*, 659-672. doi: :10.1016/j.conbuildmat.2018.06.075.

Wanna, S., Toochinda, P., Saengsoy, W., & Tangtermsirikul, S. (2021). Deterioration in sulfuric acid of cement pastes incorporating high CaO and low CaO fly ashes. *Engineering Journal*, *25*(2), 71-83. doi: 10.4186/ej.2021.25.2.71.

Yeğinobalı, A. (2009). Utilization of Silica Fume and Cement in the Concrete Mixture. *TÇMB*, Ankara.

Zhong, R., & Wille, K. (2018). Deterioration of residential concrete foundations: The role of pyrrhotite-bearing aggregate. *Cement and Concrete Composites*, *94*, 53-61. doi: 10.1016/j.cemconcomp.2018.08.012.

Zunino, F., & Scrivener, K. (2021). The reaction between metakaolin and limestone and its effect in porosity refinement and mechanical properties. *Cement and Concrete Research*, *140*, 106307. doi: 10.1016/j.cemconres.2020.106307.

BIOGRAPHY

Name	Niraporn Pornsiri
Education	2019: Bachelor of Engineering (Civil Engineering)
	Sirindhorn International Institute of Technology
	Thammasat University

Publications

Pornsiri, N., Saengsoy, W., & Tangtermsirikul, S. (2021). Effects of High CaO and Low CaO Fly Ashes and Limestone Powder on Iron Sulfide Oxidation of Aggregates in Concrete. *Proceedings of the 9th International Conference of Asian Concrete Federation (ACF2020/2021): Advanced & Innovative Concrete Technology*. Pathum Thani, Thailand.

Jeyakaran, T., Pornsiri, N., Saengsoy, W., & Tangtermsirikul, S. (2023). Test methods for performance-based evaluation of concrete containing iron sulfide-bearing aggregates: Development and application. *Results in Engineering*, *18*, 101068.